Fisheries and Oceans Canada | Pêches et Océans Canada
Ecosystems and Oceans Science | Sciences des écosystèmes et des océans

Canadian Science Advisory Secretariat (CSAS)

Research Document 2017/044

Quebec Region

Physical Oceanographic Conditions in the Gulf of St. Lawrence in 2016

P.S. Galbraith[1], J. Chassé[2], C. Caverhill[3], P. Nicot[3], D. Gilbert[1], B. Pettigrew[1], D. Lefaivre[1], D. Brickman[4], L. Devine[1], and C. Lafleur[1]

[1] Fisheries and Oceans Canada, Québec Region,
Maurice Lamontagne Institute,
P.O. Box 1000, Mont-Joli, Québec, G5H 3Z4

[2] Fisheries and Oceans Canada, Gulf Region,
P.O. Box 5030, Moncton, New Brunswick, E1C 9B6

[3] Institut des sciences de la mer de Rimouski
Université du Québec à Rimouski
310 allée des Ursulines, Rimouski, Québec, G5L 3A1

[4] Fisheries and Oceans Canada, Maritimes Region,
Bedford Institute of Oceanography
P.O. Box 1006, Dartmouth, Nova Scotia, B2Y 4A2

July 2017

Canada

Foreword

This series documents the scientific basis for the evaluation of aquatic resources and ecosystems in Canada. As such, it addresses the issues of the day in the time frames required and the documents it contains are not intended as definitive statements on the subjects addressed but rather as progress reports on ongoing investigations.

Research documents are produced in the official language in which they are provided to the Secretariat.

Published by:

Fisheries and Oceans Canada
Canadian Science Advisory Secretariat
200 Kent Street
Ottawa ON K1A 0E6

http://www.dfo-mpo.gc.ca/csas-sccs/
csas-sccs@dfo-mpo.gc.ca

ISSN 1919-5044

Correct citation for this publication:

Galbraith, P.S., Chassé, J., Caverhill, C., Nicot, P., Gilbert, D., Pettigrew, B., Lefaivre, D., Brickman, D., Devine, L., and Lafleur, C. 2017. Physical Oceanographic Conditions in the Gulf of St. Lawrence in 2016. DFO Can. Sci. Advis. Sec. Res. Doc. 2017/044. v + 91 p.

TABLE OF CONTENTS

ABSTRACT

An overview of physical oceanographic conditions in the Gulf of St. Lawrence (GSL) in 2016 is presented as part of the Atlantic Zone Monitoring Program (AZMP). AZMP data as well as data from regional monitoring programs are analysed and presented in relation to long-term means. The annual average freshwater runoff of the St. Lawrence River measured at Québec City was normal and its combination with rivers flowing into the Estuary (RIVSUM II) was about above-normal in 2016 (+0.5 SD and +0.6 SD respectively). The mild early winter of 2016 created a surface mixed layer that was not near-freezing over the entire Gulf, and led to the third lowest sea ice cover maximum volume since 1969. The August cold intermediate layer (CIL) showed warmer than normal minimum temperature (+1.4 SD) and less than normal volume colder than 1°C (-2.1 SD). Sea-surface temperatures averaged over the Gulf were near normal or above normal from May to November 2016, leading to an above-normal May-November average (+0.6°C, +0.9 SD). The May to November average was however at a record high (since 1985) for the Estuary (+1.4°C, +2.4 SD). Record highs were reached in November averaged over the Gulf (+1.7°C, +2.2 SD) and in the following regions: Estuary (+1.8°C, +2.2 SD), Northwest Gulf (+1.9°C, +2.1 SD), Esquiman Channel (+2.5°C, +2.2 SD), Cabot Strait (+2.2°C, +2.5 SD), and Magdalen Shallows (+2.0°C, +2.5 SD). The timing of summer warming onset and fall cooling were normal. Deep water temperatures have been increasing overall in the Gulf, with inward advection from Cabot Strait where temperature had reached a record high (since 1915) in 2012 at 200 m. Temperature averaged over the Gulf at depths of 250 and 300 m were at record highs in 2016 at 6.1 and 6.2°C respectively. The bottom area covered by waters warmer than 6°C finally decreased in 2016 in Anticosti Channel and Esquiman Channel, but increased sharply in Central Gulf and made its first appearance in the northwest Gulf.

Conditions océanographiques physiques dans le golfe du Saint-Laurent en 2016

RÉSUMÉ

Le présent document donne un aperçu des conditions d'océanographie physique qui ont prévalu dans le golfe du Saint-Laurent en 2016 et est un produit du Programme de monitorage de la zone Atlantique (PMZA). Les données du PMZA ainsi que de programmes de monitorage régionaux sont analysées et présentées en relation avec des moyennes à long terme. Les débits du fleuve Saint-Laurent et de l'indice RIVSUM II étaient respectivement près et au-dessus de la normale en 2016 (+ 0,5 É.T. et + 0,6 É.T. respectivement). Le début de l'hiver 2016 a été doux, ce qui a permis à la couche de surface de maintenir des températures largement au-dessus du point de congélation sur une importante superficie du golfe, ainsi que le troisième plus faible volume de glace saisonnier maximal depuis 1969. La couche intermédiaire froide (CIF) du mois d'août était chaude (+ 1,4 É.T.) et mince (- 2,1 É.T. pour le volume des eaux sous 1 °C). Les températures de l'eau à la surface de étaient généralement près ou au-dessus de la normale de mai à novembre, conduisant à une moyenne de mai à novembre qui a été au-dessus de la normale (+ 0,6 °C, + 0,9 É.T.). La moyenne de mai à novembre était à un niveau record dans l'estuaire (+ 1,4 °C;+ 2,4 SD).Le mois de novembre a connu un record de + 1,7 °C au-dessus de la climatologie (+ 2,2 É.T.). Des records ont aussi été battus dans les régions suivantes : estuaire (+ 1,8 °C; + 2,2 É.T.), nord-ouest du golfe (+ 1,9 °C; + 2,1 É.T.), chenal Esquiman (+ 2,5 °C; + 2,2 É.T.), détroit de Cabot (+ 2,2 °C; + 2,5 É.T.) et le Plateau madelinien (+ 2,0 °C; + 2,5 É.T.). Le réchauffement estival et le refroidissement d'automne se sont produits à des dates près des normales. Les températures des eaux profondes du golfe ont depuis quelques années été en augmentation avec le transport depuis le détroit de Cabot d'eaux qui avaient atteint une température record (depuis 1915) en 2012 à 200 m. Globalement, les températures à 250 m et 300 m de profondeur ont atteint un record de série depuis 1915, à respectivement 6,1 et 6,2 °C respectively. La superficie du fond marin recouvert par des températures plus grandes que 6 °C a finalement diminué dans le chenal d'Anticosti et le chenal Esquiman, mais a augmenté beaucoup dans le centre du golfe et a fait sa première apparition dans le nord-ouest du golfe.

INTRODUCTION

This document examines the physical oceanographic conditions and related atmospheric forcing in the Gulf of St. Lawrence in 2016 (Fig. 1). It complements similar reviews of the environmental conditions on the Newfoundland and Labrador Shelf and the Scotian Shelf and Gulf of Maine as part of the Department of Fisheries and Oceans' (DFO) Atlantic Zone Monitoring Program (AZMP; see Therriault et. al. 1998 for background information on the program and Colbourne et al. 2016, and Hebert et al. 2016 for examples of past reviews in other AZMP regions). The last detailed report of physical oceanographic conditions in the Gulf of St. Lawrence was produced for the year 2015 (Galbraith et al. 2016). Specifically, it discusses air temperature, freshwater runoff, sea-ice volume, surface water temperature and salinity, winter water mass conditions (e.g., the near-freezing mixed layer volume, the volume of dense water that entered the Gulf through the Strait of Belle Isle), the summertime cold intermediate layer (CIL), and the temperature, salinity, and dissolved oxygen of the deeper layers. Some of the variables are spatially averaged over distinct regions of the Gulf (Fig. 2). The report uses data obtained from the AZMP, other DFO surveys, and other sources. Environmental variables are usually expressed as anomalies, i.e., deviations from their long-term mean. The long-term mean or normal conditions are calculated for the standard 1981–2010 reference period when possible. Furthermore, because these series have different units (°C, m^3, m^2, etc.), each anomaly time series is normalized by dividing by its standard deviation (SD), also calculated for the standard reference when possible. This allows a more direct comparison of the various series. Missing data are represented by grey cells in the tables, values within ±0.5 SD of the average as white cells, and conditions corresponding to warmer than normal (higher temperatures, reduced ice volumes, reduced cold-water volumes or areas) by more than 0.5 SD as red cells, with more intense reds corresponding to increasingly warmer conditions. Similarly, blue represents colder than normal conditions. Higher than normal freshwater inflow is shown as red, but does not necessarily correspond to warmer-than-normal conditions. Higher than normal stratification values are shown in blue because they are usually caused by lower upper layer salinity.

The summertime water column in the Gulf of St. Lawrence consists of three distinct layers: the surface layer, the cold intermediate layer (CIL), and the deeper water layer (Fig. 3). Surface temperatures typically reach maximum values in early to mid-August (Galbraith et al 2012). Gradual cooling occurs thereafter, and wind forced mixing during the fall leads to a progressively deeper and cooler mixed layer, eventually encompassing the CIL. During winter, the surface layer thickens partly because of buoyancy losses (cooling and reduced runoff) and brine rejection associated with sea-ice formation, but mostly from wind-driven mixing prior to ice formation (Galbraith 2006). The surface winter layer extends to an average depth of 75 m, but may reach >150 m in places such as the Mécatina Trough where near freezing waters (-1.8 to 0ºC) from the Labrador shelf entering through the Strait of Belle Isle may extend from the surface to the bottom in depths >200 m) (Galbraith 2006). During spring, surface warming, sea-ice melt waters, and continental runoff produce a lower-salinity and higher-temperature surface layer. Underneath this surface layer, cold waters from the previous winter are partly isolated from the atmosphere and form the summer CIL. This layer will persist until the next winter, gradually warming up and deepening during summer (Gilbert and Pettigrew 1997; Cyr et al. 2011) and more rapidly during the fall as vertical mixing intensifies.

This report considers these three layers in turn, but first air temperature and the freshwater runoff are examined because they are significant drivers of the surface layer. The winter sea ice and winter oceanographic conditions are described; these force the summer CIL, which is presented next. The deeper waters, mostly isolated from exchanges with the surface, are presented last along with a summary of major oceanographic surveys.

AIR TEMPERATURE

The air temperature data are the second generation of homogenized surface air temperature data, part of the Adjusted and Homogenized Canadian Climate Data (AHCCD), which accounts for shifts due to the relocation of stations, changes in observing practices and automation (Vincent et al. 2012). The monthly air temperature anomalies for several stations around the Gulf are shown in Fig. 4 for 2015 and 2016, as well as the average of all station anomalies.

Fig. 5 shows the annual, winter (December-March), and April-November mean air temperature anomalies averaged over all available stations shown in Fig. 4 since 1873. Record-high annual and winter temperatures occurred in 2010 and record-high April-November temperatures in 2012. Galbraith et al. (2012) found the average April-November air temperature over the Gulf from Environment Canada's National Climate Data and Information Archive (NCDIA) to be a good proxy for May-November sea-surface temperature over the Gulf (but excluding the estuary) and found within the former a warming trend of 0.9°C per century between 1873 and 2011; the same trend is found here over the selected ACCHD stations between 1873 and 2016 (Fig. 5). The NCDIA December-March air temperatures in the western Gulf were found to be highly correlated (R^2=0.67) with sea-ice properties, as well as with winter mixed layer volumes (Galbraith et al. 2010). Galbraith et al. (2013) found slightly higher correlations (R^2=0.72) with sea-ice using December-February ACCHD averages, possibly because March temperature are of less importance during low sea-ice cover since much of the sea-ice cover decrease has occurred much earlier in February.

No monthly records were set at individual stations in 2016. Overall, the winter began with above-normal air temperatures but finished with below-normal temperatures. The summer was characterized with near-normal to above-normal temperatures, and the fall temperatures were above-normal including the warmest November since 2006. Averaged over all stations, the December-March air temperature average was above-normal (+1.5°C, +1.0 SD), as was the April-November average (+0.4°C, +0.6 SD) and the annual average (+0.5°C, +0.5 SD).

PRECIPITATION AND FRESHWATER RUNOFF

Freshwater runoff data for the St. Lawrence River are updated monthly (Fig. 6, lower curve) using the water level method from Bourgault and Koutitonsky (1999). A hydrological watershed model was used to estimate the monthly runoff since 1948 for all other major rivers flowing into the Gulf of St. Lawrence, with discharge locations as shown in Fig. 7. The precipitation data (NCEP reanalysis, six hourly intervals) used as input in the model were obtained from the NOAA-CIRES Climate Diagnostics Center (Boulder, Colorado, USA; Kalnay et al. 1996). The data were interpolated to a ¼° resolution grid and the water routed to river mouths using a simple algorithm described here. When air temperatures were below freezing, the water was accumulated as snow in the watershed and later melted as a function of warming temperatures. Water regulation is modelled for three rivers that flow into the estuary (Saguenay, Manicouagan, Outardes) for which the annual runoff is redistributed following the climatology of the true regulated runoffs for 12 months thereafter. Runoffs were summed for each region shown and the climatology established for the 1981–2010 period. The waters that flow into the Estuary (region 1, Fig 7.) were added to the St. Lawrence River runoff measured at Québec City to produce the RIVSUM II index, although no advection lags were introduced (Fig. 6, upper curve).

Monthly anomalies of the summed runoffs for 2015 and 2016 are shown in Fig. 8. Rivers other than the St. Lawrence contribute about 5,000 $m^3 s^{-1}$ runoff to the Estuary, the equivalent of 40% of the St. Lawrence River, while the other tributaries distributed along the border of the GSL provide an additional 3,500 $m^3 s^{-1}$ in freshwater runoff to the system. River regulation has a strong impact on the relative contributions of sources. For example, in May 2015 the higher-

than-average river runoff into the Estuary (an effect of the heavy precipitation in 2014 and river regulation) was almost as important as the below-normal St. Lawrence run-off. The 2016 hydrological simulation shows that rivers in regions 2, 3, 4 and 5 behaved similarly from July to December, with typically near-normal to below-normal runoff. The long-term time series are shown, summed by large basins, in Fig. 9. Broad long-term patterns of runoff over the large basins were similar to that of the St. Lawrence River but interannual variability is low in the Northeast basin and Magdalen Shallows basin. The average run-off into the Estuary was above-normal at +0.5 SD. The annual average runoff of the St. Lawrence River measured at Québec City and RIVSUM II both show a general downward trend from the mid-1970s until 2001, an upwards trend between 2001 and 2011 and were respectively normal and above-normal in 2016 (Fig. 9) at 12,400 m^3s^{-1} (+0.5 SD) and 17,600 m^3s^{-1} (+0.6 SD). Runoff was generally high from January through June. The spring freshet was normal at +0.1 SD in April for the St. Lawrence River but above-normal at +0.7 SD in May for RIVSUM II, but its timing was normal (Fig. 6). The fall freshet was also near normal.

SURFACE LAYER

The surface layer conditions of the Gulf are monitored by several complementary methods. The shipboard thermosalinograph network (Galbraith et al. 2002) consists of temperature-salinity sensors (SBE-21; Sea-Bird Electronics Inc., Bellevue, WA) that have been installed on various ships starting with the commercial ship Cicero of Oceanex Inc. in 1999 (retired in 2006) and on the Cabot from 2006 to fall 2013. The Oceanex Connaigra, was outfitted with a thermosalinograph in early 2015.

The second data source is the thermograph network (Pettigrew et al. 2016), which consists of a number of stations with moored instruments recording water temperature every 30 minutes (Fig. 10). Most instruments are installed on Coast Guard buoys that are deployed in the ice-free season, but a few stations are monitored year-round. The data are typically only available after the instruments are recovered except for oceanographic buoys that transmit data in real-time.

The third data source are 1 km resolution monthly composite Sea Surface Temperature (SST) generated using National Oceanic and Atmospheric Administration (NOAA) and European Organisation for the Exploitation of Meteorological Satellites (EUMETSAT) Advanced Very High Resolution Radiometer (AVHRR) satellite images available from the Maurice Lamontagne Institute sea surface temperature processing facility (details in Galbraith and Larouche 2011, and Galbraith et al. 2012). These data are available for the period of 1985-2013. From 2014, AVHRR composites of 1.5-km resolution provided by the Bedford Institute of Oceanography (BIO) Operational Remote Sensing group complete the data set. Monthly climatologies for the period of 1998-2012 common to both products were compared at the 1.5-km pixel level for cross-calibration. The BIO product is adjusted to the MLI product climatology as $SST_{IML} = 0.9794\ SST_{BIO} - 0.13$ (-0.13°C adjustment at 0°C; -0.54°C at 20°C). This is in part explained by the fact that the MLI product used all available SST images while the BIO product uses only daytime passes, introducing a slight diurnal bias.

SST SEASONAL CYCLE CLIMATOLOGY

The May to November cycle of weekly averaged surface temperature is illustrated in Fig. 11 using a 1985–2010 climatology based on AVHRR remote sensing data for ice-free months complemented by 2001–2010 thermosalinograph data for the winter months. Galbraith et al. (2012) have shown that Gulf-averaged air temperature and SST monthly climatologies match up quite well with SST lagging air temperature by half a month. Maximum sea-surface temperatures are reached on average during the second week of August but that can vary by a

few weeks from year to year. The maximum surface temperature averages to 15.6ºC over the Gulf during the second week of August (1985–2010), but there are spatial differences: temperatures on the Magdalen Shallows are the warmest in the Gulf, averaging 18.1ºC over that area, and the coolest are at the head of the St. Lawrence Estuary and upwelling areas along the lower north shore.

Fig. 12 shows a mean annual cycle of water temperature at a depth of 8 m along the Montréal to St. John's shipping route based on thermosalinograph data collected from 2000 to 2016. The data were averaged for each day of the year at intervals of 0.1 degree of longitude within the main shipping route to create a composite along the ship track. The most striking feature is the area at the head of the Laurentian Trough (69.5°W), where strong vertical mixing leads to cold summer water temperatures (around 5°C to 6°C and sometimes lower) and winter temperatures that are always above freezing (see also Fig. 11). The climatology shows the progression to winter conditions, first reaching near-freezing temperatures in the Estuary and then progressing eastward with time, usually reaching Cabot Strait by the end of the winter (but no further).

Temperature anomaly time series and the 2000–2016 climatologies were constructed for selected sections that are crossed by the ship (Fig. 13). The near-surface temperature climatology at Tadoussac (head of the Laurentian Trough) contrasts with that nearby in the Estuary, as noted above. Winter temperatures are on average 0.7°C warmer at the Tadoussac section; the maximum monthly mean temperature in summer is only 7.1°C compared with 8.6°C at the nearby Estuary section and up to 13.2°C at the Mont-Louis section. The table in Fig. 13 provides a quick reference to the interannual near-surface temperature variations at the selected sections as well as monthly averages for the year in review.

SST IN 2016

Thermosalinograph data show that near-freezing surface layer conditions first appeared later than normal (Fig. 12), consistent with the well above normal December and January air temperatures over the Gulf (Fig. 4). The 2016 monthly mean sea-surface temperatures from AVHRR imagery are shown in Fig. 14 as colour-coded maps and the corresponding temperature anomaly maps are shown in Fig. 15 referenced to 1985–2010 monthly climatologies. Missing anomaly pixels are due to incomplete climatologies during the ice covered winter months. The SST information is summarized in Fig. 16, showing the 2016 monthly average temperatures versus the climatology spatially averaged over the Gulf and over each of the eight regions delimited by the areas shown in Fig. 2. The information also appears again in tabular form in Fig. 17 with the same averaging regions and further into sub-regions of the Estuary as shown in Fig. 18. Fig. 16 displays anomalies expressed in degrees while Fig. 17 displays average temperatures.

Near-surface water temperatures were near normal or above normal from May to November 2016, leading to an above-normal May-November average (+0.6°C, +0.9 SD). The May to November average was however at a record high (since 1985) for the Estuary, at 8.3°C (+2.4 SD) which is 1.4°C higher than the climatological mean. Record highs were reached in November averaged over the Gulf (6.1°C, above normal by +1.7°C and 2.2 SD) and in the following regions: Estuary (+1.8°C, +2.2 SD), Northwest Gulf (+1.9°C, +2.1 SD), Esquiman Channel (+2.5°C, +2.2 SD), Cabot Strait (+2.2°C, +2.5 SD) and Magdalen Shallows (+2.0°C, +2.5 SD). Figures 19 and 20 show the 1985–2016 time series of monthly surface temperature anomalies spatially averaged over the Gulf of St. Lawrence and over the eight regions of the Gulf. The thermosalinograph data show above-normal surface layer conditions in December as well (Figs. 12 and 13).

Sea-surface temperature monthly climatologies and time series were also extracted for more specific regions of the Gulf. The monthly average SST for the St. Lawrence Estuary as a whole (region 1) is repeated in Fig. 21 along with averages for the proposed Manicouagan Marine Protected Area (MPA), the proposed St. Lawrence Estuary MPA, and the Saguenay – St. Lawrence Marine Park. The overall pattern is similar across regions, but there are differences associated with episodic local events such as eddies and upwellings. The climatology averages also differ, for example the Manicouagan maximum monthly average temperature is 1.0°C warmer than for the Estuary as a whole.

The Magdalen Shallows, excluding Northumberland Strait, is divided into western and eastern areas as shown in Fig. 22. The monthly average SST for the Magdalen Shallows as a whole (region 8) is repeated in Fig. 23 along with averages for the western and eastern areas. Climatologies differ by roughly 0.5°C to 1°C between the western and eastern regions. Temperatures were below-normal to normal from May to July and normal to above-normal from August until November.

The number of weeks in the year that the mean weekly temperature is above 10°C for each pixel (Fig. 24) integrates summer surface temperature conditions into a single map displaying the length of the warm season. The average number of weeks with mean weekly temperature above 10°C are shown for each region as time series in Fig. 25. The Estuary had a longer than normal warm season (+1.5 SD, about three weeks longer), while the lengths in other regions of the Gulf were near-normal.

Seasonal trends in relation to air temperature are examined by first displaying weekly averaged AVHRR SST in the GSL for all years between 1985 and 2016 (Fig. 26) with years on the x-axis and weeks of the year on the y-axis (See Galbraith and Larouche 2013 for a full description). Isotherms show the first and last occurrences of weekly temperature averages of 12°C over the years. These temperatures are chosen to be representative of spring (and fall) transitions to (and from) typical summer temperatures. Although the selected temperature is arbitrary, the results that follow are not particularly sensitive to the exact temperature chosen because the surface mixed layer tends to warm and cool linearly in spring and fall (e.g. Fig. 11). The Gulf has experienced earlier summer onset and later fall cooling between 1985 and 2016, with trends of -0.5 and +0.5 weeks per decade respectively (confidence intervals of ±0.4 weeks per decade, therefore significantly different from zero). In 2016, the timing of summer onset and fall cooling were both near-normal. The interannual variability in the time of year when the 12°C threshold is crossed is correlated with June-July average air temperature for the summer onset (1.1 week sooner per 1°C increase; R^2=0.56) and with September average air temperature for the fall (0.7 week later per 1°C increase; R^2=0.43). These air temperature averages, shown in Fig. 26, can be used as proxies prior to 1985. The implication is that the Gulf of Lawrence warm season will be longer by about 2 weeks for each 1°C of warming associated with climate change.

Thermograph network observations are compared to daily average temperatures calculated using all available data for each day of the year at each station and depth (Figs. 27-29). The seasonal cycle of near-surface temperature is measured by shallow instruments, while Cold Intermediate Layer warming from spring to fall is captured by instruments moored between 30 and 120 m depth. Monthly average temperatures are also shown, with the magnitude of their anomaly colour-coded. Salinities are shown in a similar fashion in Fig. 30. The average monthly temperatures for each station at shallow sampling depths (< 20 m) for 2015 and 2016 are also shown in Fig. 31, while Fig. 32 shows information for sensors moored deeper than 20 m and Fig. 33 shows the history of monthly averaged temperature anomalies for selected stations.

Monthly shallow-water anomalies were fairly consistent across all stations of each of the three regions listed in Fig. 31. As with AVHRR data sources and in spite of different climatological

periods, summer months shows mostly near-normal to above-normal temperatures (especially in the Estuary and Northwest Gulf) and well above-normal temperatures in October (few sites have full November data).

The Île Shag (10 m) station shows bottom temperatures close to Îles-de-la-Madeleine that are important to the lobster fishery. April and May temperatures were near normal at this station (Fig. 29 and Fig. 33). The Île Shag panel (Fig. 29) shows with a red line the span of historical dates when spring temperature increased over 1.5°C, a temperature associated with increased lobster mobility, as well as the mean date plus and minus 0.5 SD. In 2016, this occurred on April 25th, just a day later than the average recorded date. Station La Perle is also relevant to the lobster fishery because it is located in deeper waters (26 m) where the fishery tends to start. Because the thermograph is attached to a Coast Guard buoy, even the bottom temperature is usually already above 1.5°C by the time it get deployed in spring. The data are not yet available at this time. The lobster fishery began on May 1th and must therefore have been in cold waters (<1.5°C) since it can take up to two weeks for waters to warm at 30 m starting from the time recorded at 10 m.

SEA ICE

Ice volume is estimated from three gridded databases of ice cover and ice categories obtained from the Canadian Ice Service (CIS). Weekly Geographic Information System (GIS) charts covering the period 1969-2016 and daily charts covering the period 2009-2016 were gridded on a 0.01° latitude by 0.015° longitude grid (approximately 1 km resolution), and 5-km resolution gridded daily files were obtained directly from the CIS covering the period 1998-2008. Some of the analyses described below were done using the weekly data exclusively, for long-term consistency, while for others daily data were used when available with results filtered using a 3-day running mean in order to make them more comparable to results calculated from weekly data.

Ice typically forms first in December in the St. Lawrence estuary and in shallow waters along New Brunswick, Prince Edward Island and the lower north shore and melts last in the northeast Gulf where the ice season duration tends to be longest apart from shallow bays elsewhere (Fig. 34). Offshore sea ice is typically produced in the northern parts of the Gulf and drifts towards Îles-de-la-Madeleine and Cabot Strait during the ice season. The maximum estimated ice volume in 2016 occurred the week of March 7th and is compared with the 1981-2010 climatology in Fig. 35 (upper panels). The 1981-2010 climatology and 2016 distribution of the thickest ice recorded during the season at any location is also shown in Fig. 35 (lower panels); the climatological thick areas in the northeast are mostly associated with ice that has entered the Gulf through the Strait of Belle Isle and are pushed by the wind either on the lower north shore or on the coast of Newfoundland.

Fig. 36 shows the daily evolution of the estimated sea-ice volume in relation to the climatology and historical extremes. Fig. 37 shows the estimated seasonal maximum ice volumes within the Gulf as well as on the Scotian Shelf. The volume shown on the bottom panel of Fig. 37 corresponds to that found seaward of Cabot Strait (defined by its narrowest crossing). It would represent the volume of ice exported from the Gulf provided that no melt had already occurred. The combined Gulf and Scotian Shelf ice volume shown separately as top and bottom panels of Fig. 37 is indicative of the total volume of ice produced in the Gulf, including the advection out of the Gulf, but it also includes the thicker sea ice that drifts into the Gulf from the Strait of Belle Isle.

Fig. 38 shows the day of first and last occurrence of ice in each of the regions of the Gulf of St. Lawrence as well as duration of the ice season and maximum observed volume during each season.

Fig. 39 shows the time series of seasonal maximum ice volume and area (excluding thin new ice), ice season duration and December-to-March air temperature anomaly (from Fig. 5). The figure shows declining trends in ice cover severity since 1990 with rebounds in 2003 and 2014. The correlation between annual maximum ice volume (including the cover present on the Scotian Shelf) and the December-February air temperature averaged over five Western Gulf stations (Sept-Îles, Mont-Joli, Gaspé, Charlottetown and Îles-de-la-Madeleine) accounted for 72% of the variance using the 1969–2012 time series (Galbraith et al. 2013). Fig. 39 shows a similar comparison using ice volume and the ACCHD December-to-March air temperature anomaly from Fig. 5 yielding $R^2 = 0.73$. The correlation between air temperature and the ice parameters season duration and area are also very high ($R^2 = 0.74$-0.83). Correlation coefficients are slightly higher when using January to February air temperatures, perhaps because March air temperatures have no effect on ice cover that has almost disappeared by then during very mild winters. Sensitivity of the ice cover to climate change can be estimated using past co-variations between winter air temperature and sea-ice parameters, which indicate losses of 17 km^3, 30,000 km^2 and 14 days of sea-ice season for each 1°C increase in winter air temperature

In 2016, the seasonal maximum ice volume based on weekly ice charts was 14 km^3 (Fig. 38), well below-normal (-1.8 SD) and third lowest of the time series that began in 1969, partly consistent with above-normal winter air temperatures (+1.5°C, +1.0 SD). Five of the seven lowest maximum ice volumes of the time series have occurred in the previous seven years. No ice was exported from the Gulf of St. Lawrence onto the Scotian Shelf in 2016. The sea-ice cover throughout the season was typically close to historical minimums until mid-February (Fig. 36). The peak sea-ice volume is typically reached early during low sea-ice year, but the (low) seasonal maximum was reached at a near-normal time of year in mid-March, probably due to below-normal air temperatures in March (-1.4°C, -0.6 SD). First occurrence of sea-ice was late and last occurrence was early, leading to well below-normal durations everywhere by more than 5 weeks (Figs. 34 and 38).

WINTER WATER MASSES

A wintertime survey of the Gulf of St. Lawrence waters (0–200 m) has been undertaken in early March since 1996, typically using a Canadian Coast Guard helicopter but from Class 1100 Coast Guard buoy tenders in 2016. The survey, sampling methods, and results of the cold-water volume analysis in the Gulf and the estimate of the water volume advected into the Gulf via the Strait of Belle Isle over the winter are described in Galbraith (2006) and in Galbraith et al. (2006). Figs. 40 and 41 show gridded interpolations of near-surface temperature, temperature above freezing, salinity, cold layer thickness and bottom contacts, and thickness of the Labrador Shelf water intrusion for 2016 as well as climatological means.

The March surface mixed layer is usually very close (within 0.1°C) to the freezing point in most regions of the Gulf but thickness of the surface layer varies, leaving only variability in the cold-water volume between mild and severe winters. However, his was not the case in 2010 for the first time since the inception of the winter survey, when the mixed layer was on average 1°C above freezing. During typical winters, surface waters in the temperature range of ~ 0°C to -1°C are only found from the northeast side of Cabot Strait and into the Gulf. Some of these warm waters have presumably entered the Gulf during winter and flowed northward along the west coast of Newfoundland, however it is also possible that local waters could have simply not

cooled close to freezing. Conditions in March 2016 were warm in the triangle formed roughly by Gros Morne (NL), Heath Point on Anticosti and Port aux Basques (NL) (Fig. 40), consistent with the lack of sea-ice in that part of the Gulf in the observed maximum ice cover field (Fig. 35).

Near-freezing waters with salinities of around 32 are responsible for the (local) formation of the CIL since that is roughly the salinity at the temperature minimum during summer. These are coded in green-blue in the salinity panel of Fig. 40 and are typically found to the north and east of Anticosti Island. Surface salinities were a bit lower than the climatology in this part of the Gulf during the winter of 2016.

Near-freezing waters with salinity >32.35 (colour-coded in violet) are considered to be too saline to have been formed from waters originating within the Gulf (Galbraith 2006) and are presumed to have been advected from the Labrador Shelf through the Strait of Belle Isle. These waters were present at the surface in Mécatica Trough at only one station in March 2016 (Fig. 40). A T-S water mass criterion from Galbraith (2006) was used to identify intruding Labrador Shelf waters that have exhibited no evidence of mixing with warm and saline deep Gulf water. These waters occupied a thick sub-surface layer within Mécatina Trough in March 2016, but its extent was limited (top-right panel of Fig. 41). The recent history of Labrador Shelf water intrusions is shown in Fig. 42, where its volume is shown as well as the fraction it represents of all the cold-water volume in the Gulf. This volume was below-normal in March 2016, at 560 km³ (-0.8 SD) representing only 5% (-0.9 SD) of the cold water (T< -1°C) in the Gulf.

The thermograph network also provides some information on the winter intrusion of Labrador Shelf waters. There are large differences in springtime bottom temperature at the Strait of Belle Isle (71 m) station depending on how late the cold inflow of Labrador Shelf Water persists (Fig. 33). Deep temperatures in the Strait of Belle Isle were below -1°C up to April 24th (Fig. 28), coinciding with the earliest date on record for that transition to occur and indicating an early stop of the entry of cold Labrador Shelf waters into the Gulf.

The cold mixed layer depth typically reaches about 75 m in the Gulf and is usually delimited by the -1°C isotherm because the mixed layer is typically near-freezing and deeper waters are much warmer (Galbraith 2006). In March 2010 and 2011 much of the mixed layer was warmer than -1°C such that the criterion of T<0°C was also introduced (see middle panels of Fig. 41). The cold surface layer is the product of local formation as well as cold waters advected from the Labrador Shelf, and can consist either of a single water mass or of layers of increasing salinity with depth. This layer reaches the bottom in many regions of the Gulf, with interannual variability in whether the deepest parts of the Magdalen Shallow or of Mécatina Trough are reached (see bottom panels of Fig. 41).

Integrating the cold layer depth over the area of the Gulf (excluding the Estuary and the Strait of Belle Isle) yields a cold-water (< -1°C) volume of 10 300 km³ in 2016 (Fig. 43), 0.5 SD below the 1996–2016 average and similar to the volumes observed in 2000 and 2012. The time series of winter cold-water (<-1°C) volume observed in the Gulf is shown in Fig. 49. The mixed layer volume increases to 13 800 km³ when water temperatures <0°C are considered which is 1 SD below the 1996–2016 average. This last volume of cold water corresponds to 41% of the total water volume of the Gulf (33 500 km³, excluding the Estuary).

COLD INTERMEDIATE LAYER

PREDICTION FROM THE MARCH SURVEY

The summer CIL minimum temperature index (Gilbert and Pettigrew 1997) has been found to be highly correlated with the Gulf (excluding the estuary) volume of cold water (<-1°C) measured the previous March when much of the mixed layer is near-freezing (Galbraith 2006; updated relation in right panel of the present document Fig. 43). This is expected because the CIL is the remnant of the winter cold surface layer. A measurement of the volume of cold water present in March is therefore a valuable tool for forecasting the coming summer CIL conditions. The winter mixed layer in 2016 was not near-freezing throughout the Gulf. The overall thickness and volume of the layer colder than -1°C was 0.5 SD below normal in 2016. The Cold Intermediate Layer for summer 2016 was therefore forecasted to be warmer than in 2015, with a Gilbert and Pettigrew (1997) index of around +0.1°C compared to -0.3°C in 2015 (Galbraith et al. 2016).

AUGUST CIL BASED ON THE MULTI-SPECIES SURVEY

The CIL minimum temperature, thickness and volume for T<0°C and <1°C were estimated using temperature profiles from all sources for August and September. Most data are from the multi-species surveys in September for the Magdalen Shallows and August for the rest of the Gulf. Using all available temperature profiles, each 1-m depth layer of the Gulf was spatially interpolated for temperature, with the interpolated field bound between the minimum and maximum values observed within each of the different regions of the Gulf (Fig. 2) to avoid spurious extrapolations. The CIL thickness at each grid point is simply the sum of depth bins below the threshold temperature, and the CIL minimum temperature is only defined at grid points where temperature rises by at least 0.5°C at depths greater than that of the minimum, or if the grid point minimum temperature is below the CIL spatial average of the Gulf.

Fig. 44 shows the gridded interpolation of the CIL thickness <1°C and <0°C and the CIL minimum temperature for August–September 2016 as well their 1985-2010 climatology (1994-2010 for Mécatina Trough). The CIL thickness for T<0°C and T<1°C decreased again compared to 2015, with conditions similar to 2006 (not shown). Similar maps were produced for all years back to 1971 (although some years have no data in some regions), allowing the calculation of volumes for each region for each year as well as the climatologies shown on the left side of Fig. 44. The 2016 CIL water mass was thinner and warmer than the 1985-2010 climatologies, with particularly warm conditions in the Estuary, with minimum temperatures well above 1°C in the western half.

The time series of the regional August–September CIL volumes are shown in Fig. 45 (for <0°C and <1°C). Many regions show decreased CIL volumes in 2016 compared to 2015. Fig. 46 shows the total volume of CIL water (<0°C and <1°C) and the average CIL core temperature from the August–September interpolated grids (e.g., Fig. 44). The CIL areal minimum temperature average and volume shown in Fig. 46 exclude data from Mécatina Trough which has very different water masses from the rest of the Gulf; it is influenced by inflow through the Strait of Belle Isle and is therefore not indicative of the climate in the rest of the Gulf. The CIL volume as defined by T<1°C decreased significantly (to -2.1 SD) compared to 2015 conditions (-1.5 SD) and reached a volume similar to 2006 (also -2.1 SD). The volume delimited by 0°C also decreased, to -2.1 SD.

The time series of the CIL regional average minimum core temperatures are shown in Fig. 47. All regions, again except for Mécatina Trough, show an increase in core temperature. The 2016 average temperature minimum (excluding Mecatina Trough, the Strait of Belle Isle and the

Magdalen Shallows) was 0.2°C, an increase of 0.2°C over 2015, and is shown in Fig. 46 (bottom panel, green line). The overall 2016 CIL water mass properties are similar to observations of 2006.

NOVEMBER CIL CONDITIONS IN THE ST. LAWRENCE ESTUARY

The AZMP November survey provides a high-resolution conductivity-temperature-depth (CTD) sampling grid in the St. Lawrence estuary since 2006 although measurements are sparser in some years. This allows a higher resolution display of the CIL minimum temperature in the Estuary (Fig. 48). The data also show the temporal warming (Fig. 45) and thinning (Fig. 47) of the CIL since the August survey. The CIL was slightly warmer in November 2016 than in 2015, and again none of it was below 1°C. Fig. 47 shows that the fairly rapid increase of the CIL minimum temperature occurring between August and November is fairly constant inter-annually in spite of the differences in August temperature.

SUMMER MEAN CIL INDEX

The Gilbert and Pettigrew (1997) CIL index is defined as the mean of the CIL minimum core temperatures observed between 1 May and 30 September of each year, adjusted to 15 July with a region-dependant warming rate. It was updated using all available temperature profiles measured within the Gulf between May and September inclusively since 1947 (black line of the bottom panel of Fig. 46). As expected, the CIL core temperature interpolated to 15 July is almost always colder than the estimate based on August and September data for which no temporal corrections were made. This is because the CIL is eroded over the summer and therefore its core warms over time.

This CIL index for summer 2016 was -0.10°C, 0.8 SD above normal. The 0.18°C increase from the summer 2014 CIL index is consistent with the decrease in CIL volume between August 2015 and 2016 discussed above and the decrease of 0.17°C in the areal average of the minimum temperature in August. The warm winter conditions from 2010 to 2012 led to CIL indices that were still far below the record high observed in the 1960s and 1980s. The earlier CIL temperature minimums will need to be re-examined to confirm that they were calculated using data with sufficient vertical resolution to correctly resolve the core minimum temperature. It is also becoming increasingly clear that the winter mixed layer is not the only factor explaining summertime CIL conditions and that mechanisms having a multi-year cumulative effect are required to explain the interannual autocorrelations observed. For example, this may be linked to temperatures below the CIL, which in warm years may create a higher temperature gradient that leads to higher heat fluxes and faster summertime CIL warming rates.

As a summary, Fig. 49 shows selected time series of winter and summertime CIL conditions (June and September bottom temperatures also related to the CIL are outlined below) and highlights the strong correlations between these various time series. The CIL had warmer than normal conditions both in August and in this May-September average, consistent with winter air temperatures that were above-normal and with the seasonal maximum sea-ice cover smaller than normal. The August CIL was warmer and thinner in 2016 than in 2015 with conditions similar to those of 1999. The Gilbert and Pettigrew index which considers data from earlier in the season was warmer than in 2015 by a similar amount, and similar to the 2005 index.

MAGDALEN SHALLOWS JUNE SURVEY

A long-standing assessment survey covering the Magdalen Shallows has taken place in June for mackerel assessments and was since merged with the June AZMP survey. This survey provides good coverage of the temperature conditions that are greatly influenced by the cold intermediate layer that reaches the bottom at roughly half of the surface area at this time of the year.

Near-surface waters warm quickly in June, mid-way between the winter minimum and the annual maximum in early August. This can introduce a bias if the survey dates are not the same each year. To account for this, the seasonal warming observed at the Shediac Valley AZMP monitoring station was evaluated. A linear regression was performed of temperature versus time for each meter of the water column for each year with monitoring data at Shediac Valley between May and July. Visual inspection showed that the depth-dependent warming rate was fairly constant for all years and an average was computed for every depth. Warming is maximal at the surface at 18°C per 100 days and, in spite of some uncertainties between 30 and 55 m, decreases almost proportionally with depth to reach 2°C per 100 days at 40 m, followed by a further linear decrease to reach 1°C per 100 days at 82 m (Galbraith and Grégoire 2015).

All available temperature profiles taken in June from a given year are binned at 1 m depth intervals (or interpolated if the resolution is too coarse) and then adjusted according to the sampling date to offset them to June 15th according to the depth-dependent warming rate extracted from Shediac Valley monitoring data. An interpolation scheme is used to estimate temperature at each 1 m depth layer on a 2 km resolution grid. Fig. 50 shows temperatures and anomalies at depths of 20, 30 and 50 m. Fig. 51 shows averages over the grids at 0, 10, 20, 30, 50 and 75 m for all years when interpolation was possible, as well as SST June averages since 1985, for both western and eastern regions of the Magdalen Shallows (Fig. 22). Temperatures were on average below-normal at 10 to 50 m and above-normal at 75 m (Figs. 50 and 51).

BOTTOM WATER TEMPERATURES ON THE MAGDALEN SHALLOWS

Bottom temperature is also estimated at each point of the grids constructed from the June survey by looking up the interpolated temperature at the depth level corresponding to a bathymetry grid provided by the Canadian Hydrographic Service with some corrections applied (Dutil et al. 2012). The method is fully described in Tamdrari et al. (2012). A climatology was constructed by averaging all available temperature grids between 1981 and 2010 and anomaly grids were computed for each year. The June bottom temperature climatology as well as the 2016 reconstructed temperature and anomaly fields are shown in Fig. 52. The same method was applied using the available CTD data from August and September, thus including the multispecies surveys for the northern Gulf in August and for the Magdalen Shallows in September. These results are also shown in Fig. 52. While much of the deeper bottom water temperatures are climatologically still below 0°C in June, a remnant from the winter near-freezing mixed layer that reached the bottom, most of the area usually warms to below 1°C by August-September. Temperature anomalies in coastal shallow waters range from <-2.5°C to >+2.5°C, but anomalies tend to be of smaller magnitude in deeper waters.

Time series of the bottom area covered by water in various temperature intervals were estimated from the gridded data for the June surveys as well as for the September multispecies survey on the Magdalen Shallows (Fig. 53). The time series of areas of the Magdalen Shallows covered by water colder than 0, 1, 2, and 3°C in June and September are also shown in Fig. 49 as part of the CIL summary. Almost none of the bottom of the Magdalen Shallows was covered by water with temperatures <-1°C in June 2016 and very little of it was covered by water with temperatures <0°C by August-September; these are nevertheless colder conditions than during

the recent 2010-2013 period. The area covered by water temperatures <1°C in September had reached a low not seen since 1982 in 2012, but rebounded to near-normal in 2014 and 2015, and were again above-normal in 2016. At higher threshold temperatures, areas with T< 2°C and < 3°C were near-normal in both June and September 2016 (Fig. 49). The thermograph network (Fig. 29) also showed bottom temperatures at Shediac Valley (86 m) to be well above-normal (using a different reference period) from May through October.

DEEP WATERS (>150 M)

The deeper water layer (>150 m) below the CIL originates at the entrance of the Laurentian Channel at the continental shelf and circulates towards the heads of the Laurentian, Anticosti, and Esquiman channels without much exchange with the upper layers. The layer from 150 to 540 m is characterized by temperatures between 1 and >7°C and salinities between 32.5 and 35 (except for Mécatina Trough where near-freezing waters may fill the basin to 235 m in winter and usually persist throughout the summer). Interdecadal changes in temperature, salinity, and dissolved oxygen of the deep waters entering the Gulf at the continental shelf are related to the varying proportion of the source cold–fresh and high dissolved oxygen Labrador Current water and warm–salty and low dissolved oxygen slope water (McLellan 1957, Lauzier and Trites 1958, Gilbert et al. 2005). These waters travel from the mouth of the Laurentian Channel to the Estuary in roughly three to four years (Gilbert 2004), decreasing in dissolved oxygen from in situ respiration and oxidation of organic material as they progress to the channel heads. The lowest levels of dissolved oxygen (around 20 percent saturation in recent years) are therefore found in the deep waters at the head of the Laurentian Channel in the Estuary.

BOTTOM WATER TEMPERATURES IN AUGUST AND SEPTEMBER

The same method used to calculate bottom water temperature on the Magdalen Shallows was applied to the entire Gulf by combining all available CTD data from August and September, thus including the multispecies surveys for the northern Gulf in August and for the Magdalen Shallows in September into a single map (Fig. 54). All of the Gulf deep bottom water temperatures were above normal, with large areas of Anticosti and Esquiman Channels above 6°C, spreading into the northwest Gulf on the flanks of the Laurentian Channel.

Time series of the bottom area covered by water in various temperature intervals were also estimated for the other regions of the Gulf based on August-September temperature profile data (Figs. 55 and 56). Many areas had bottom waters colder than 0°C, and Mécatina Trough had bottom waters colder than -1°C. The figures also show compression of the bottom habitat area in the temperature range of 5–6°C in 1992, offset by larger 5–6°C habitat. In 2012, a return of >6°C temperatures to the sea floor began. By 2015, it had caused a large decrease of the 5–6°C habitat in Anticosti and Esquiman Channels. The area decreased a bit in these Channels in 2016, but increased sharply in Central Gulf and made its first appearance in the northwest Gulf.

The warm waters found at the bottom of Esquiman Channel and elsewhere are associated with the deep temperature maximum evident in the temperature profiles in these areas (e.g. Fig. 3). The progression from a cold anomaly within the Gulf in 2009 to current conditions of the deep temperature maximum is shown on Fig. 57. In 2012, 2015 and again in 2016, temperatures above 7°C were recorded in the Gulf near Cabot Strait. The Gulf-wide average and regional areal averages are shown in Fig. 58 for temperature and in Fig. 59 for salinity and dissolved oxygen. The deep maximum temperature Gulf-wide average was at a series record high in 2016, at 6.26°C, however the regional averages for Anticosti Channel and Esquiman Channel decreased from record highs set in 2015.

TEMPERATURE AND SALINITY MONTHLY MEANS

Monthly temperature and salinity averages were constructed for various depths using a method used by Petrie et al. (1996) but using the geographical regions shown in Fig. 2. In this method, all available data obtained during the same month within a region and close to each depth bin are first averaged together for each year. Monthly averages from all available years and their standard deviations are then computed. This two-fold averaging process reduces the bias that occurs when the numbers of profiles in any given year are different. These monthly averages were further averaged into regional yearly time series that are presented in Figs. 58 (temperature) and 59 (salinity) for 200 and 300 m. The 300 m observations in particular suggest that temperature anomalies are advected up-channel from Cabot Strait to the northwestern Gulf in two to three years, consistent with the findings of Gilbert (2004). The regional averages are weighted into a Gulf-wide average in accordance to the surface area of each region at the specified depth. These Gulf-wide averages are shown for 150, 200 and 300 m in Figs. 58-60. Linear trends in temperature and salinity at 300 m of 2.2°C and 0.3 per century, respectively are shown on Fig. 60 (See also Galbraith et al. 2013 for other long term trends).

In 2016, the gulf-wide average salinities decreased at all depths shown in Figs. 59 and 60 from 2015 levels but remained above-normal at 200, 250 and 300 m. Temperature decreased from 2015 record highs at 150 and 200 m, remaining above-normal (3.5°C, +2.1 SD and 5.3°C, +2.1 SD) but increased to new record levels at 250 (6.1°C, +2.9 SD) and 300 m (6.2°C, +4.4 SD). At 300 m, temperature increased to regional record highs in all deep regions of the Gulf: Estuary (5.5°C, +2.3 SD), Northwest Gulf (5.9°C, +3.4 SD), Central Gulf (6.3°C, +4.1 SD) and Cabot Strait (6.5°C, +3.4 SD).

The warm anomaly present since 2010 at Cabot Strait has been progressing up the channel towards the Estuary since then, but waters that have followed into the gulf have also remained very warm and even increased in temperature such that the average overall temperature may continue to increase (Fig. 57). The potential for still warmer waters entering the Gulf exists, as evidenced by an average temperature of 9.2°C observed at the Laurentian Mouth at 200 m in 2016 (Fig. 58), a record since the series began in 1914.

DISSOLVED OXYGEN AND HYPOXIA IN THE ST. LAWRENCE ESTUARY

Fig. 60 shows an update of the Gilbert et al. (2005) oxygen time series of the mean dissolved oxygen value at depths ≥295 m in the St. Lawrence Estuary. The value of 100 µmol l^{-1} corresponds approximately to 30% saturation, below which is considered to be hypoxic. Since some of the variability is associated with changing water masses, the temperature at 300 m in the Estuary is also shown. The deep waters of the Estuary were briefly hypoxic in the early 1960s and have consistently been hypoxic since 1984. Dissolved oxygen decreased to its lowest annual average in 2016, at 54.1 µmol l^{-1} (-1.7 SD), corresponding to 18% saturation (Fig. 59).

Based on interdecadal variability, the inflow of warmer waters to the Estuary is expected to deteriorate the hypoxic conditions since these waters are typically poorer in dissolved oxygen (McLellan 1957, Lauzier and Trites 1958, Gilbert et al. 2005). Although other factors are at play in the determination of dissolved oxygen of the waters that enter the Gulf of St. Lawrence, such as temporal changes in source water masses or of bacterial activity, a change of dissolved oxygen of 147.4 µmol l^{-1} was accounted for by a 10.09°C temperature difference in source water masses in Gilbert et al 2005, implying that a decrease of 1.46 µmol l^{-1} might be expected for each 0.1°C temperature increase observed at Cabot Strait from variability of the mixing ratio of source waters. Recent interannual variability in the Gilbert et al. 2005 updated time series had not shown changes in dissolved oxygen that would have been expected to be associated with

the increases in temperature. However during the last three years, the dissolved oxygen concentration decrease (-12.1 µmol l^{-1}) has been greater than expected considering the observed warming of Estuary bottom waters. The correlation between the temperature and oxygen timeseries in the St. Lawrence Estuary (bottom panel of Fig. 60) explains 74% of the variance (R^2 = 0.74). Other factors that can cause oxygen variability include interannual changes in the vertical flux of organic matter to the bottom waters of the Lower St. Lawrence Estuary.

Dissolved oxygen obtained using sensors on CTD profilers are shown for 300-m regional averages in Fig. 59 and show a strong decrease in the Gulf in 2016, reaching the lowest observed values since 2000 in all regions.

SEASONAL AND REGIONAL AVERAGE TEMPERATURE STRUCTURE

In order to show the seasonal progression of the vertical temperature structure, regional averages are shown in Figs. 61 to 64 based on the profiles collected during the March helicopter survey, the June AZMP and mackerel surveys, the August multi-species survey (September survey for the Magdalen Shallows), and the October-November AZMP survey. All additional archived CTD data for those months were also used. The temperature scale was adjusted to highlight the CIL and deep-water features; the display of surface temperature variability is best suited to other tools such as remote sensing and thermographs. Average discrete depth layer conditions are summarized for the months of the 2015 and 2016 AZMP surveys in Fig. 65 for temperature and in Fig. 66 for salinity and 0-50 m stratification. For each survey the anomalies were computed relative to monthly temperature and salinity 1981-2010 climatologies calculated for each region, shown in grey as the mean value ± 0.5 SD in Figs. 61 to 64.

Caution is needed in interpreting the March profiles. Indeed, regional averaging of winter profiles does not work very well in the northeast Gulf (regions 3 and 4) because very different water masses are present in the area such as the cold Labrador Shelf intrusion with saltier and warmer deeper waters of Anticosti Channel or Esquiman Channel. For example, the sudden temperature changes near the bottom of Mécatina Trough resulted from the deepest cast used in each of the averages, which contained warmer than surrounding waters in 2015 and colder waters in 2016. The highlights of March water temperatures shown in Fig. 61 include the previously discussed winter mixed layer, with near-freezing temperatures in the northwest and above-normal southeast of Anticosti Island. The thermocline was much shallower than usual in most regions, associated with temperatures well above normal at 200 m although not as pronounced as in 2015. Waters in the deepest parts of Mécatina Trough were near-freezing, indicating renewal from a Labrador Shelf intrusion. Deep water masses in Mécatina Trough changed from June to August, showing considerable warming.

Temperatures in June and August 2016 were characterized by CIL conditions that were typically below normal in thickness. The CIL temperature minimum was usually high in the Estuary. Deep-water temperatures were above normal in all regions along the Laurentian Channel, with most regions showing increases compared with 2015 conditions in waters deeper than 250 m depth. Temperatures at the depth of the temperature maximum (200 to >250 m) remained above normal in Esquiman Channel and central Gulf, exceeding 6°C at depth, presumably advected in from the Cabot Strait recent record-high conditions. Temperatures exceeded 7°C around 250 m in Cabot Strait in the Fall and were generally very warm to 350 m.

CURRENTS AND TRANSPORTS

Currents and transports are derived from a numerical model of the Gulf of St. Lawrence, Scotian Shelf, and Gulf of Maine. The model is prognostic, i.e., it allows for evolving temperature and salinity fields. It has a spatial resolution of 1/12° with 46 depth-levels in the vertical. The atmospheric forcing is taken from the Global Environmental Multiscale (GEM) model running at the Canadian Meteorological Center (CMC). Freshwater runoff is obtained from observed data and the hydrological model, as discussed in the freshwater runoff section. A simulation was run for 2006–2016 from which transports were calculated. The reader is reminded that the results outlined below are not measurements but simulations and improvements in the model may lead to changes in the transport values.

Figs. 67–69 show seasonal depth-averaged currents for 0–20 m, 20–100 m, and 100 m to the bottom for 2016. Currents are strongest in the surface mixed layer, generally 0–20 m, except in winter months when the 20–100 m and the 100m to bottom averages are almost as high (note the different scale for this depth). Currents are also strongest along the slopes of the deep channels. The Anticosti Gyre is always evident but strongest during winter months, when it even extends strongly into the bottom-average currents.

Monthly averaged transports across seven sections of the Gulf of St. Lawrence are shown in Fig. 70 for sections with estuarine circulation, and in Fig. 71 for sections where only net transports are relevant. In Fig. 70, the net transport integrates both up and downstream circulation and, for example, corresponds to freshwater runoff at the Pointe-des-Monts section. The outflow transport integrates all currents heading toward the ocean, while the estuarine ratio corresponds to the outflow divided by the net transports.

Transports through sections under the direct estuarian influence of the St. Lawrence River (e.g., Pointe-des-Monts) have a more direct response to change in freshwater runoff while others (e.g., Cabot Strait, Bradelle Bank) have a different response, presumably due to redistribution of circulation in the GSL under varying runoff. The estuarine circulation ratio is determined by the mixing intensities within the estuary and is greatly influenced by stratification. It is on average greatest during winter months and weakest during the spring freshet. In fact, it is sufficiently reduced in spring that the overall outward transport at Pointe-des-Monts reaches its minimum value in June even though this month corresponds to the third highest net transport of the year, i.e. the estuary becomes sufficiently stratified that fresh water runoff tends to slip on top of the denser salty waters underneath. In 2016, the estuarine ratio at Pointe-des-Monts was below-normal during the May freshet but above-normal and higher in absolute value in June (11.6 vs 7.3 in May), leading to greater outward transport at the Pointe-des-Monts section in June than in May (e.g. via enhanced estuarine entrainment).

HIGH FREQUENCY SAMPLING AZMP STATIONS

Sampling by the Maurice Lamontagne Institute began in 1991 at a station offshore of Rimouski (48° 40' N 68° 35' W, 320 m depth; Plourde et al. 2009), typically once a week during summer and less often during spring and fall and almost never in winter (Fig. 72). In 2013, following several analyses that identified good correlations and correspondences between the prior AZMP Anticosti Gyre and Gaspé Current stations with the Rimouski station, it was decided to drop sampling efforts at these logistically difficult stations and integrate the Rimouski station officially in the AZMP program and begin winter sampling there when opportunities arose. The AZMP station in the Shediac Valley (47° 46.8' N, 64° 01.8' W, 84 m depth) is sampled on a regular basis by the Bedford Institute of Oceanography as well as occasionally by DFO Gulf Region and by the Maurice Lamontagne Institute during their Gulf-wide surveys (Fig. 72). This station has been sampled irregularly since 1947, nearly every year since 1957, and more

regularly during the summer months since 1999 when the AZMP program began. However, observations were mostly limited to temperature and salinity prior to 1999. In 2016, an oceanographic buoy equipped with an automatic temperature and salinity profiler was deployed at Shediac Valley station and carried out 866 casts between May 25 and October 31.

Isotherms and isohalines as well as monthly averages of layer temperature and salinity, stratification, and CIL core temperature and thickness at <1°C are shown for 2012-2016 for the Rimouski station in Fig. 73 and for the Shediac Valley station in Fig. 74. The scorecard climatologies are calculated from 1991-2010 data for Rimouski station, and for 1981-2016 for Shediac Valley (The time span of the climatology is extended at Shediac Valley because of the sparseness of data prior to 1999).

At the Rimouski station in 2016, the CIL typically had much below-normal thickness and above-normal minimum temperature, with higher anomalies than those prevailing in the Gulf. At 200-300 m, the gradual shift of cold-fresh waters present in 2010 to warmer-saltier waters advected from Cabot Strait lead to a shift to warm anomalies by May 2013 and series records in temperature (5.63°C) observed in September of 2016. The thermograph network also shows a Rimouski station series record of the daily average temperature (since 2005) of 5.79°C occurring in September (not shown), and a record-high monthly average of 5.63°C (Figs. 27 and 33).

A mooring measuring temperature and salinity at multiple depths has been was deployed at Shediac Valley station since June 2015, and the data from September 2016 are currently available. Because of the sparse winter sampling at this station, the monthly averages at 20, 30 and 75 m of Fig. 74 were calculated using the mooring for months when the automatic buoy was not in operation. This eliminated strong anomalies that would have been estimated for the shallower depths but did not alter the anomalies significantly at 75 m. Temperatures were generally near-normal at Shediac Valley station over the season.

Fig. 75 shows the interannual variability of some bulk layer averages from May to October for the two stations. Both bulk surface layer temperatures, as well as near-bottom temperature and CIL minimum temperature were record highs at Rimouski station. Stratification was normal and bulk surface salinity was below-normal. Bulk surface layer temperatures and near-bottom temperature were above-normal at Shediac Valley station in 2016, while stratification and bulk surface salinity were normal.

OUTLOOK FOR 2017

Air temperatures were respectively 2.4°C and 1.3°C above-normal over the Gulf in January and February 2017. This was the setting for the March 2017 survey, which provides an outlook for CIL conditions expected for the remainder of 2017. Fig. 76 shows the surface mixed layer temperature, salinity, and thickness (at T<-1°C and T<0°C), as well as the thickness and extent of the cold and saline layer that has intruded into the Gulf from the Labrador shelf. A smaller portion of the winter mixed layer was warmer (above -1°C) than in March 2016. The overall thickness and volume of the layer colder than -1°C was normal and the Cold Intermediate Layer for summer 2017 is therefore forecasted to be colder than in 2016, with a Gilbert and Pettigrew (1997) index of around -0.21°C compared to -0.10°C in 2015.

Concerning deep waters, recall that record high temperatures have been recorded in Cabot Strait since 2012, and that overall the Gulf waters at 250 m and 300m m were in 2016 at a 100+ year record high. There were 19 stations sampled in March 2017 with some deep-water temperatures greater than 6°C, located from Cabot Strait up to the Northwest Gulf. One Cabot

Strait station had a deep temperature maximum that reached 7.43°C. This signifies the continuation of warmer than normal conditions at depth.

SUMMARY

Fig. 77 summarizes SST, summertime CIL and deep-water average temperatures. For May-November SST, a proxy is used prior to 1985 using the April-November air temperature anomaly averaged over all stations of Fig. 4 except the two from the Estuary, similar to the index developed in Galbraith et al. (2012). For August SST, the proxy is based on July and August air temperatures. While May-November SST and August SST are well correlated (R^2 = 0.57 for the 1985-2016 AVHRR record), the August SST reached in 2012 and 2014 were very high anomalies compared the May-November averages, while in 2006 the reverse was found to be the case.

Fig. 77 shows a slight increase from 2015 values for May-November average SST, average temperature at 300 m as well as for the CIL temperature minimum, but decreases for the August SST and average temperature at 150 m and 200 m. The SST was above-normal (10.2°C and +0.9 SD), temperature at 300 m was the highest on record (6.2°C, +4.4 SD). The CIL temperature minimum was above-normal (+1.0 SD), consistent with above normal winter air temperatures (+1.5°C, +1.0 SD).

Another summary of the temperature state of the Gulf of St. Lawrence over a shorter time span (since 1971) allows the inclusion of more data sets, and three sets of four time series are chosen to represent surface, intermediate and deep conditions (Fig. 78). Here, sea-ice is grouped as an intermediate feature since all are associated with winter formation. Fig. 78 shows the sums of these three sets of anomalies representing the state of different parts of the system and is reproduced on Fig. 79 with each time series contribution shown as stacked bars (Petrie et al. 2007). These composite indices measure the overall state of the climate system with positive values representing warm conditions and negative representing cold conditions. The plot also indicates the degree of correlation between the various measures of the environment. In 2016, the surface and intermediate index were above-normal at +0.7 SD and +1.5 SD respectively, and the deep index decreased slightly to its second highest value record after the 2015 record high.

KEY FINDINGS

- The annual average runoff from the St. Lawrence River measured at Québec City and RIVSUM II were respectively normal and above-normal in 2016 (12,400 m^3s^{-1}, +0.5 SD and 17,600 m^3s^{-1}, +0.6 SD respectively). The spring freshet was normal at +0.1 SD in April for the St. Lawrence River but above-normal at +0.7 SD in May for RIVSUM II. Its timing was normal.
- The (simulated) estuarine ratio at Pointe-des-Monts was below-normal during the May freshet but above-normal and higher in absolute value in June, leading to greater outward transport at the Pointe-des-Monts section in June than in May.
- Air temperatures were above-normal, in winter (December-March) by +1.5°C (+1.0 SD), April to November by +0.4°C (+0.6 SD), and annual by +0.5°C (+0.5 SD).
- The winter surface mixed cold layer (<- 1°C) volume of 10 300 km^3 was 0.5 SD below the 1996–2016 average. The Labrador Shelf water intrusion into Mécatina Trough was below normal in March 2016, representing only 5% (-0.9 SD) of the cold water in the Gulf.

- Sea ice maximum volume was third lowest since 1969 at 14 km³ (-1.8 SD). Five of the seven lowest maximum ice volumes of the time series have occurred in the previous seven years.
- The August cold intermediate layer (CIL) showed much warmer (+1.4 SD) and thinner (-2.1 SD for volume colder than 1°C) than normal. The Gilbert and Pettigrew minimum temperature index, which includes data over a longer season, was also above-normal (+0.8 SD).
- In 2016, the timing of summer onset and post-season cooling were normal. The Estuary, had longer than normal seasons with surface temperature above 10°C (9.8 weeks compared to the 6.9 week average), while other regions had near-normal durations.
- Near-surface water temperatures were near normal or above normal from May to November 2016, leading to an above-normal May-November average (+0.6°C, +0.9 SD). The May to November average was however at a record high (since 1985) for the Estuary (+1.4°C, +2.4 SD). Record highs were reached in November averaged over the Gulf (6.1°C, above normal by +1.7°C and 2.2 SD) and in the following regions: Estuary (+1.8°C, +2.2 SD), Northwest Gulf (+1.9°C, +2.1 SD), Esquiman Channel (+2.5°C, +2.2 SD), Cabot Strait (+2.2°C, +2.5 SD) and Magdalen Shallows (+2.0°C, +2.5 SD).
- Water masses in Mécatina Trough were exchanged more frequently than usual.
- Deep water temperatures have been increasing overall in the Gulf, with inward advection from Cabot Strait where temperature had reached a record high (since 1915) in 2012 at 200 m. Temperature decreased from 2015 record highs at 150 and 200 m, remaining above-normal (3.5°C, +2.1 SD and 5.3°C, +2.1 SD) but increased to new record levels at 250 (6.1°C, +2.9 SD) and 300 m (6.2°C, +4.4 SD). At 300 m, temperature increased to regional record highs in all deep regions of the Gulf: Estuary (5.5°C, +2.3 SD), Northwest Gulf (5.9°C, +3.4 SD), Central Gulf (6.3°C, +4.1 SD) and Cabot Strait (6.5°C, +3.4 SD).
- Bottom area covered by waters warmer than 6°C finally decreased in 2016 in Anticosti Channel and Esquiman Channel, but increased sharply in Central Gulf and made its first appearance in the northwest Gulf.

ACKNOWLEDGEMENTS

We are grateful to the people responsible for CTD data acquisition during the surveys used in this report:

- Rimouski station monitoring: Roger Pigeon, Félix St-Pierre, Michel Rousseau, Sylvain Chartrand, Lily St-Amand, Line McLaughlin, Marie-Lyne Dubé, Yves Gagnon, Rémi Desmarais, François Villeneuve, Caroline Lafleur, Peter Galbraith, Isabelle St-Pierre, Laure Devine, Paul Nicot, Jean-Yves Couture, Brian Boivin, Sonia Michaud, David Leblanc, Caroline Lebel
- March survey: Peter Galbraith, Caroline Lafleur, Rémi Desmarais, Pierre Joly, Yves Gagnon, Félix St-Pierre; the officers and crew of the CCGS Martha L. Black and CCGS Edward Cornwallis.
- June AZMP transects: Yves Gagnon, Michel Rousseau, Marie-Lyne Dubé, François Villeneuve, Johanne Guérin, Isabelle St-Pierre, Rémi Desmarais, Linda Girard, Mélanie Boudreau, Élisabeth Van Beveren; the officers and crew of the CCGS Teleost.
- August Multi-species survey: Sylvain Chartrand, Caroline Lafleur, Félix St-Pierre, David Leblanc; the officers and crew of the CCGS Teleost.
- October-November AZMP survey:, Yves Gagnon, Félix St-Pierre, Sylvain Chartrand, , François Villeneuve, Sonia Michaud, Caroline Lafleur, Marie-Lyne Dubé, Roger Pigeon,

Rémi Desmarais, Isabelle St-Pierre, Brian Boivin; the officers and crew of the CCGS Hudson.
- September Multi-species survey: Luc Savoie for providing the CTD data.
- Northumberland Strait survey: Chief scientists Mark Hanson and Joël Chassé.
- Data management: Laure Devine, Caroline Lafleur, Isabelle St-Pierre, Brian Boivin.

CTD maintenance: Roger Pigeon, Félix St-Pierre, Michel Rousseau, Sylvain Chartrand. Data from the following sources are also gratefully acknowledged:

- Air temperature: Environment Canada.
- Sea-ice: Canadian Ice Service, Environment Canada. Processing of GIS files by Paul Nicot.
- Runoff at Québec City: Denis Lefaivre.
- Runoff from hydrological modelling: Joël Chassé and Diane Lavoie.
- Thermograph network: Bernard Pettigrew, Rémi Desmarais, Félix St-Pierre.
- Historical AVHRR SST remote sensing (IML): Pierre Larouche, Bernard Pettigrew.
- AVHRR SST remote sensing (BIO): Carla Caverhill.
- All figures were made using the free software Gri (Kelley and Galbraith 2000).

We are grateful to David Hebert and Frédéric Cyr for reviewing the manuscript and providing insightful comments.

REFERENCES

Benoît, H.P., Savenkoff, C., Ouellet, P., Galbraith, P.S., Chassé, J. and Fréchet, A. 2012. Impacts of fishing and climate-driven changes in exploited marine populations and communities with implications for management, in State-of-the-Ocean Report for the Gulf of St. Lawrence Integrated Management (GOSLIM) Area, H. P. Benoît, J. A. Gagné, C. Savenkoff, P. Ouellet and M.-N. Bourassa, Eds. Can. Manuscr. Rep. Fish. Aquat. Sci. 2986: viii + 73 pp.

Bourgault, D., and Koutitonsky, V.G. 1999. Real-time monitoring of the freshwater discharge at the head of the St. Lawrence Estuary. Atmos. Ocean, 37 (2): 203–220.

Colbourne, E., Holden, J., Senciall, D., Bailey, W., Snook, S., and Higdon, J. 2016. Physical Oceanographic Conditions on the Newfoundland and Labrador Shelf during 2015. DFO Can. Sci. Advis. Sec. Res. Doc. 2016/079. v +40 p.

Cyr, F., Bourgault, D., and Galbraith, P. S. 2011. Interior versus boundary mixing of a cold intermediate layer. J. Gephys. Res. (Oceans), 116, C12029, doi:10.1029/2011JC007359.

Dutil, J.-D., Proulx, S., Galbraith, P.S., Chassé, J., Lambert, N., and Laurian, C. 2012. Coastal and epipelagic habitats of the estuary and Gulf of St. Lawrence. Can. Tech. Rep. Fish. Aquat. Sci. 3009: ix + 87 p.

Galbraith, P.S. 2006. Winter water masses in the Gulf of St. Lawrence. J. Geophys. Res., 111, C06022, doi:10.1029/2005JC003159.

Galbraith, P. S., et Grégoire, F. 2015. Habitat thermique du maquereau bleu; profondeur de l'isotherme de 8 °C dans le sud du golfe du Saint-Laurent entre 1960 et 2014. Secr. can. de consult. sci. du MPO. Doc. de rech. 2014/116. v + 13 p.

Galbraith, P.S., and Larouche, P. 2011. Sea-surface temperature in Hudson Bay and Hudson Strait in relation to air temperature and ice cover breakup, 1985-2009. J. Mar. Systems, 87, 66-78.

Galbraith, P.S. and Larouche, P. 2013. Trends and variability in eastern Canada sea-surface temperatures. Ch. 1 (p. 1-18) In: Aspects of climate change in the Northwest Atlantic off Canada [Loder, J.W., G. Han, P.S. Galbraith, J. Chassé and A. van der Baaren (Eds.)]. Can. Tech. Rep. Fish. Aquat. Sci. 3045: x + 190 p.

Galbraith, P.S., Saucier, F.J., Michaud, N., Lefaivre, D., Corriveau, R., Roy, F., Pigeon, R., and Cantin, S. 2002. Shipborne monitoring of near-surface temperature and salinity in the Estuary and Gulf of St. Lawrence. Atlantic Zone Monitoring Program Bulletin, Dept. of Fisheries and Oceans Canada. No. 2: 26–30.

Galbraith, P.S., Desmarais, R., Pigeon, R., and Cantin, S. 2006. Ten years of monitoring winter water masses in the Gulf of St . Lawrence by helicopter. Atlantic Zone Monitoring Program Bulletin, Dept. of Fisheries and Oceans Canada. No. 5: 32–35.

Galbraith, P. S., Larouche, P., Gilbert, D., Chassé, J., and Petrie, B. 2010. Trends in sea-surface and CIL temperatures in the Gulf of St. Lawrence in relation to air temperature. Atlantic Zone Monitoring Program Bulletin, 9: 20-23.

Galbraith P.S., Larouche, P., Chassé, J., and Petrie, B. 2012. Sea-surface temperature in relation to air temperature in the Gulf of St. Lawrence: interdecadal variability and long term trends. Deep Sea Res. II, V77–80, 10–20.

Galbraith. P.S., Hebert, D., Colbourne, E., and Pettipas, R. 2013. Trends and variability in eastern Canada sub-surface ocean temperatures and implications for sea ice. Ch.5 In: Aspects of climate change in the Northwest Atlantic off Canada [Loder, J.W., G. Han, P.S. Galbraith, J. Chassé and A. van der Baaren (Eds.)]. Can. Tech. Rep. Fish. Aquat. Sci. 3045: x + 192 p.

Galbraith, P.S., Chassé, J., Caverhill, C., Nicot, P., Gilbert, D., Pettigrew, B., Lefaivre, D., Brickman, D., Devine, L., and Lafleur, C. 2016. Physical Oceanographic Conditions in the Gulf of St. Lawrence in 2015. DFO Can. Sci. Advis. Sec. Res. Doc. 2016/056. v + 90 p.

Gilbert, D. 2004. Propagation of temperature signals from the northwest Atlantic continental shelf edge into the Laurentian Channel. ICES CM, 2004/N:7, 12 pp.

Gilbert, D., and Pettigrew, B. 1997. Interannual variability (1948-1994) of the CIL core temperature in the Gulf of St. Lawrence. Can. J. Fish. Aquat. Sci., 54 (Suppl. 1): 57–67.

Gilbert, D., Sundby, B., Gobeil, C., Mucci, A., and Tremblay, G.-H. 2005. A seventy-two-year record of diminishing deep-water oxygen in the St. Lawrence estuary: The northwest Atlantic connection. Limnol. Oceanogr., 50(5): 1654–1666.

Hammill, M.O., and Galbraith, P.S. 2012. Changes in seasonal sea-ice cover and its effect on marine mammals, in State-of-the-Ocean Report for the Gulf of St. Lawrence Integrated Management (GOSLIM) Area, H. P. Benoît, J. A. Gagné, C. Savenkoff, P. Ouellet and M.-N. Bourassa, Eds. Can. Manuscr. Rep. Fish. Aquat. Sci. 2986: viii + 73 pp.

Hebert, D., Pettipas, R., Brickman, D., and Dever, M. 2016. Meteorological, sea ice and physical oceanographic conditions on the Scotian Shelf and in the Gulf of Maine during 2015. DFO Can. Sci. Advis. Sec. Res. Doc. 2016/083. v + 49 p.

Kalnay, E., Kanamitsu, M., Kistler, R., Collins, W., Deaven, D., Gandin, L., Iredell, M., Saha, S., White, G., Woollen, J., Zhu, Y., Chelliah, M., Ebisuzaki, W., Higgins, W., Janowiak, J., Mo, K., Ropelewski, C., Wang, J., Leetmaa, A., Reynolds, R., Jenne, R., and Josephé, D. 1996. The NCEP/NCAR 40-year reanalysis project. Bull. Am. Meteorol. Soc. 77, 437–470.

Kelley, D.E., and Galbraith, P.S. 2000. Gri: A language for scientific illustration, Linux J., 75, 92 101.

Lauzier, L.M., and Trites, R.W. 1958. The deep waters of the Laurentian Channel. J. Fish. Res. Board Can. 15: 1247–1257.

McLellan, H.J. 1957. On the distinctness and origin of the slope water off the Scotian Shelf and its easterly flow south of the Grand Banks. J. Fish. Res. Board. Can. 14: 213–239.

Petrie, B., Drinkwater, K., Sandström, A., Pettipas, R., Gregory, D., Gilbert, D., and Sekhon, P. 1996. Temperature, salinity and sigma-t atlas for the Gulf of St. Lawrence. Can. Tech. Rep. Hydrogr. Ocean Sci., 178: v + 256 pp.

Petrie, B., Pettipas, R. G., and Petrie, W. M. 2007. An overview of meteorological, sea ice and sea surface temperature conditions off eastern Canada during 2006. DFO Can. Sci. Advis. Sec. Res. Doc. 2007/022.

Pettigrew, B., Gilbert, D. and Desmarais, R. 2016. Thermograph network in the Gulf of St. Lawrence. Can. Tech. Rep. Hydrogr. Ocean Sci. 311: vi + 77 p.

Plourde, S., Joly, P., St-Amand, L., and Starr, M. 2009. La station de monitorage de Rimouski : plus de 400 visites et 18 ans de monitorage et de recherche. Atlantic Zone Monitoring Program Bulletin, Dept. of Fisheries and Oceans Canada. No. 8: 51-55.

Tamdrari, H., Castonguay, M., Brêthes, J.-C., Galbraith, P. S., and Duplisea, D. E. 2012. The dispersal pattern and behaviour of cod in the northern Gulf of St. Lawrence: results from tagging experiments, Can. J. of Fish. Aquat. Sci., 69: 112-121.

Therriault, J.-C., B. Petrie, P. Pépin, J. Gagnon, D. Gregory, J. Helbig, A. Herman, D. Lefaivre, M. Mitchell, B. Pelchat, J. Runge and D. Sameoto. 1998. Proposal for a Northwest Atlantic zonal monitoring program. Can. Tech. Rep. Hydrogr. Ocean Sci., 194: vii + 57 pp.

Vincent, L. A., Wang, X. L., Milewska, E. J., Wan, H., Yang, F., and Swail, V. 2012. A second generation of homogenized Canadian monthly surface air temperature for climate trend analysis. *J. Geophys. Res.* 117, D18110, doi:10.1029/2012JD017859.

FIGURES

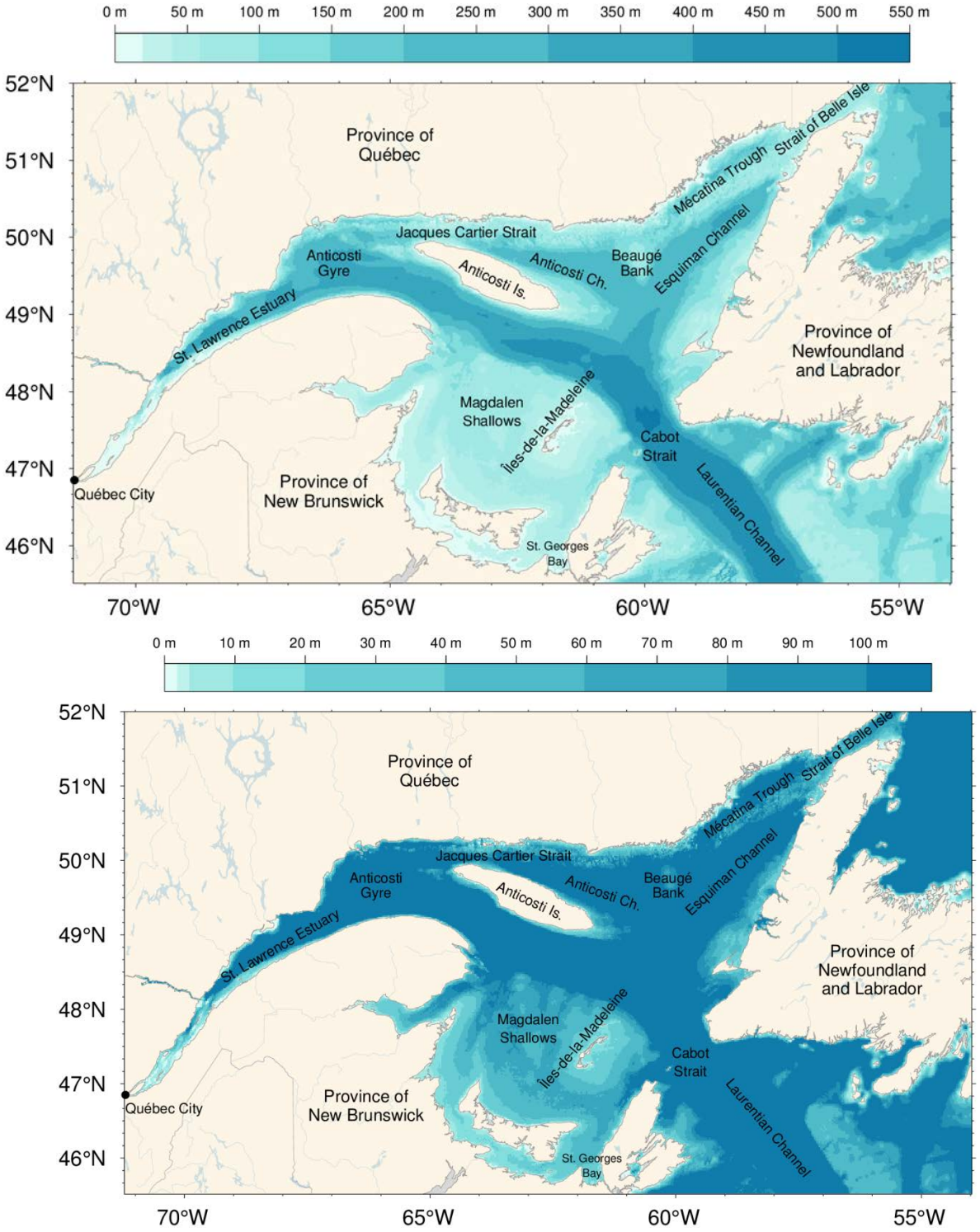

Figure 1. The Gulf of St. Lawrence. Locations discussed in the text are indicated. Bathymetry datasets used are from the Canadian Hydrographic Service to the west of 56°47' W (with some corrections applied to the baie des Chaleurs and Magdalen Shallows) and TOPEX data to the east. Bottom panel shows detail for 0-100 m bathymetry.

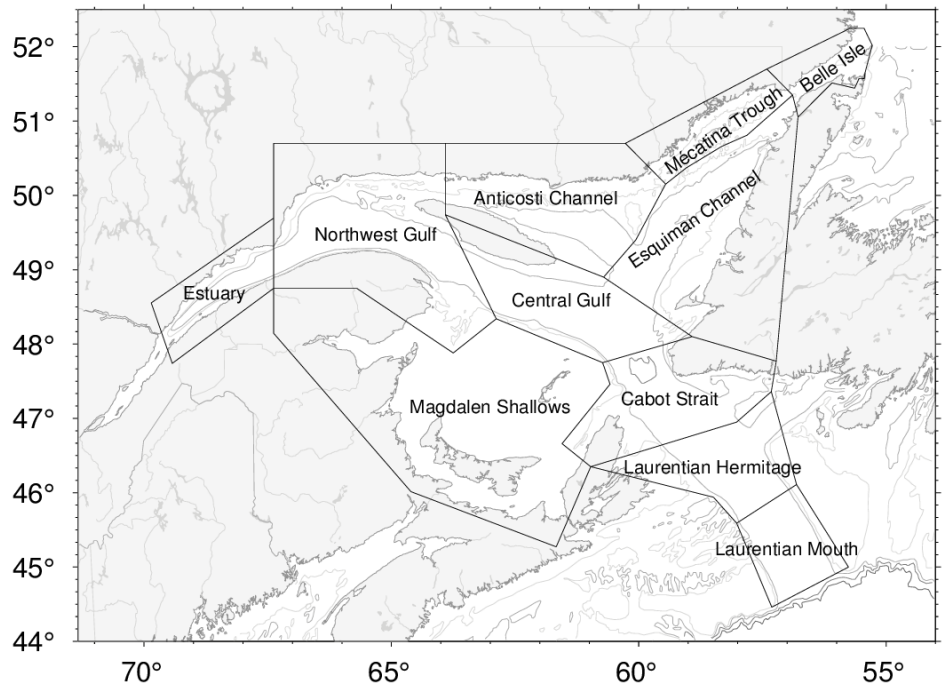

Figure 2. Gulf of St. Lawrence divided into oceanographic regions.

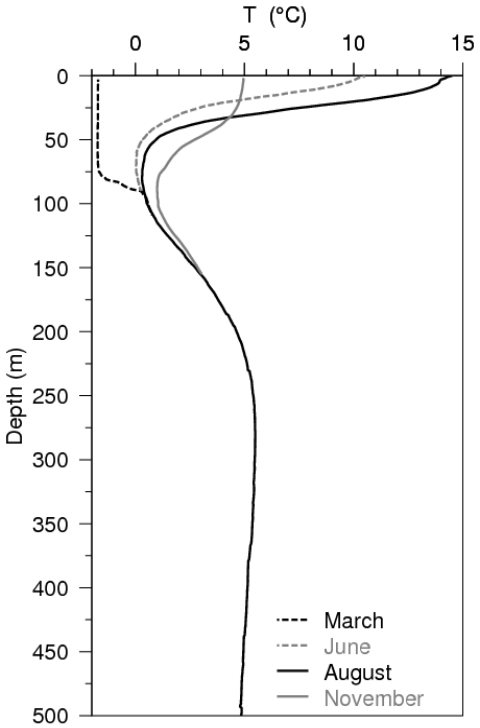

Figure 3. Typical seasonal progression of the depth profile of temperature observed in the Gulf of St. Lawrence. Profiles are averages of observations in August, June and November 2007 in the northern Gulf. The dashed line at left shows a single winter temperature profile (March 2008), with near freezing temperatures in the top 75 m. The cold intermediate layer (CIL) is defined as the part of the water column that is colder than 1°C, although some authors use a different temperature threshold. Figure from Galbraith et al. (2012).

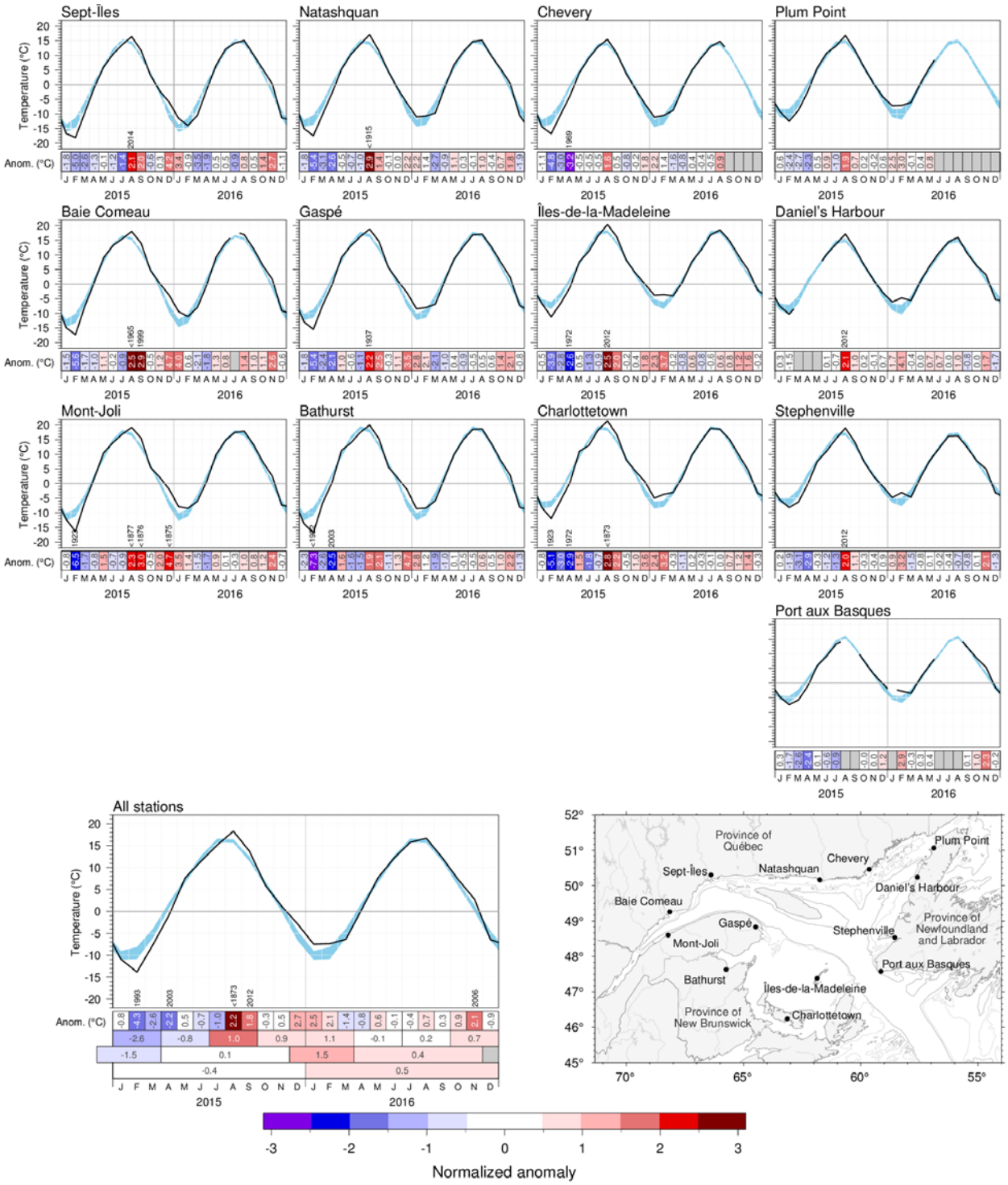

Figure 4. Monthly air temperatures and anomalies for 2015 and 2016 at selected stations around the Gulf as well as the average for all stations. The blue area represents the 1981–2010 climatological monthly mean ± 0.5 SD. Months with 4 or more days of missing data are omitted. The bottom scorecards are colour-coded according to the monthly normalized anomalies based on the 1981–2010 climatologies for each month, but the numbers are the monthly anomalies in ºC. For anomalies greater than 2 SD from normal, the prior year with a greater anomaly is indicated. Seasonal, December-March, April-November and annual anomalies are included for the all-station average.

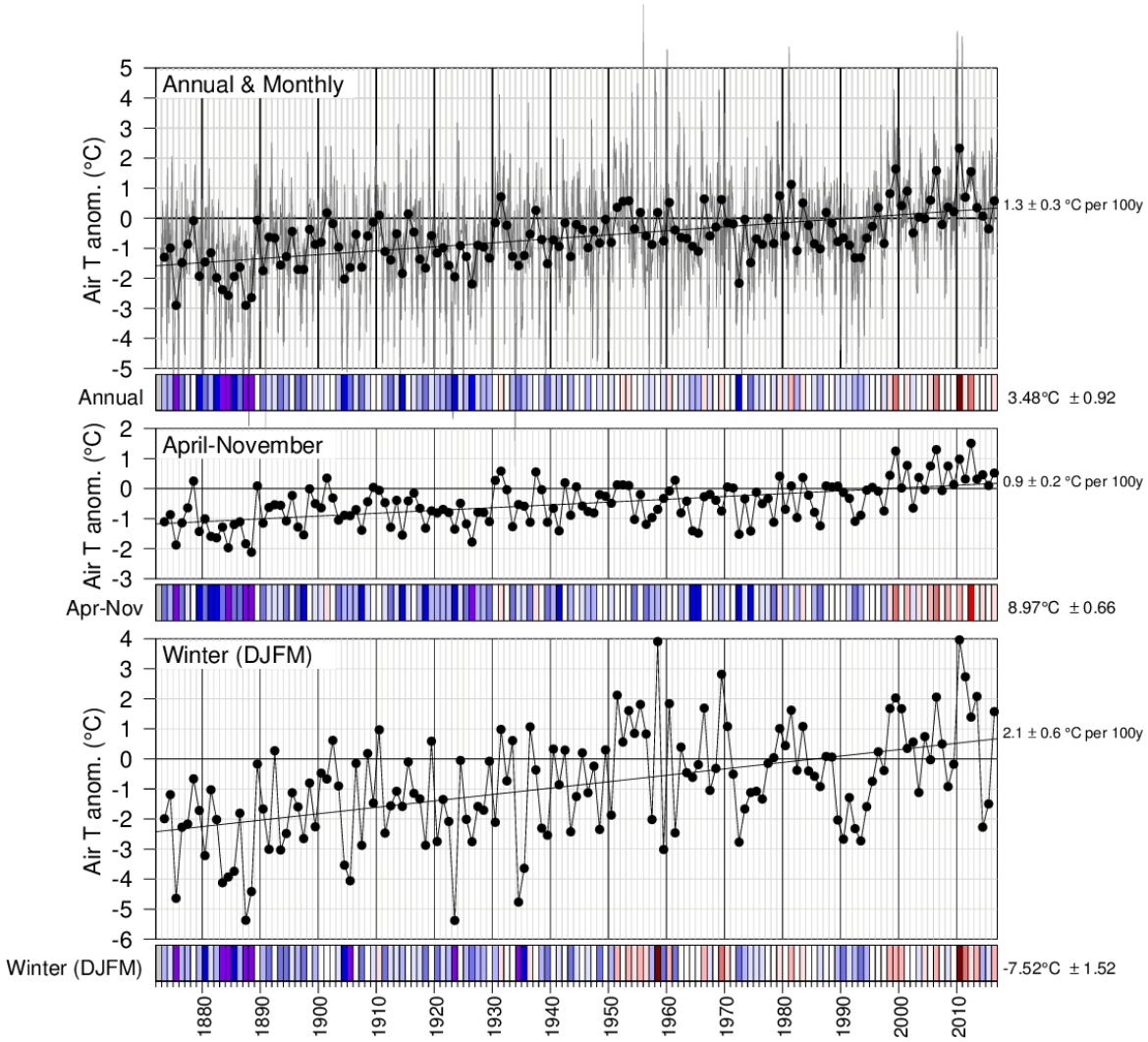

Figure 5. Annual, April-November December-March mean air temperature anomalies averaged for the selected stations around the Gulf from Fig. 4. The bottom scorecards are colour-coded according to the normalized anomalies based on the 1981–2010 climatology. Trends plus and minus their 95% confidence intervals are shown. April-November air temperature anomalies tend to be highly-correlated with May-November sea-surface temperature anomalies (Galbraith et al. 2012; Galbraith and Larouche 2013) whereas winter air temperature anomalies correlate highly with sea-ice cover parameters and winter mixed-layer volumes (Galbraith et al. 2010; Galbraith et al. 2013).

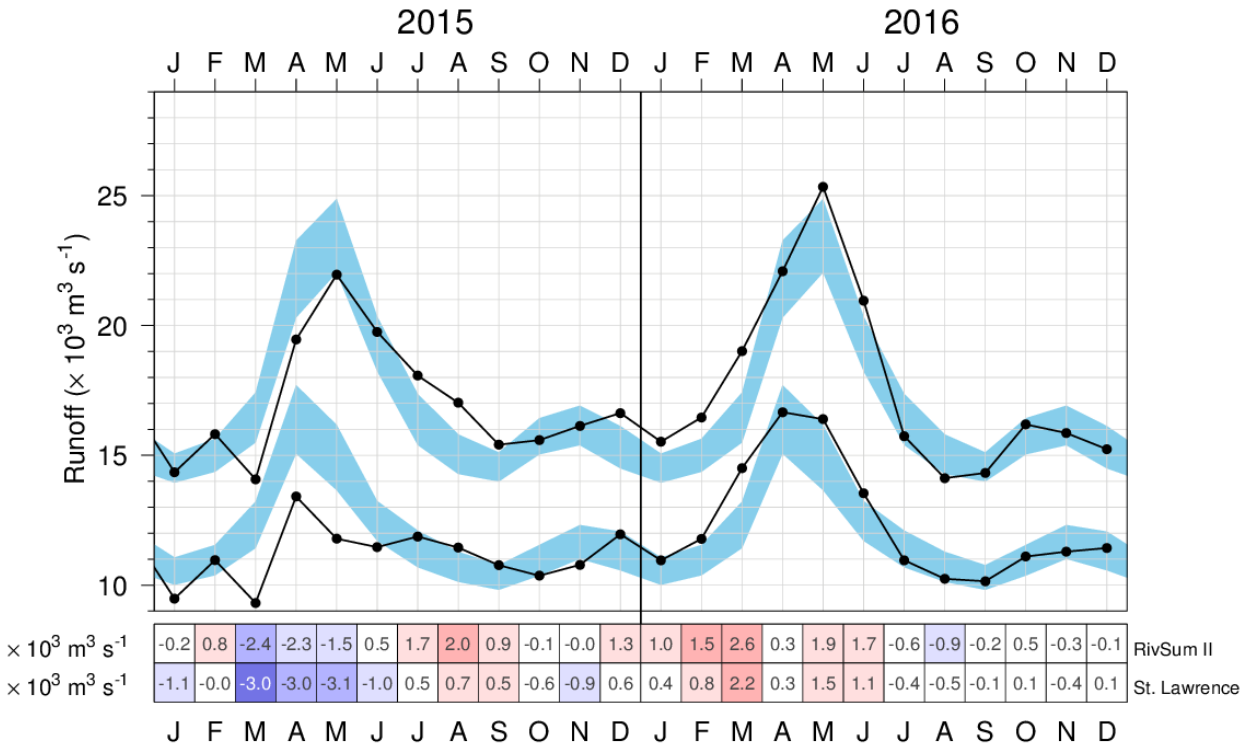

Figure 6. Monthly mean freshwater flow of the St. Lawrence River at Québec City (lower curve) and its sum with rivers flowing into the St. Lawrence Estuary (RIVSUM II, upper curve). The 1981–2010 climatological mean (± 0.5 SD) is shown (blue shading). The scorecards are colour-coded according to the monthly anomalies normalized for each month of the year, but the numbers are the actual monthly anomalies in 10^3 m^3s^{-1}.

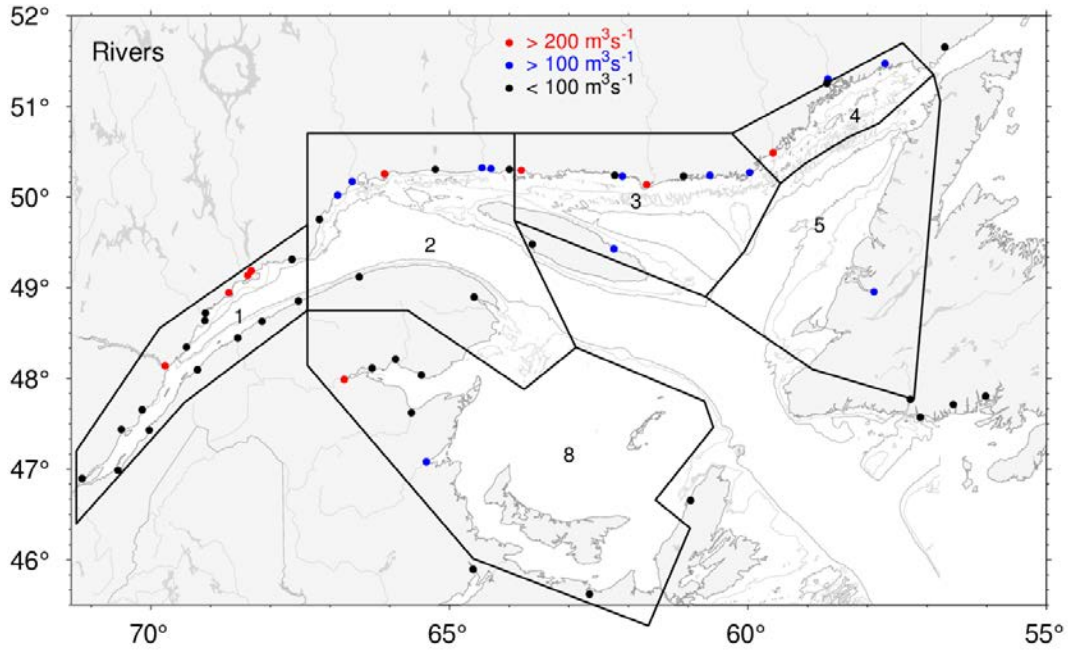

Figure 7. River discharge locations for the regional sums of runoffs listed in Table 2. Red and blue dots indicate rivers that have climatological mean runoff greater than 200 m^3s^{-1} and between 100 and 200 m^3s^{-1}, respectively.

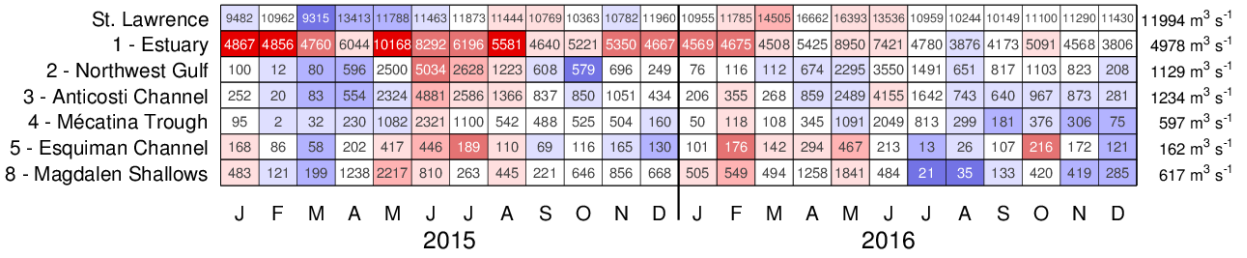

Figure 8. Monthly anomalies of the St. Lawrence River runoff and sums of all other major rivers draining into separate Gulf regions for 2015 and 2016. The scorecards are colour-coded according to the monthly normalized anomalies based on the 1981–2010 climatologies for each month, but the numbers are the monthly average runoffs in $m^3 s^{-1}$. Numbers on the right side are annual climatological means. Runoff regulation is simulated for three rivers that flow into the Estuary (Saguenay, Manicouagan, Outardes).

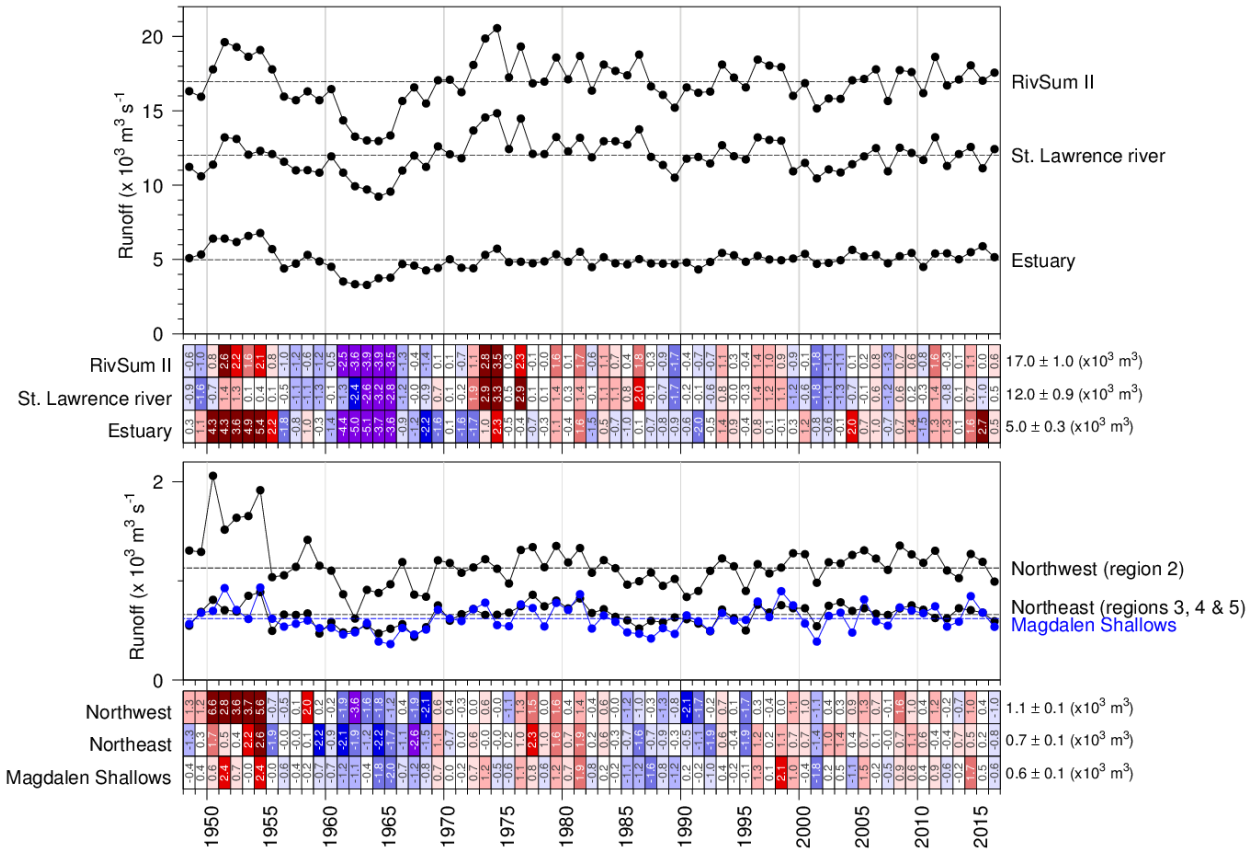

Figure 9. Annual mean freshwater flow of the St. Lawrence River at Québec City and of the sum of all rivers flowing into regions of the Estuary and Gulf. The 1981–2010 climatological mean is shown as horizontal lines and indicated on the right side of the scorecards. Numbers in scorecards are normalized anomalies.

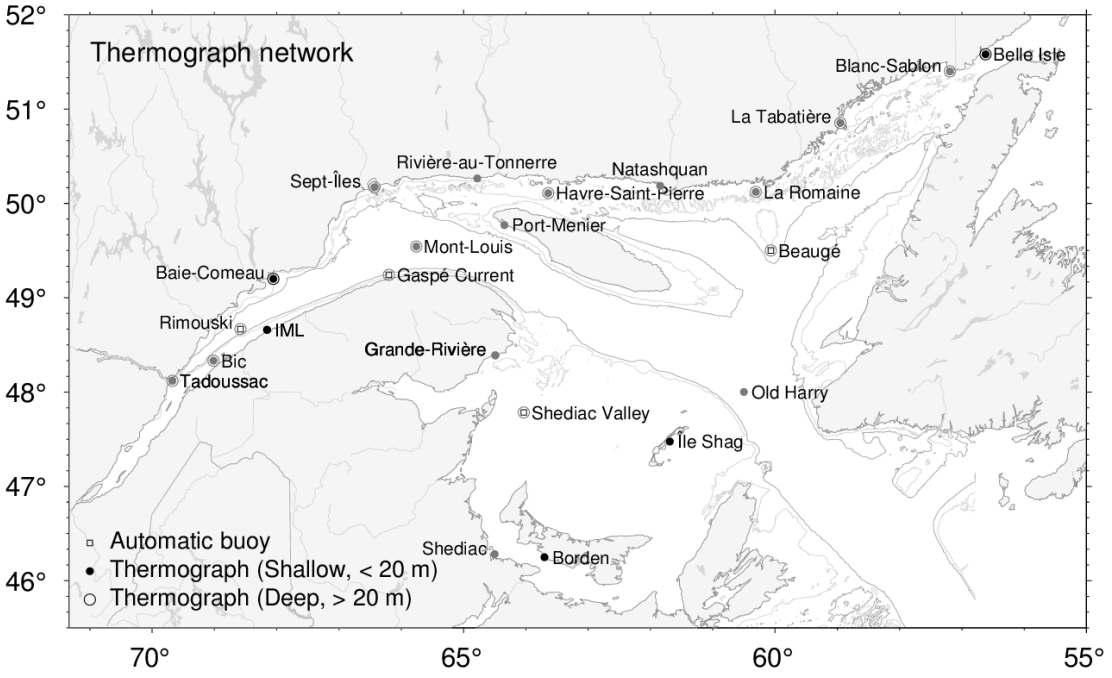

Figure 10. Locations of the Maurice Lamontagne Institute thermograph network stations in 2016, including oceanographic buoys that transmit data in real time (squares). Deep and shallow instruments are denoted by open circles and dots, while seasonal and year-round deployments are denoted by gray and black symbols. Shediac station from DFO Gulf Region is also shown.

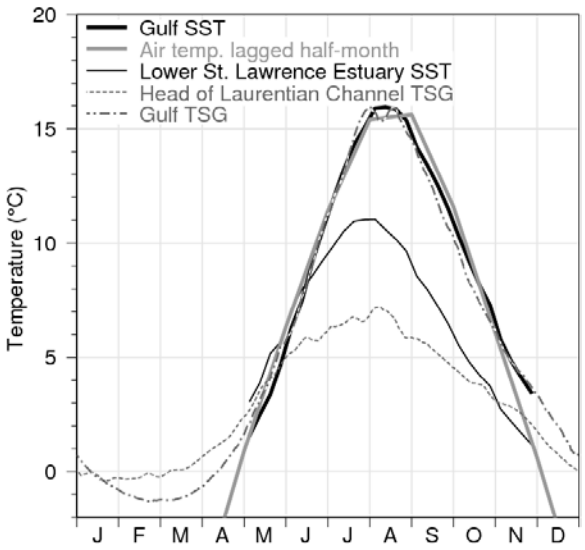

Figure 11. Sea-surface temperature climatological seasonal cycle in the Gulf of St. Lawrence. AVHRR temperature weekly averages for 1985 to 2010 are shown from May to November (ice-free months) for the entire Gulf (thick black line) and the cooler Lower St. Lawrence Estuary (thin black line), defined as the area west of the Pointe-des-Monts section and east of approx 69°30'W. Thermosalinograph data averages for 2000 to 2010 are shown for the head of the Laurentian Channel (at 69°30'W, grey dashed line) and for the average over the Gulf waters along the main shipping route between the Pointe-des-Monts and Cabot Strait sections (gray dash-dotted line). Monthly air temperature averaged over eight stations in the Gulf of St. Lawrence are shown offset by 2 weeks into the future (thick grey line; winter months not shown). Figure from Galbraith et al. (2012).

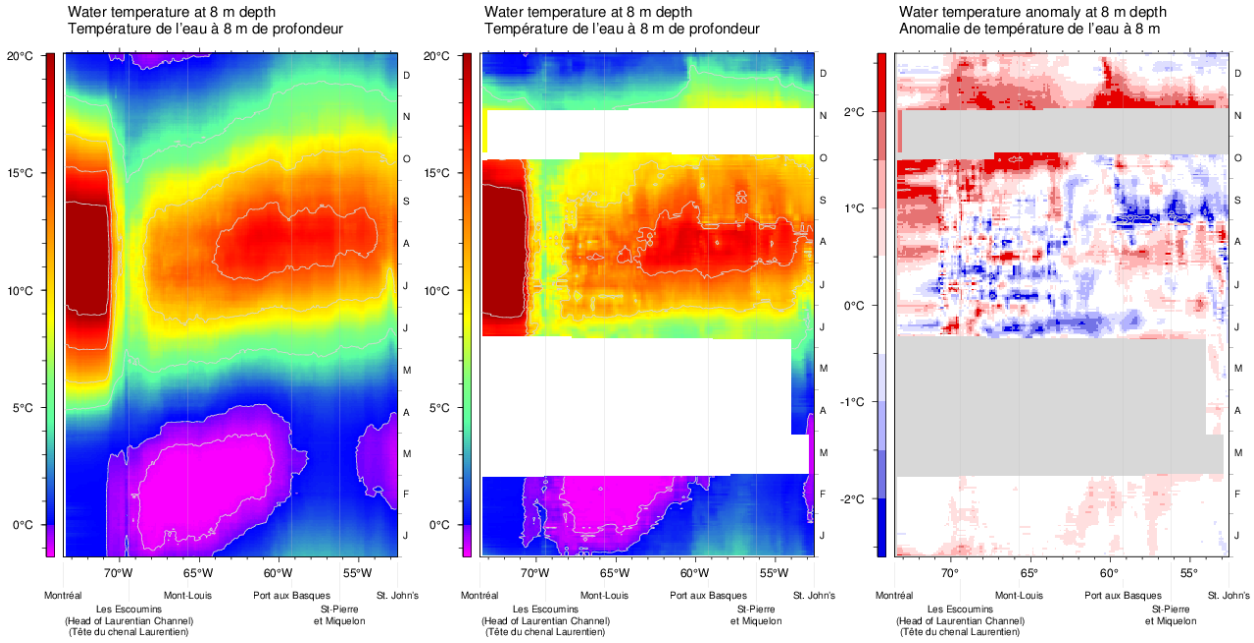

Figure 12. Thermosalinograph data at 8 m depth along the Montréal to St. John's shipping route: composite mean annual cycle of the water temperature for the 2000–2016 period (left panel),composite annual cycle of the water temperature for 2016 (middle panel), and water temperature anomaly for 2016 relative to the 2000–2016 composite (right panel).

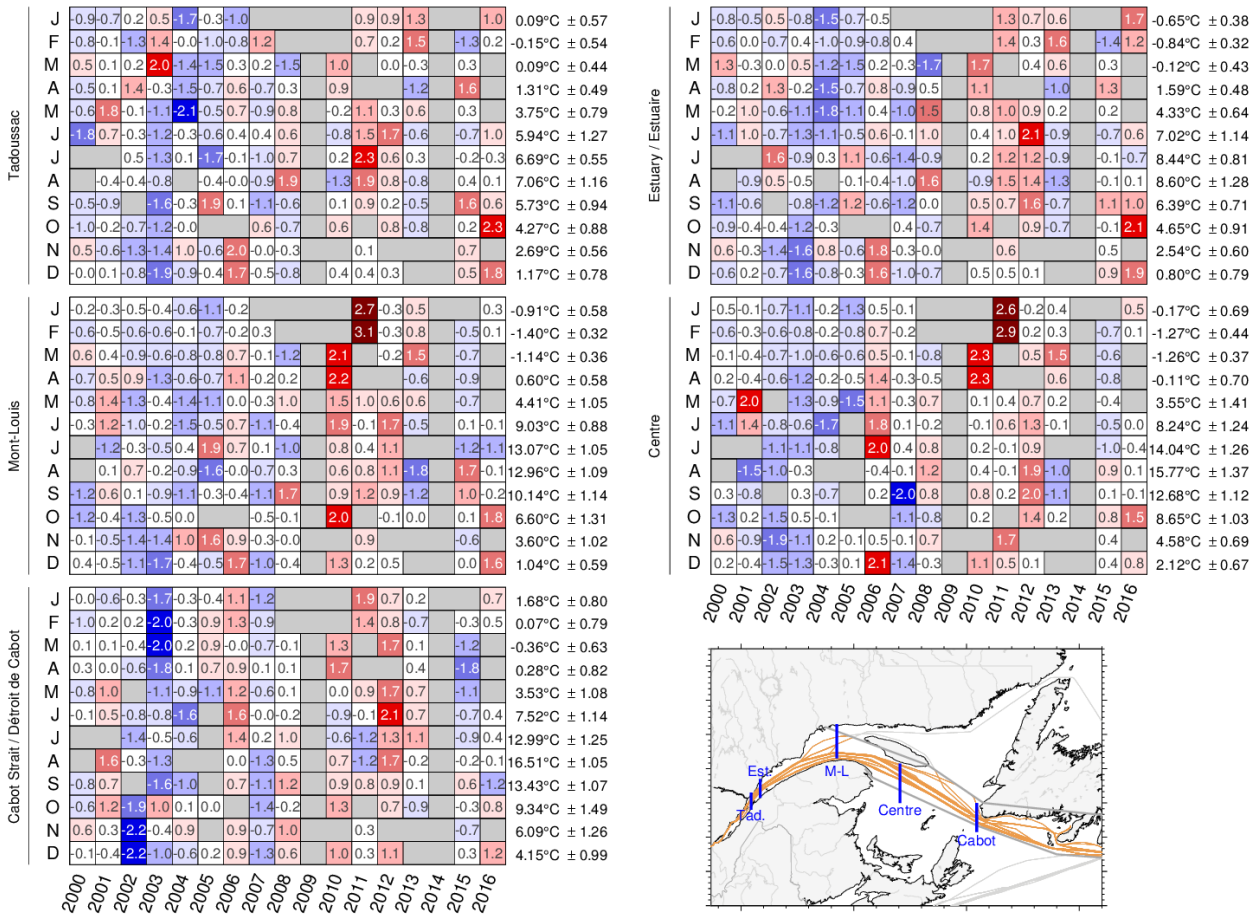

Figure 13. Thermosaligraph near-surface temperature monthly anomalies for various sections along the main shipping lane. The numbers on the right are the 2000–2016 climatological means and standard deviations. The numbers in the boxes are normalized anomalies. The map shows all TSG data sampled in 2016. Those drawn in colour are within the main shipping corridor and are used in this report. Monthly average anomalies of temperatures measured close to the indicated blue section lines are shown in the other scorecard panels.

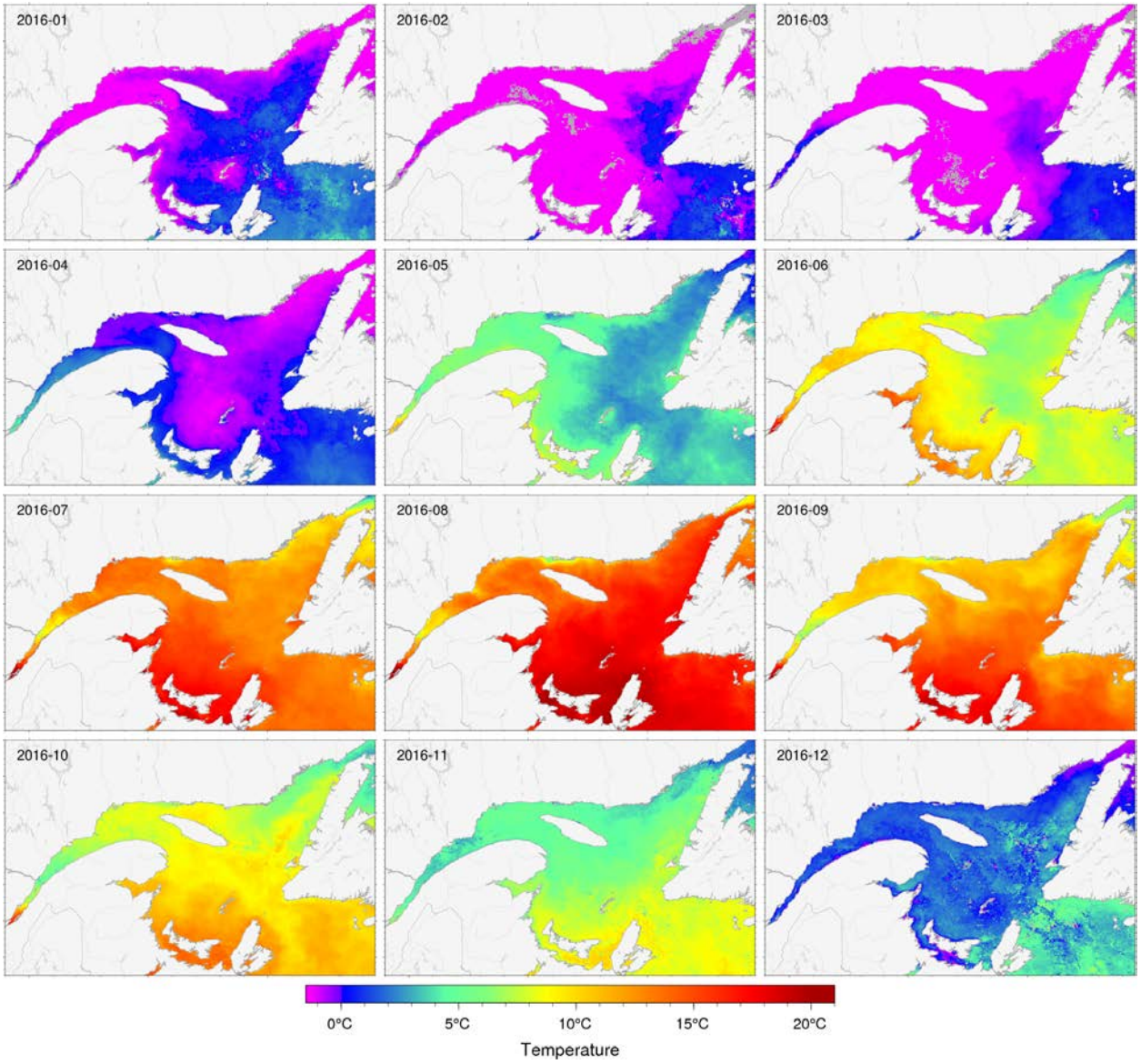

Figure 14. Sea-surface temperature monthly averages for 2016 as observed with AVHRR remote sensing. Grey areas have no data for the period due to ice cover or clouds.

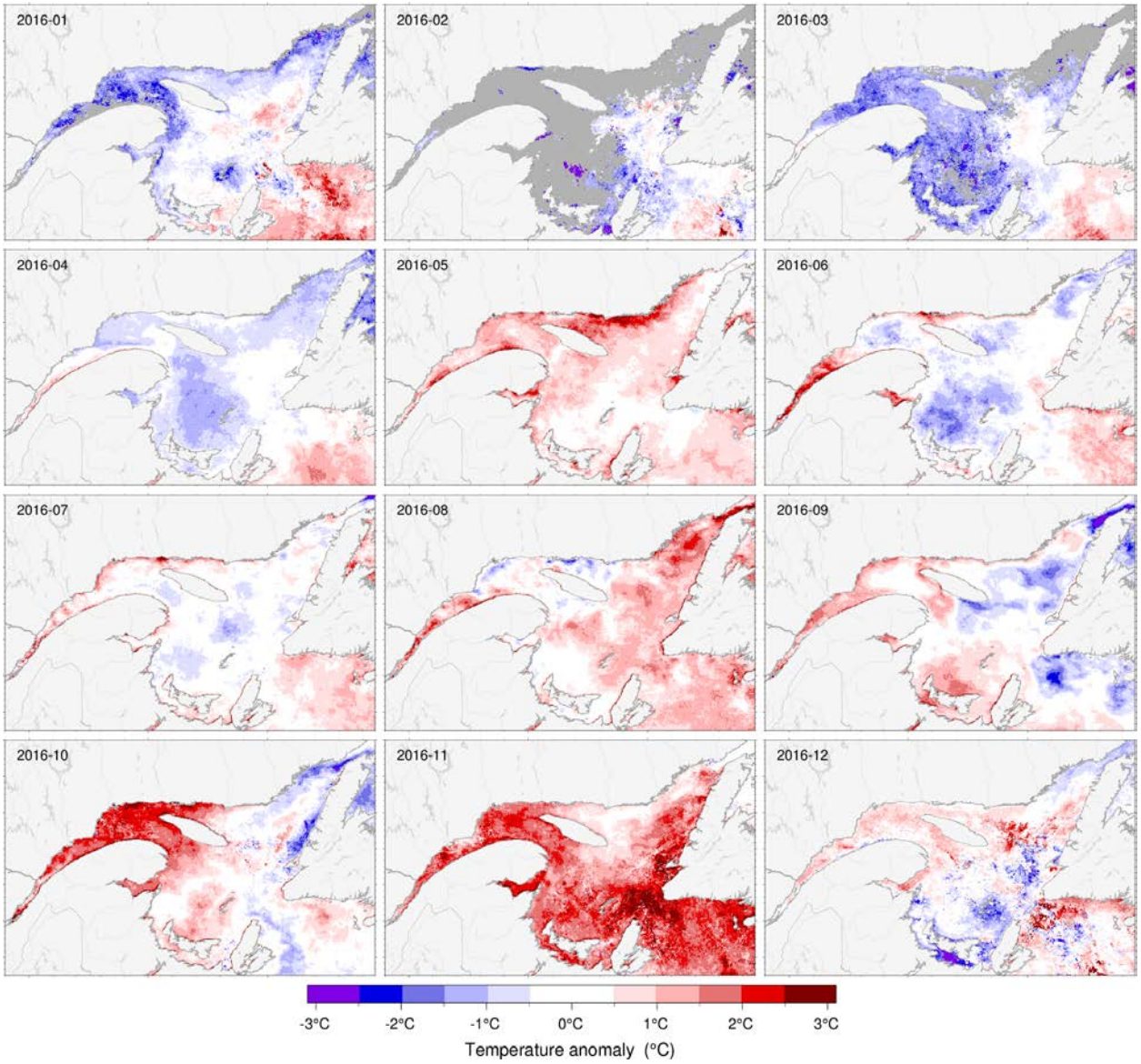

Figure 15. Sea-surface temperature monthly anomalies for 2016 based on monthly climatologies calculated for the 1985–2010 period observed with AVHRR remote sensing. Gray area either had sea-ice cover or missing climatologies due to recurrent sea-ice cover.

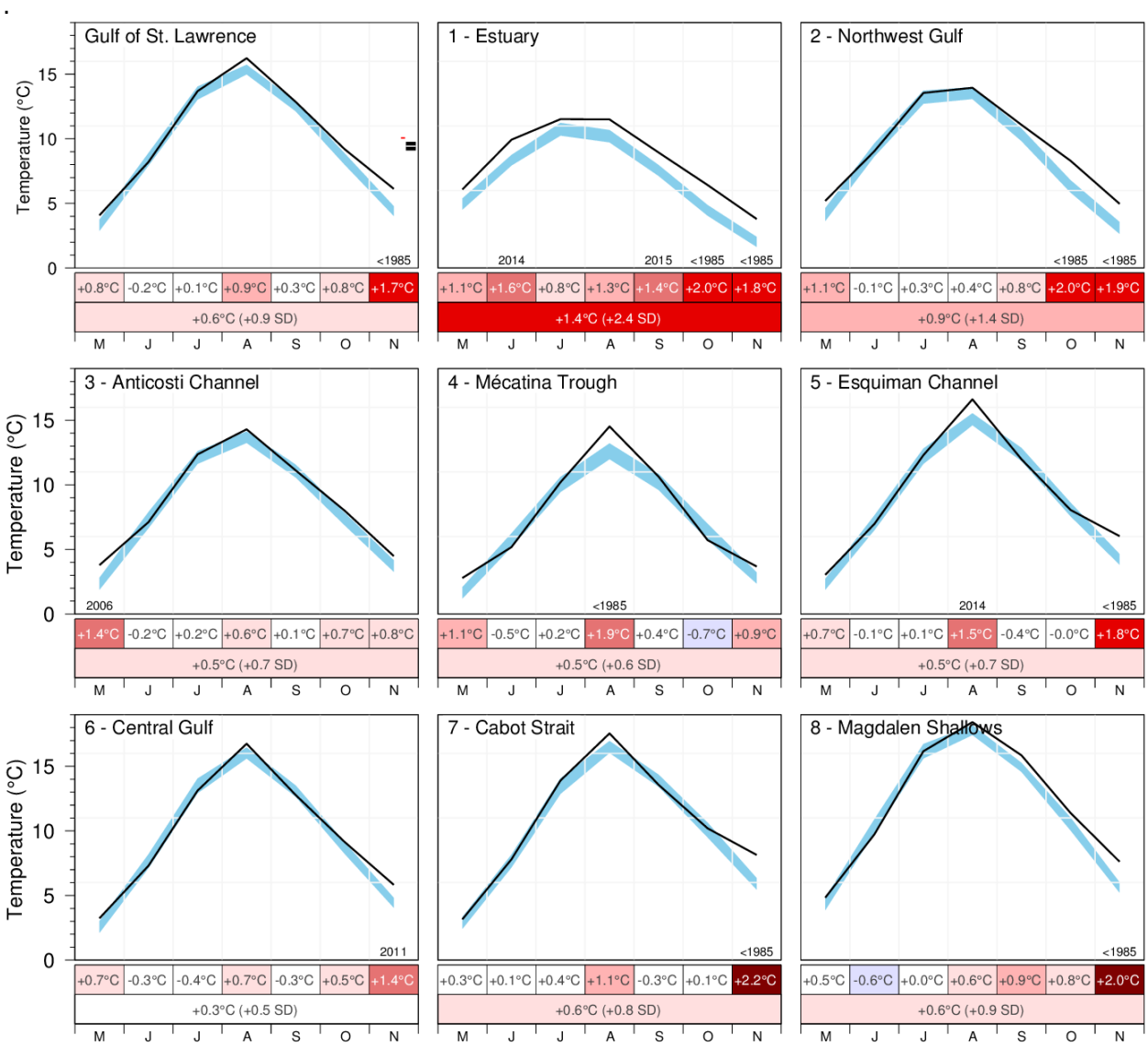

Figure 16. AVHRR SST May to November monthly averages over the Gulf and over the eight regions of the Gulf. The blue area represents the 1981–2010 climatological monthly mean ± 0.5 SD. The scorecards are colour-coded according to the monthly normalized anomalies based on the 1985–2010 climatologies for each month, but the numbers are the monthly average temperature anomalies.

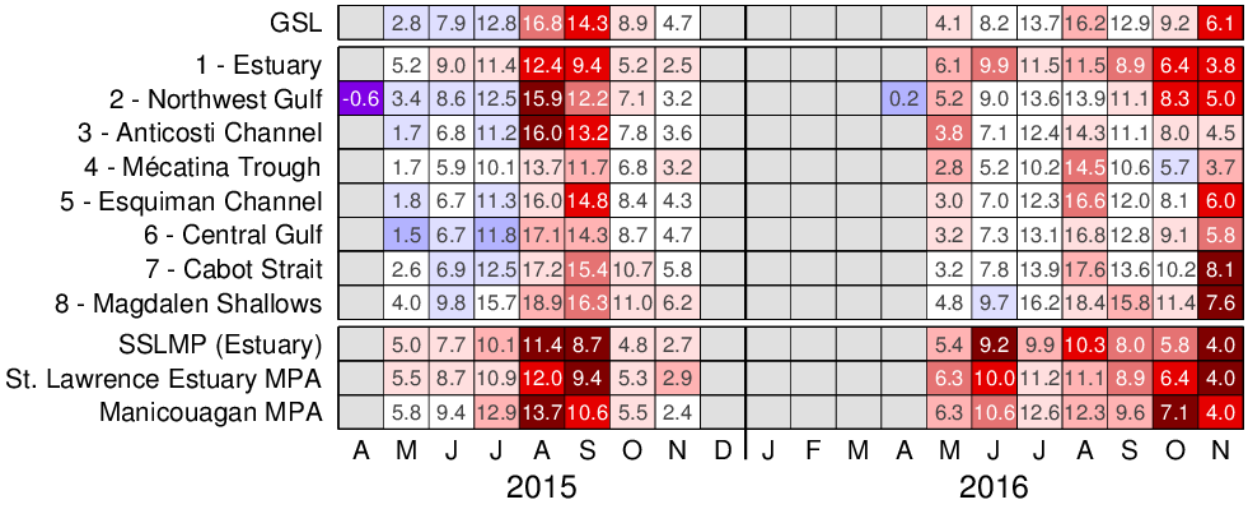

Figure 17. AVHRR SST May to November monthly anomalies averaged over the Gulf, the eight regions of the Gulf, and management regions of the St. Lawrence Estuary for 2015 and 2016 (April results are also shown for the Northwest Gulf). The scorecards are colour-coded according to the monthly normalized anomalies based on the 1985–2010 climatologies for each month, but the numbers are the monthly average temperatures.

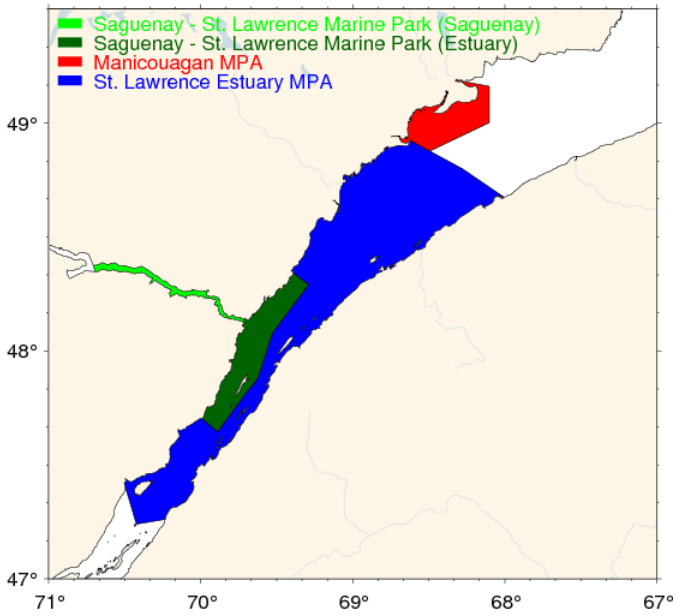

Figure 18. Map showing the proposed Manicouagan MPA, the proposed St. Lawrence Estuary MPA, and the Saguenay – St. Lawrence Marine Park for the purpose of SST extraction from NOAA imagery (Fig. 17).

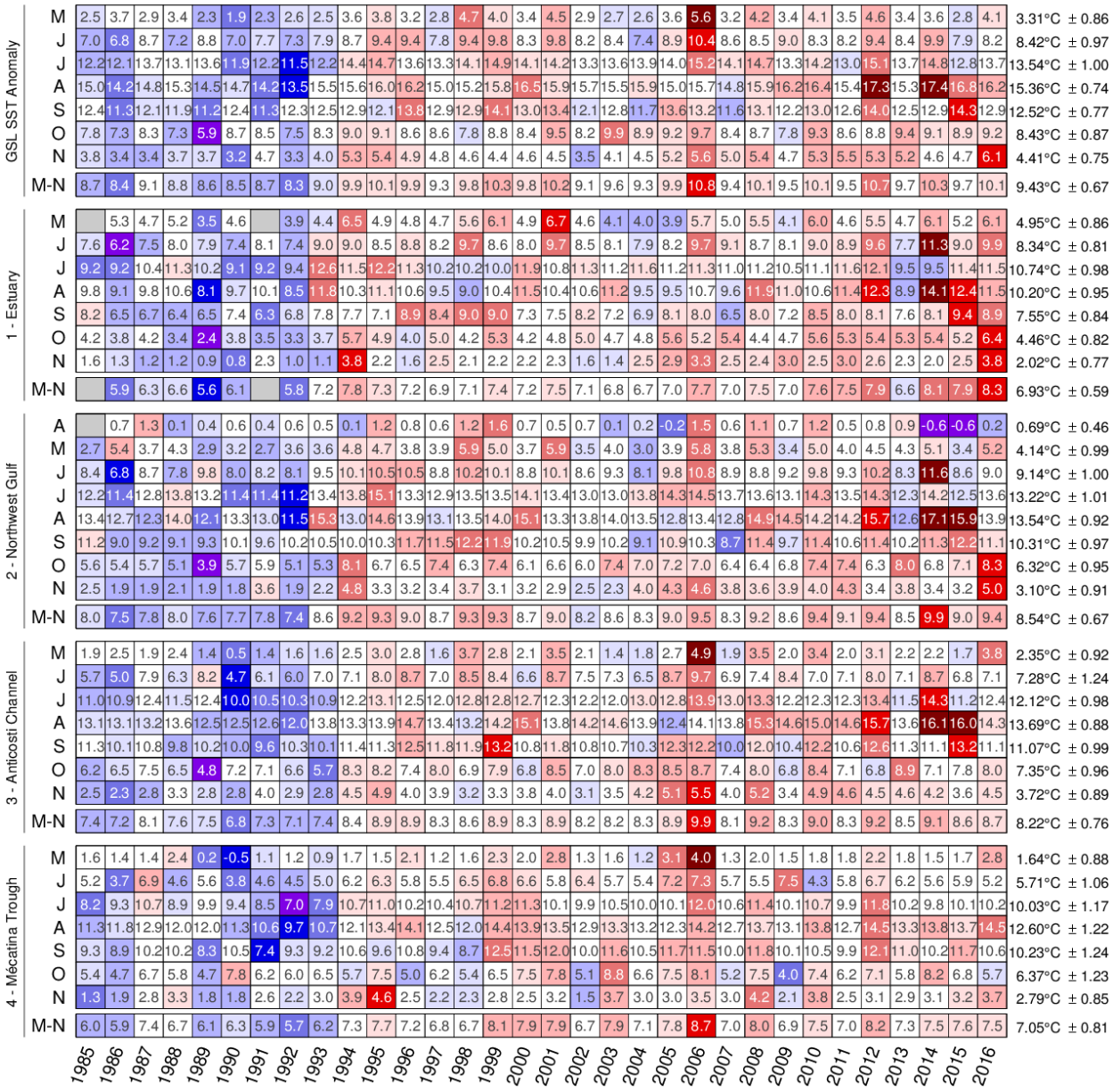

Figure 19. AVHRR SST May to November monthly anomalies averaged over the Gulf of St. Lawrence and over the first four regions of the Gulf. The scorecards are colour-coded according to the monthly normalized anomalies based on the 1985–2010 climatologies for each month, but the numbers are the monthly average temperatures in ºC. The 1985-2010 mean and standard deviation are indicated for each month on the right side of the table. April anomalies are included for the Northeast Gulf because those regions are typically ice-free by then. The May to November average is also included.

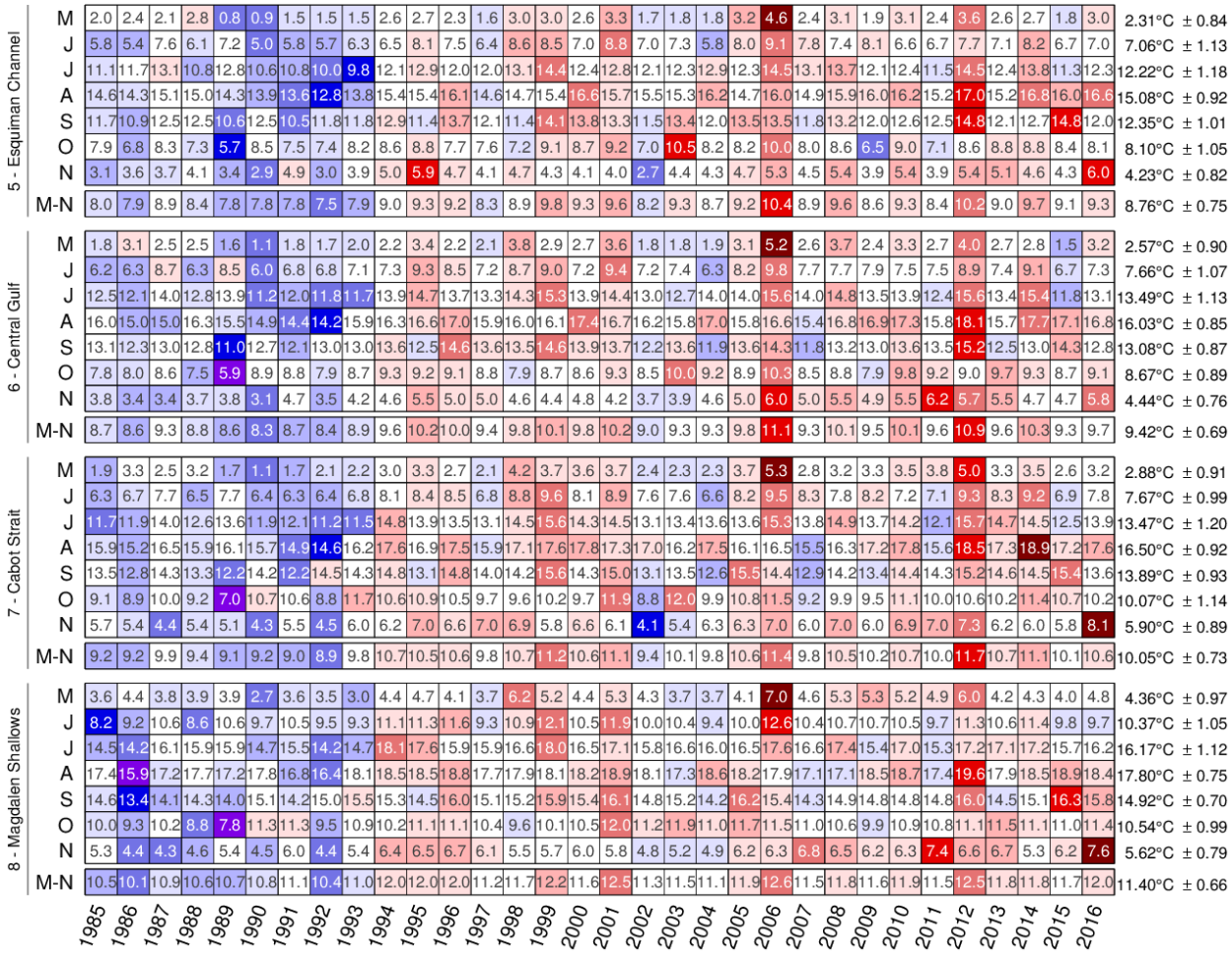

Figure 20. AVHRR SST May to November monthly anomalies averaged over the remaining four regions of the Gulf. The scorecards are colour-coded according to the monthly normalized anomalies based on the 1985–2010 climatologies for each month, but the numbers are the monthly average temperatures in ºC. The 1985-2010 mean and standard deviation are indicated for each month on the right side of the table. The May to November average is also included.

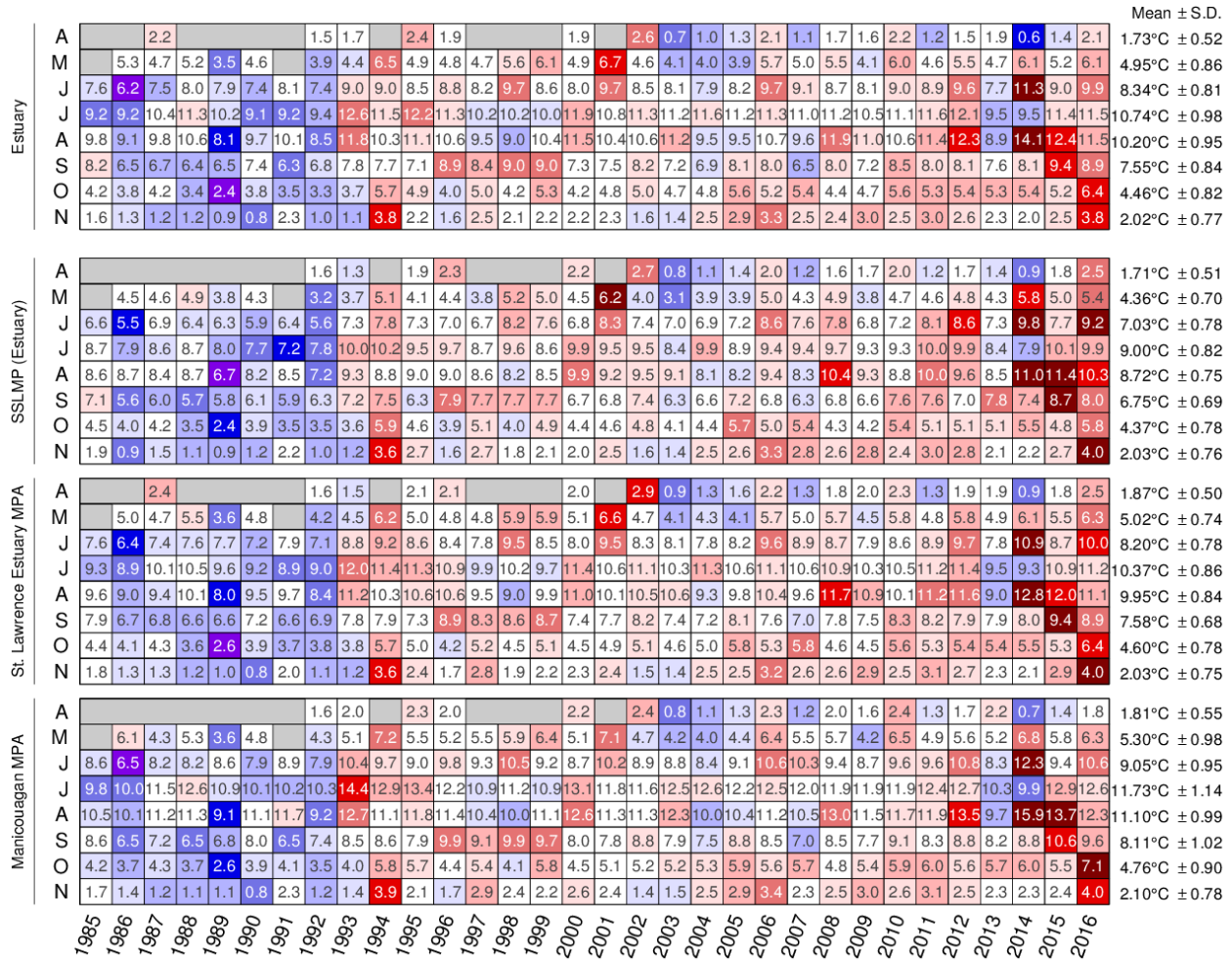

Figure 21. AVHRR SST April to November monthly anomalies averaged over the Estuary (region 1 of the Gulf) and the Estuary subregion of the Saguenay – St. Lawrence Marine Park (PMSSL), the proposed St.Lawrence Estuary Marine Protected Area (MPA), and Manicouagan MPA. The scorecards are colour-coded according to the monthly normalized anomalies based on the 1985–2010 climatologies for each month, but the numbers are the monthly average temperatures in ºC. The 1985-2010 mean and standard deviation are indicated for each month on the right side of the table.

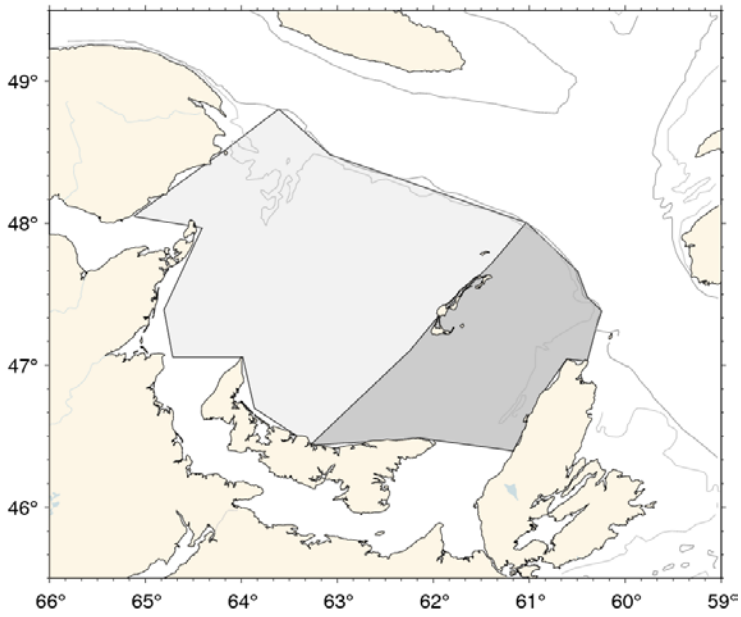

Figure 22. Areas defined as the western and eastern Magdalen Shallows.

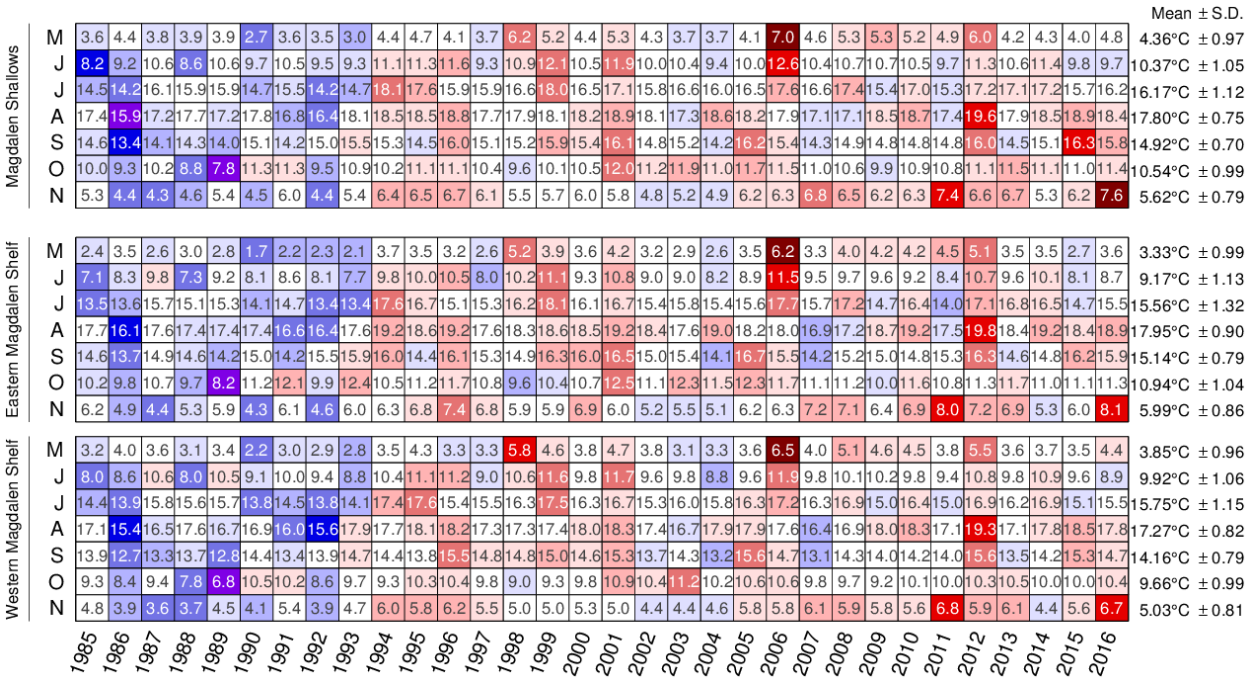

Figure 23. AVHRR SST May to November monthly anomalies averaged over the Magdalen Shallows (region 8 of the Gulf) and the eastern and western subregions of the Magdalen Shallows. The scorecards are colour-coded according to the monthly normalized anomalies based on the 1985–2010 climatologies for each month, but the numbers are the monthly average temperatures in ºC. The 1985-2010 mean and standard deviation are indicated for each month on the right side of the table.

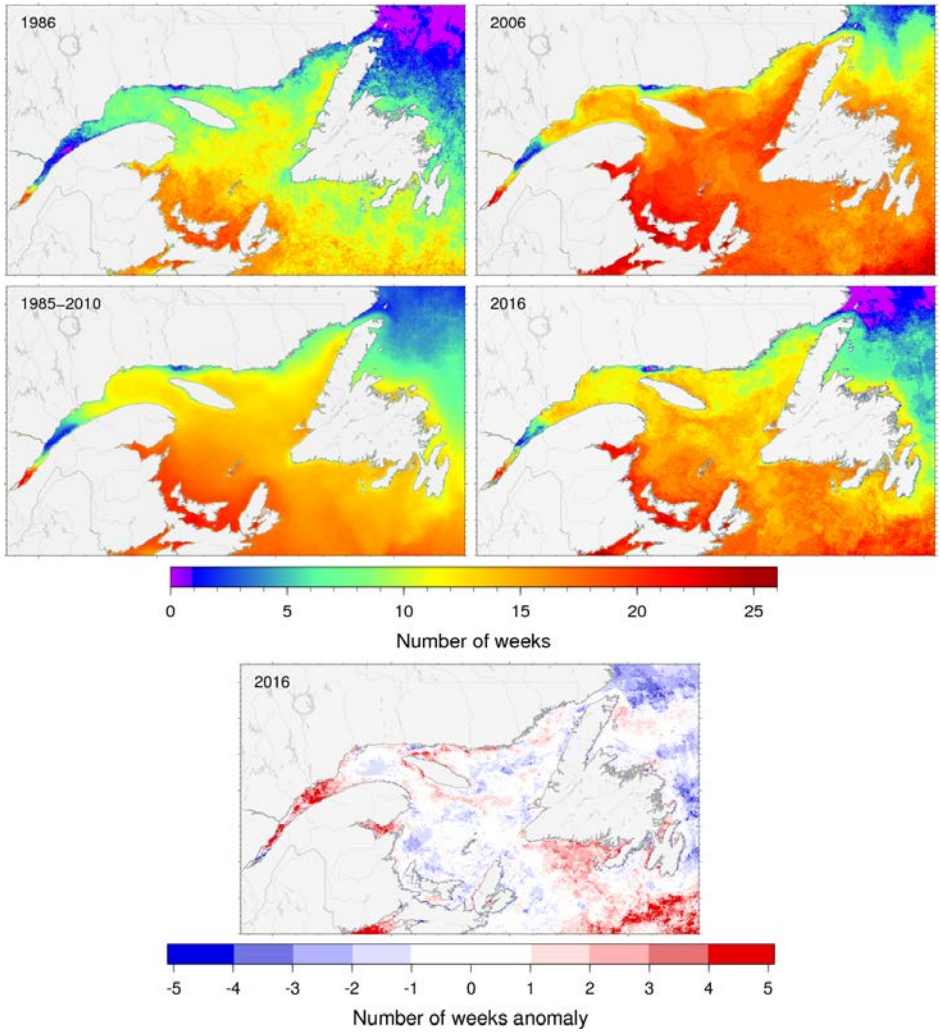

Figure 24. Yearly number of weeks with mean weekly surface temperature >10°C. (Top) Years with the minimum (1986, top left) and maximum (2006, top right) number of weeks are shown along with the 1985–2010 climatological average (lower left) and the chart for 2016. (Bottom) Anomaly for 2016 relative to 1985-2010 climatology, expressed in numbers of weeks.

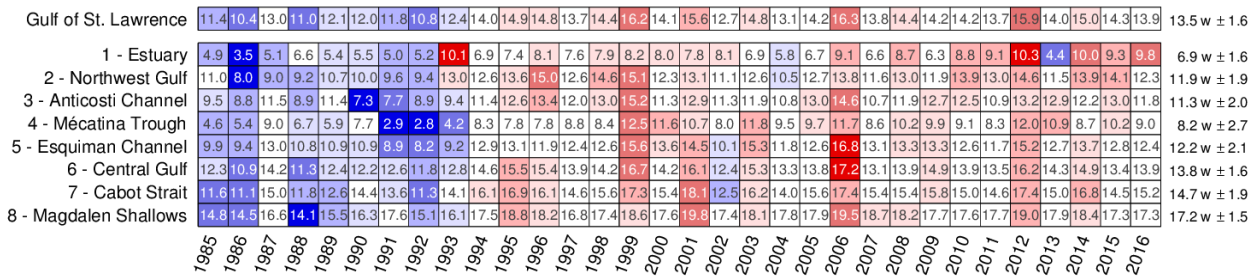

Figure 25. Yearly number of weeks with mean weekly surface temperature >10°C, averaged for the entire Gulf and each region of the Gulf. The scorecards are colour-coded according to the normalized anomalies based on the 1985–2010 time series, but the numbers are the average number of weeks above 10°C for each year.

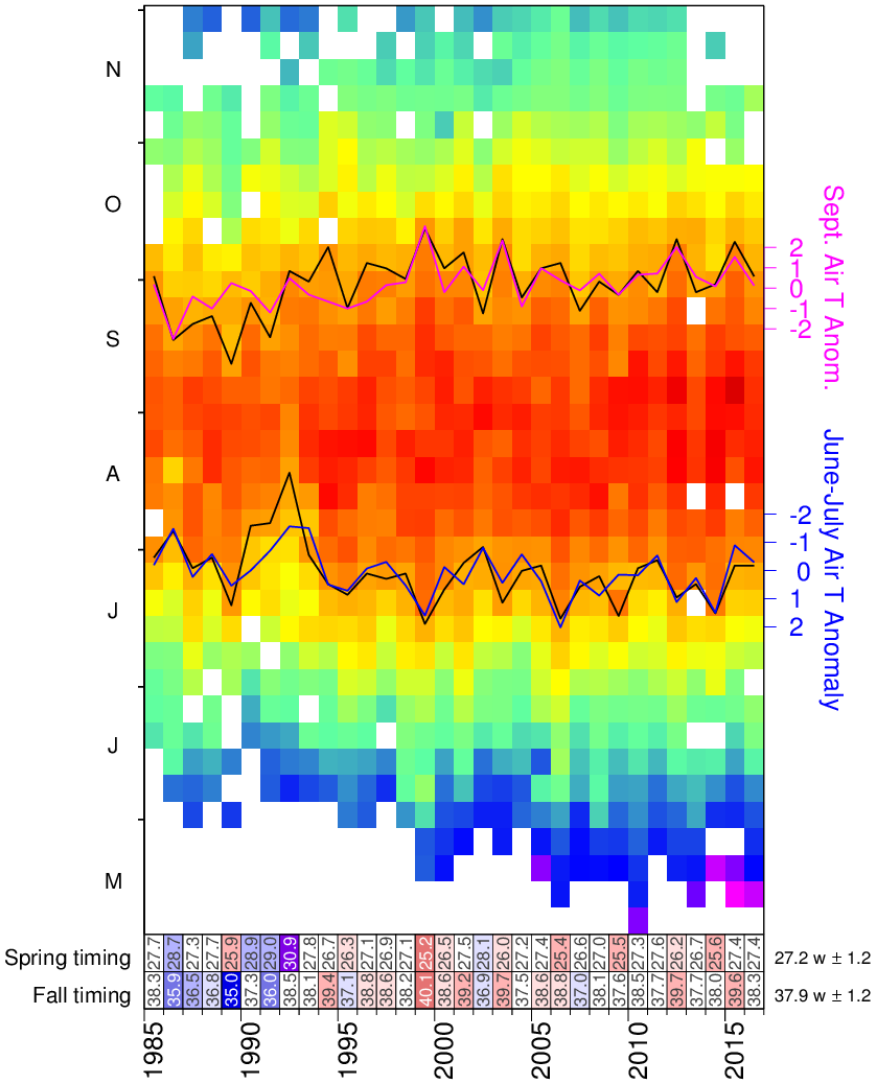

Figure 26. Weekly average SST (1985-2016) matrices for the Gulf of St. Lawrence. Black lines show first and last occurrence of the 12°C isotherm and proxies based on June-July and September average air temperature are also shown in colour (axes on right). The scorecards are colour-coded according to the normalized anomalies based on the 1985–2010 time series, but the numbers are week numbers when the threshold was crossed. Updated from Galbraith and Larouche 2013.

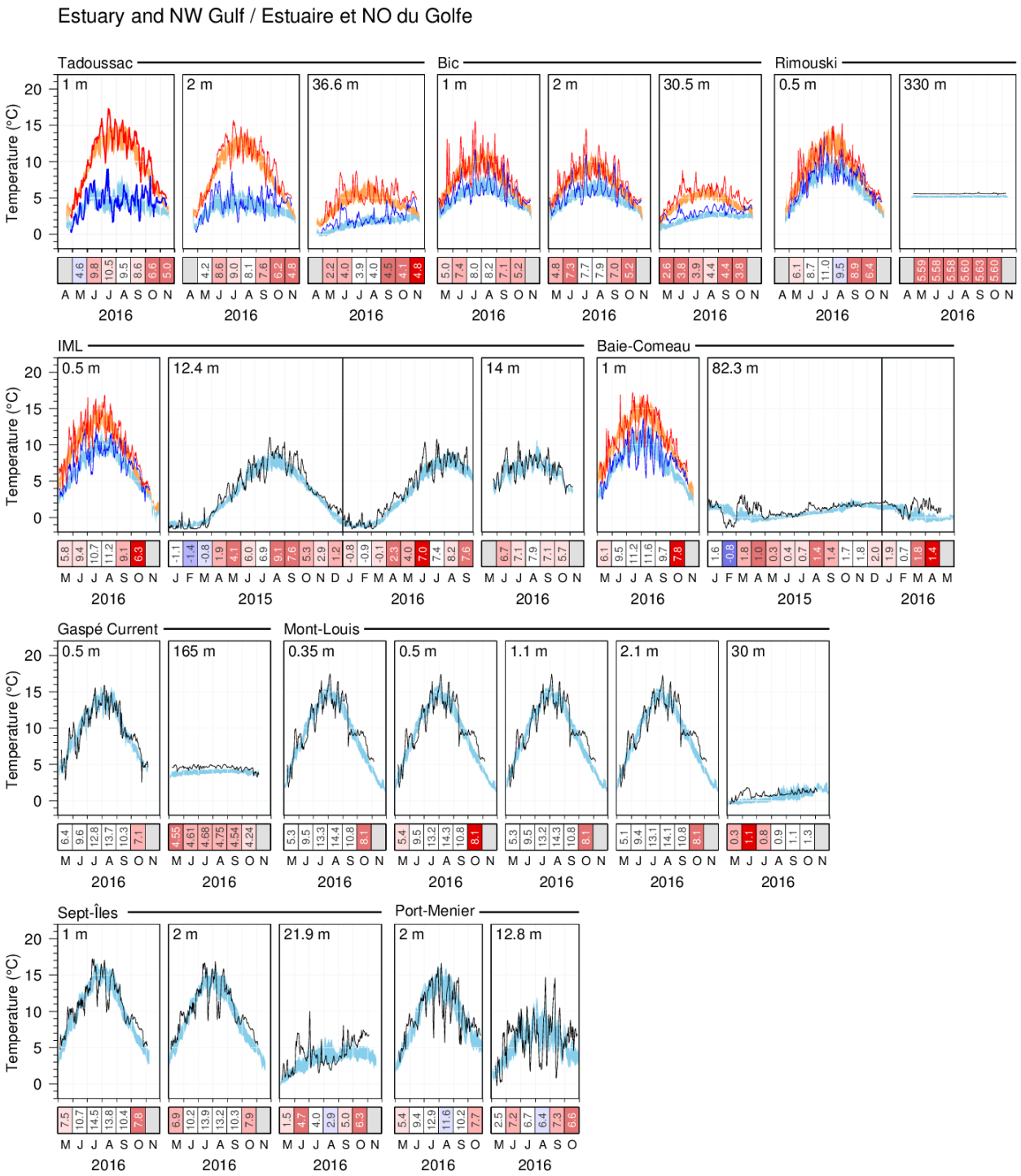

Figure 27. Thermograph network data. Daily mean 2016 temperatures compared with the daily climatology (blue areas are daily averages ± 0.5 SD, orange areas are daily average maximums ± 0.5 SD and bright blue areas are daily average minimums ± 0.5 SD) for stations in the Estuary and northwestern Gulf. Scorecards show monthly average temperature.

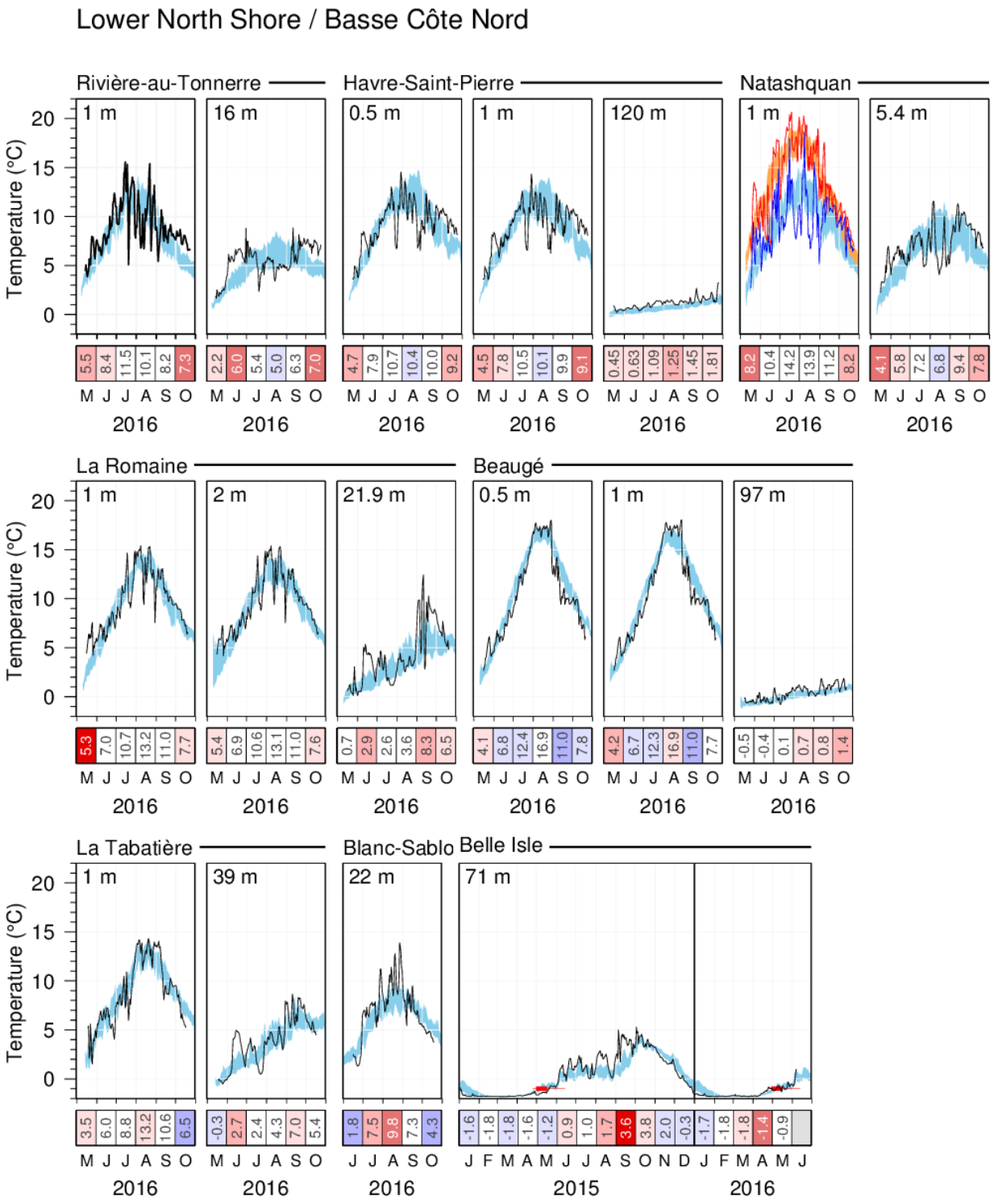

Figure 28. Thermograph network data. Daily mean 2016 temperatures compared with the daily climatology (blue areas are daily averages ± 0.5 SD, orange areas are daily average maximums ± 0.5 SD and bright blue areas are daily average minimums ± 0.5 SD) for stations of the lower north shore. Data from 2015 are included if they were not all shown in last year's report. Thin red lines in the Belle Isle panel span the historical dates when spring temperature increased over -1°C, a temperature associated with inflow of Labrador Shelf Water into the Gulf. Thick red line indicates mean date plus and minus 0.5 SD.

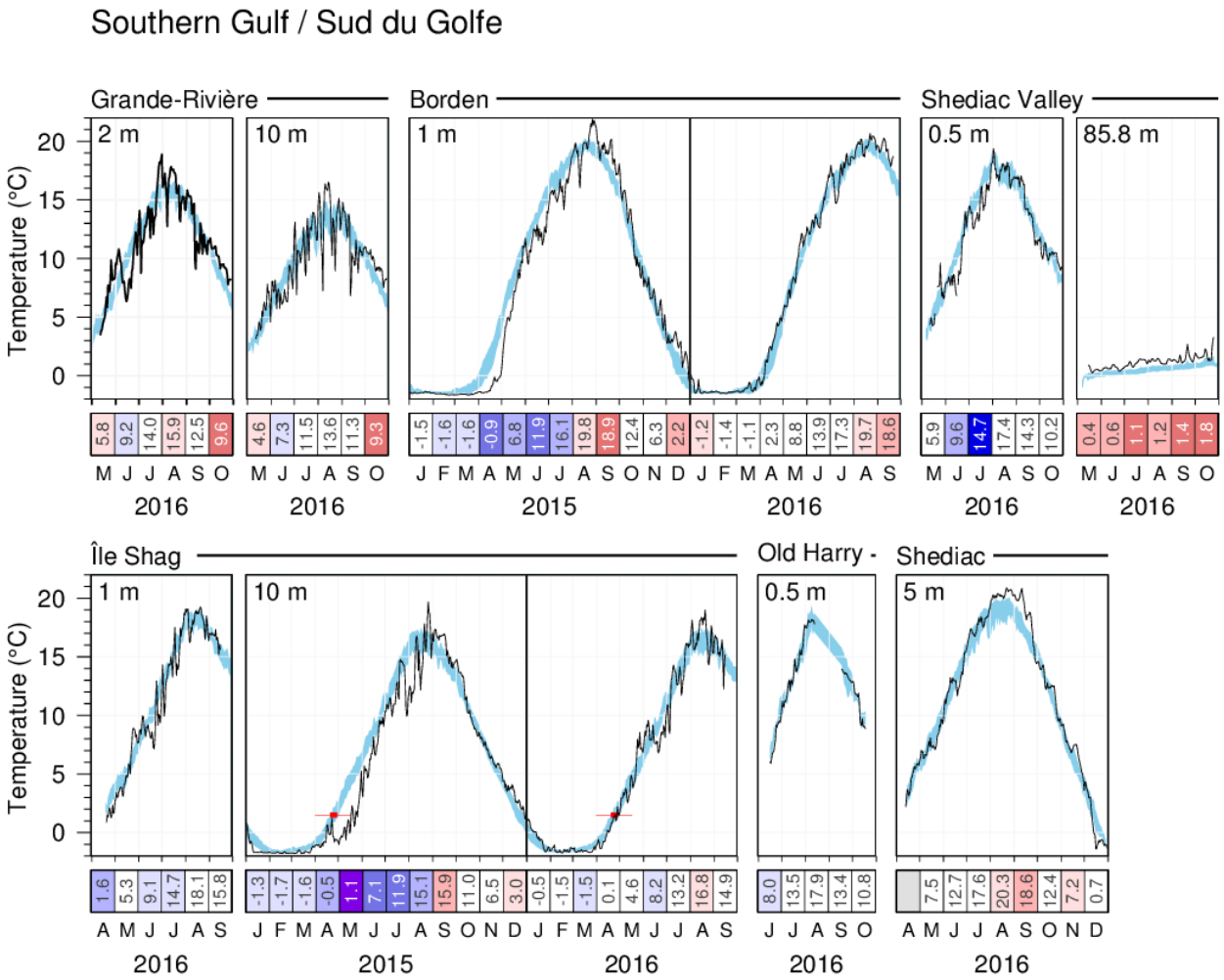

Figure 29. Thermograph network data. Daily mean 2016 temperatures compared with the daily climatology (daily averages ± 0.5 SD; blue area) for stations of the southern Gulf. Data from 2015 are included if they were not all shown in last year's report. Thin red lines in the Île Shag panel span the historical dates when spring temperature increased over 1.5°C, a temperature associated with increased lobster mobility. Thick red line indicates mean date plus and minus 0.5 SD. Shediac station is from the Southern Gulf network.

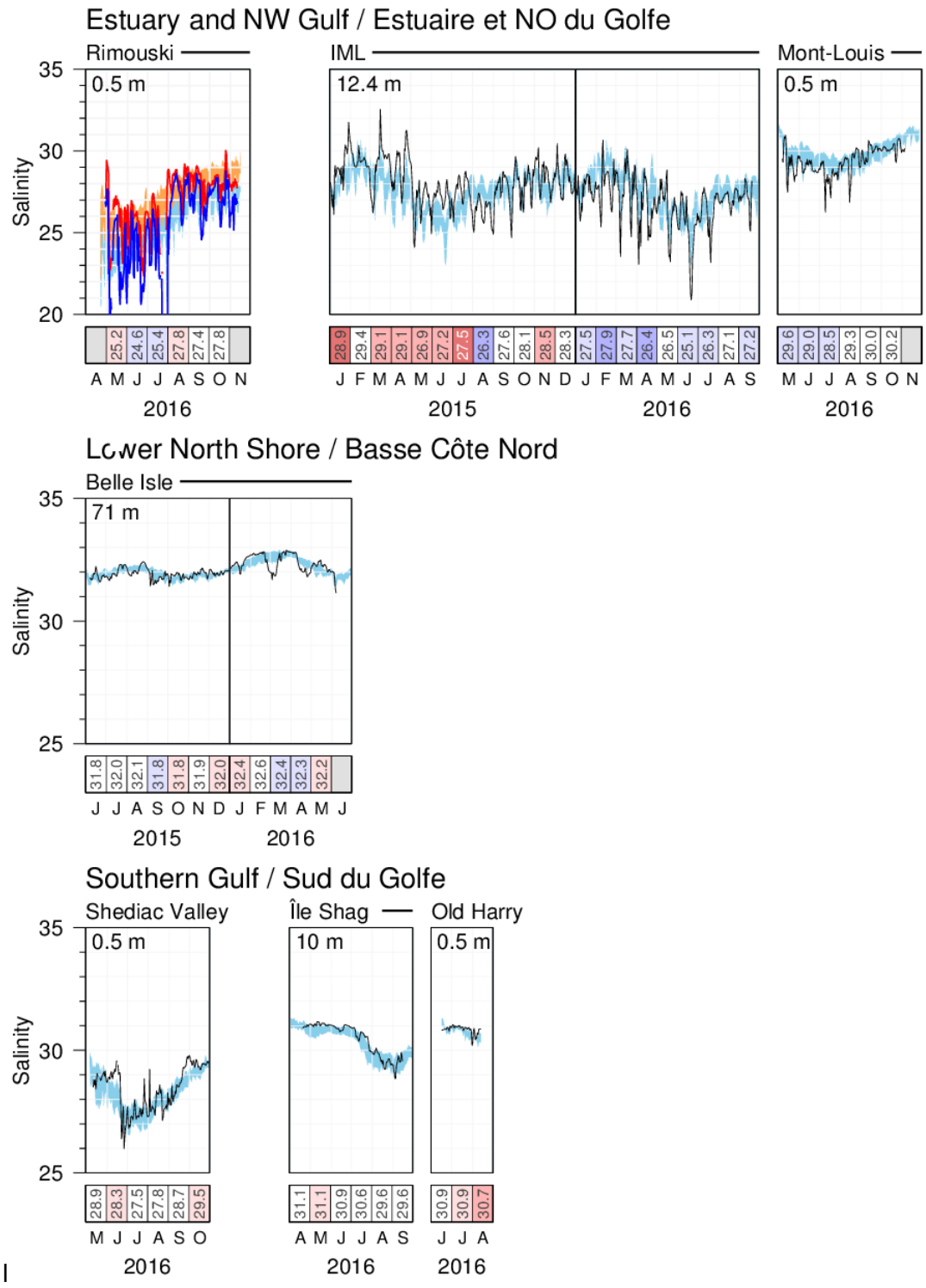

Figure 30. Thermograph network data. Daily mean 2016 salinities compared with the daily climatology (daily averages ± 0.5 SD; blue area) computed from all available stations. Data from 2015 are included if they were not all shown in last year's report.

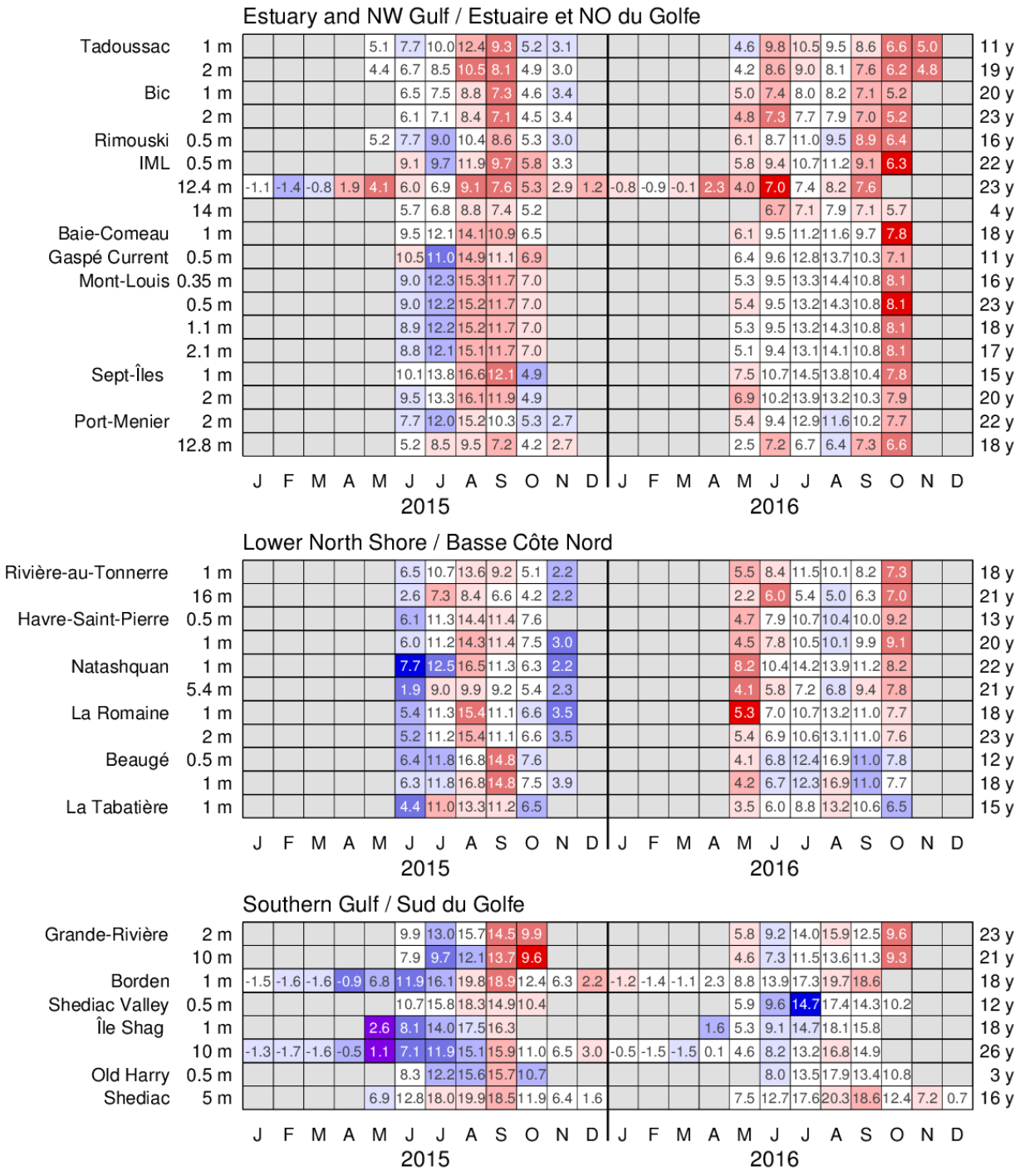

Figure 31. Monthly mean temperatures at all shallow sensors of the Maurice Lamontagne Institute thermograph network in 2015 and 2016. The number of years that each station and depth has been monitored is indicated on the far right. The colour-coding is according to the temperature anomaly relative to the climatology of each station for each month. Numbers are monthly average temperatures.

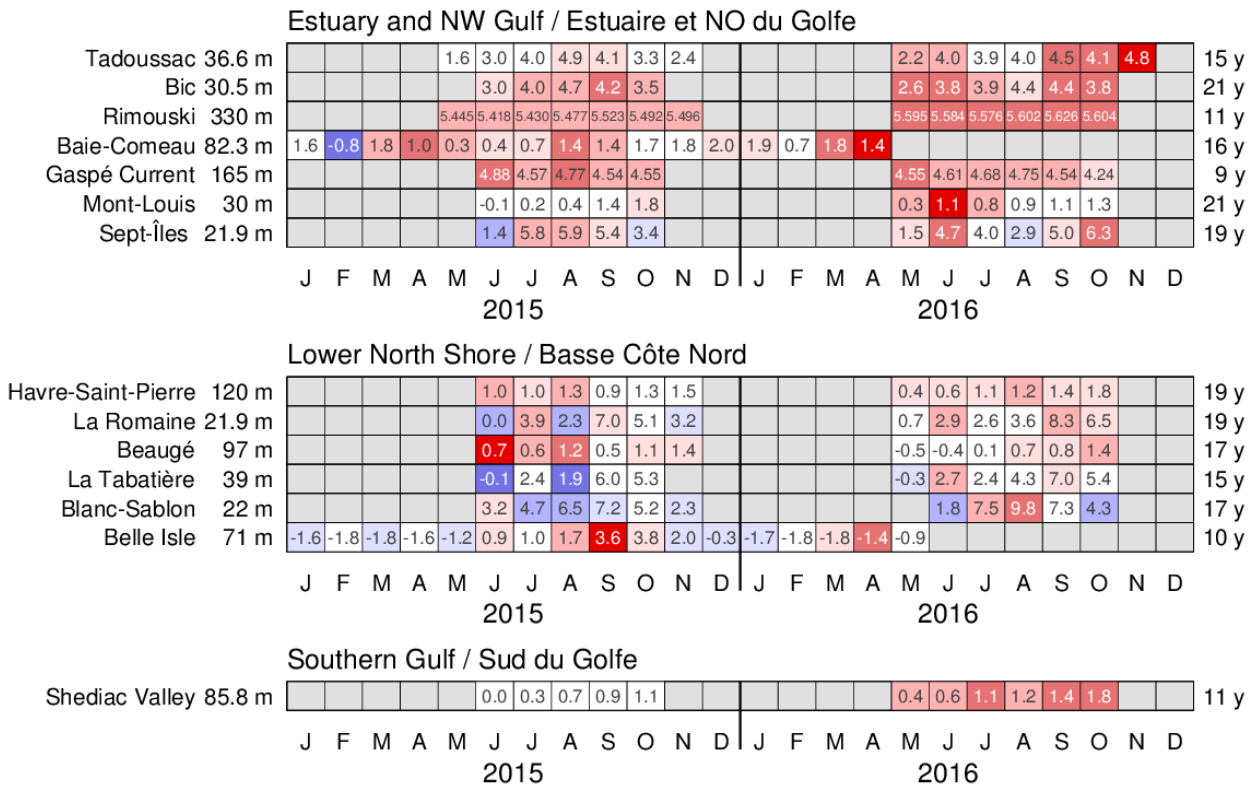

Figure 32. Monthly mean temperatures at all sensors deeper than 20 m of the Maurice Lamontagne Institute thermograph network in 2015 and 2016.The number of years that each station and depth has been monitored is indicated on the far right. The colour-coding is according to the temperature anomaly relative to the climatology of each station for each month. Numbers are monthly average temperatures, with greater number of significant digits included when variance is lower.

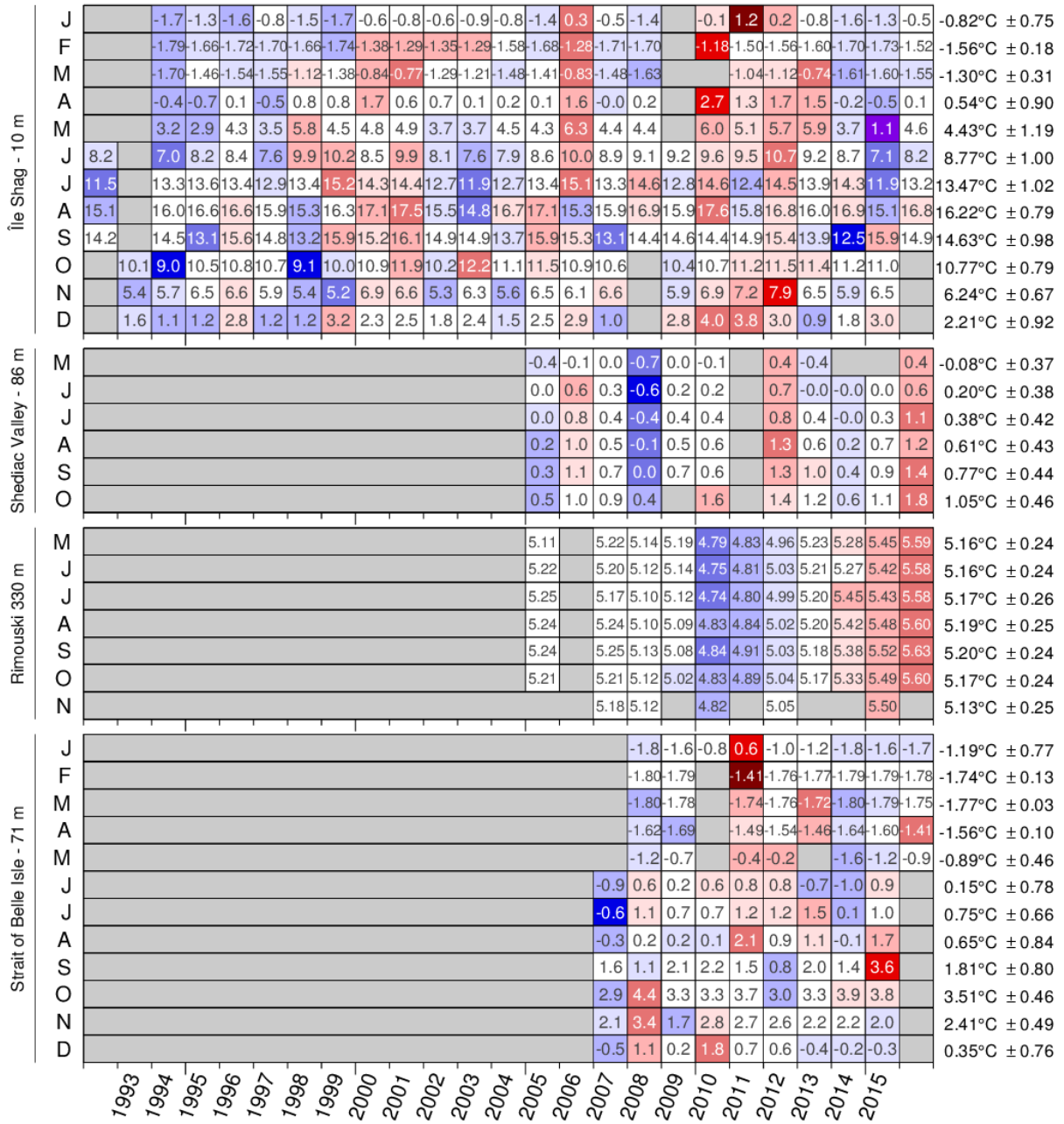

Figure 33. Time series of the monthly averaged temperature anomalies for selected stations of the thermograph network. The colour-coding is according to the temperature anomaly relative to the climatology of each station for each month. Numbers are monthly average temperatures. The mean and standard deviation are indicated for each month on the right side of the figure.

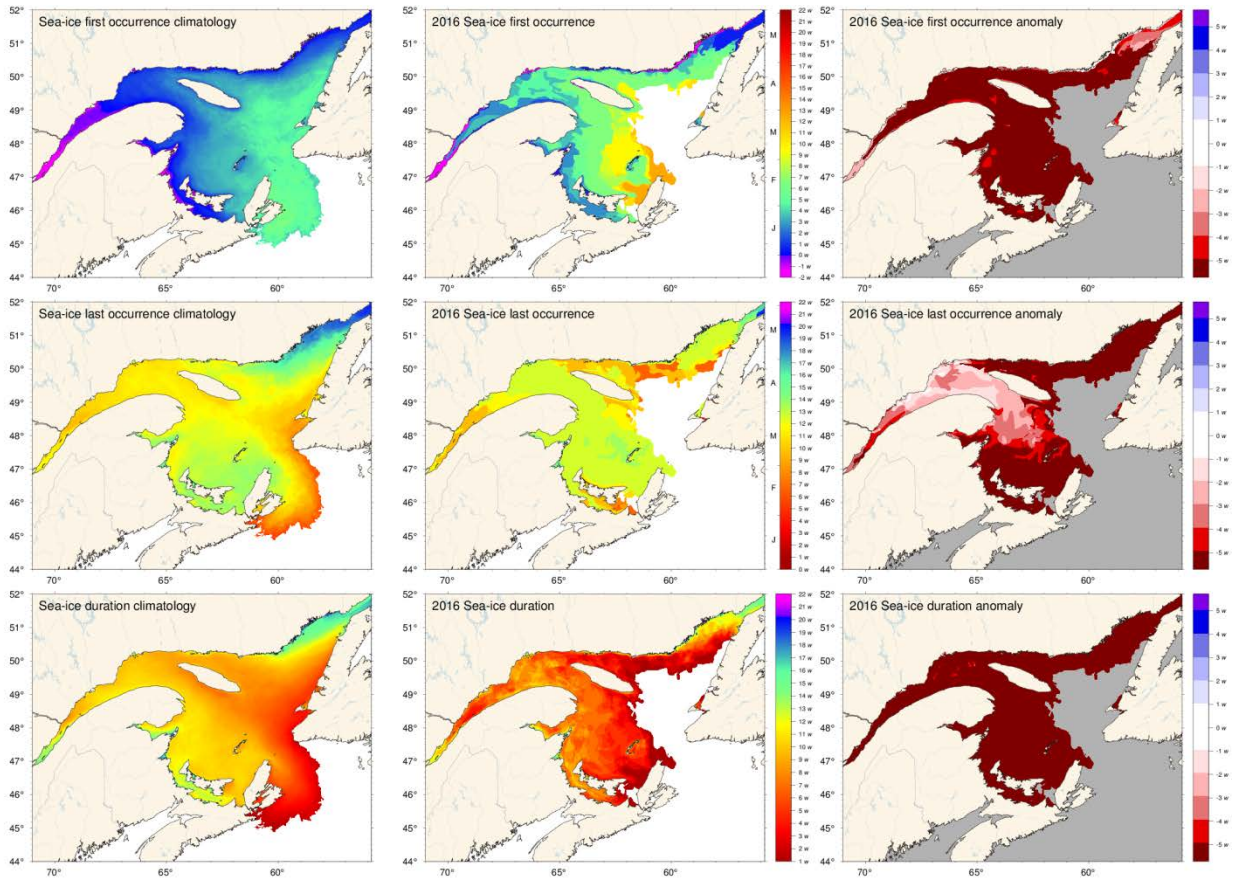

Figure 34. First and last occurrence of ice and ice season duration based on weekly data. The 1981-2010 climatologies are shown (left) as well as the 2016 values (middle) and anomalies (right). First and last occurrence is defined here as the first and last weekly chart in which any amount of ice is recorded for each pixel and are illustrated as day-of-year. Ice duration sums the number of weeks with ice cover for each pixel. Climatologies are shown for pixels that had at least 15 years out of the 30 with occurrence of sea-ice, and therefore also show the area with 50% likelihood of having some sea-ice at any time during any given year.

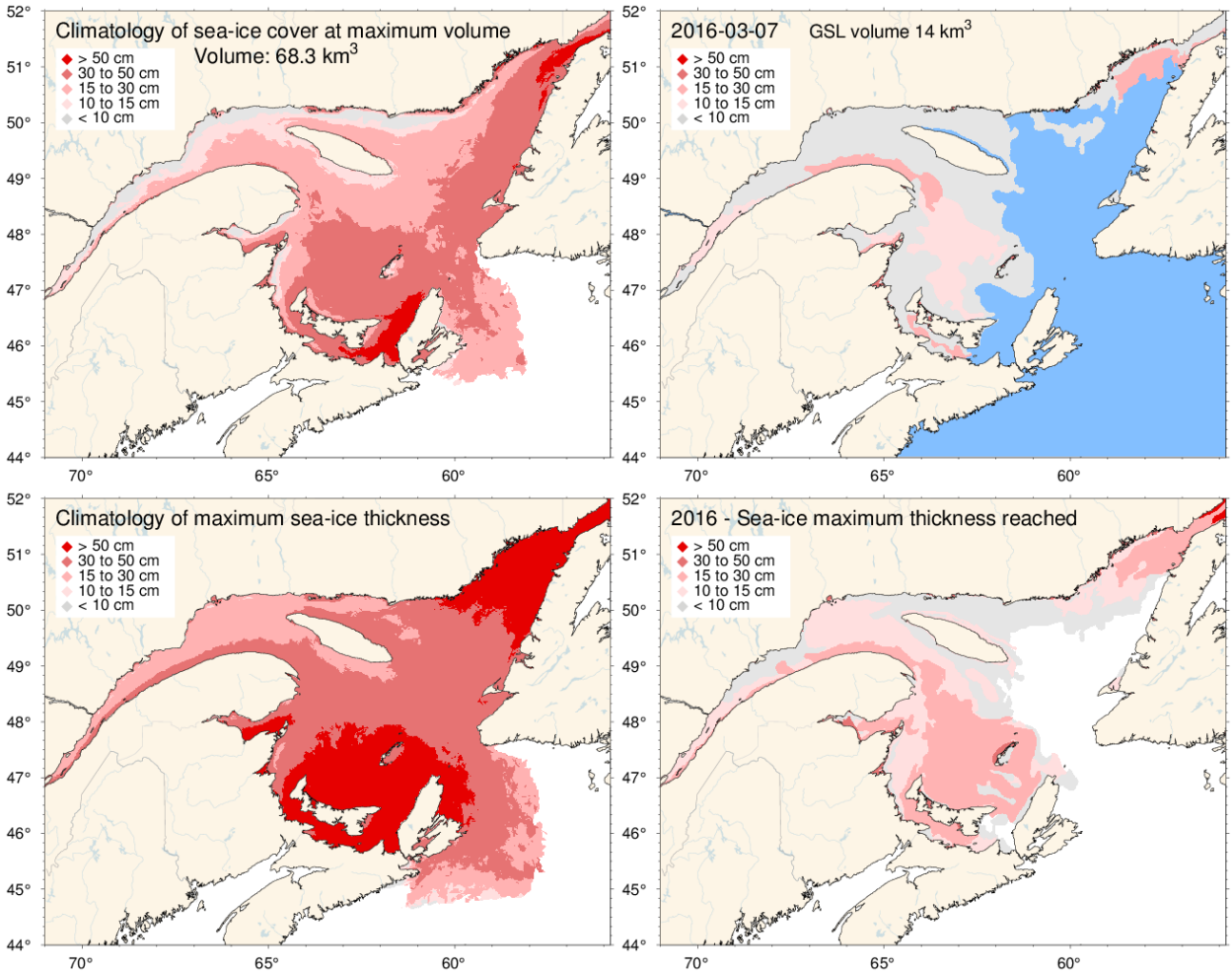

Figure 35. Ice thickness map for 2016 for the week of the year with the maximum annual volume including the portion covering the Scotian Shelf (upper right panel) and similarly for the 1981-2010 climatology of the weekly maximum (upper left panel). Note that these maps reflect the ice thickness distribution on that week, and not the maximum observed at any given location during the year. That information is shown by the lower panels, showing the 1981-2010 climatology and 2016 distribution of the thickest ice recorded during the season at any location.

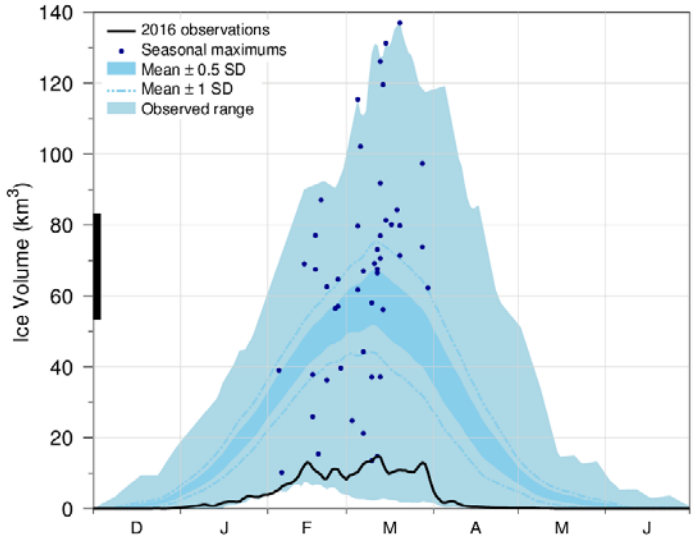

Figure 36. Time series of the 2015-2016 daily mean ice volume for the Gulf of St. Lawrence and Scotian Shelf (black line), the 1981-2010 climatological mean volume plus and minus 0.5 and 1 SD (dark blue area and dashed line), the minimum and maximum span of 1969-2016 observations (light blue) and the date and volumes of 1969-2016 seasonal maximums (blue dots). The black thick line on the left indicates the mean volume plus and minus 0.5 SD of the annual maximum ice volume, which is higher than the peak of the mean daily ice volume distribution.

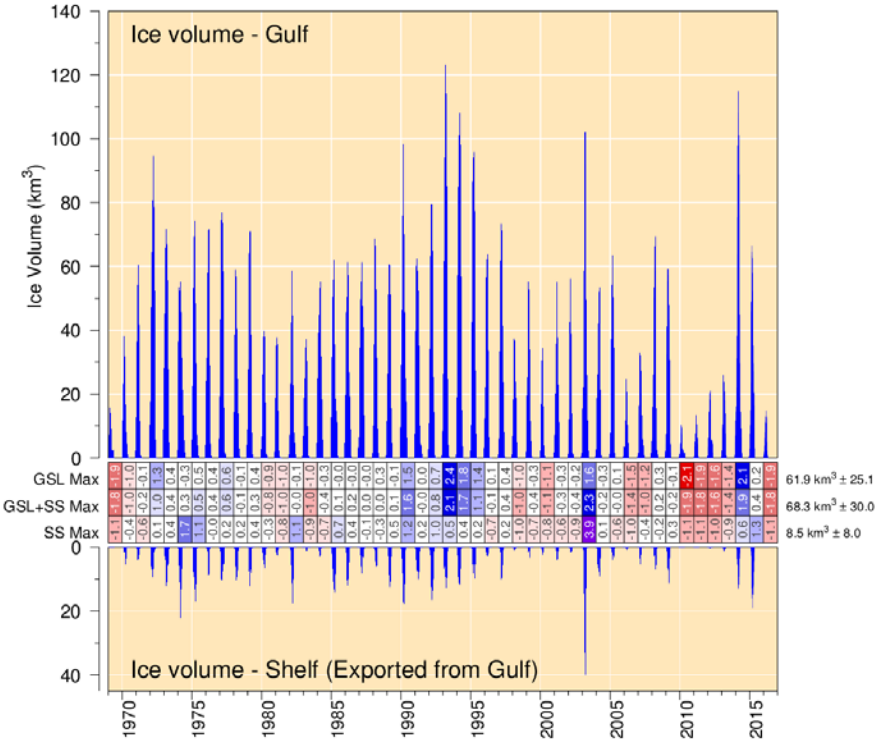

Figure 37. Estimated ice volume in the Gulf of St. Lawrence (upper panel) and on the Scotian Shelf seaward of Cabot Strait (lower panel). Scorecards show numbered normalized anomalies for the Gulf, combined Gulf and Shelf and Shelf-only annual maximum volumes from weekly ice data. The mean and standard deviation are indicated on the right side using the 1981–2010 climatology.

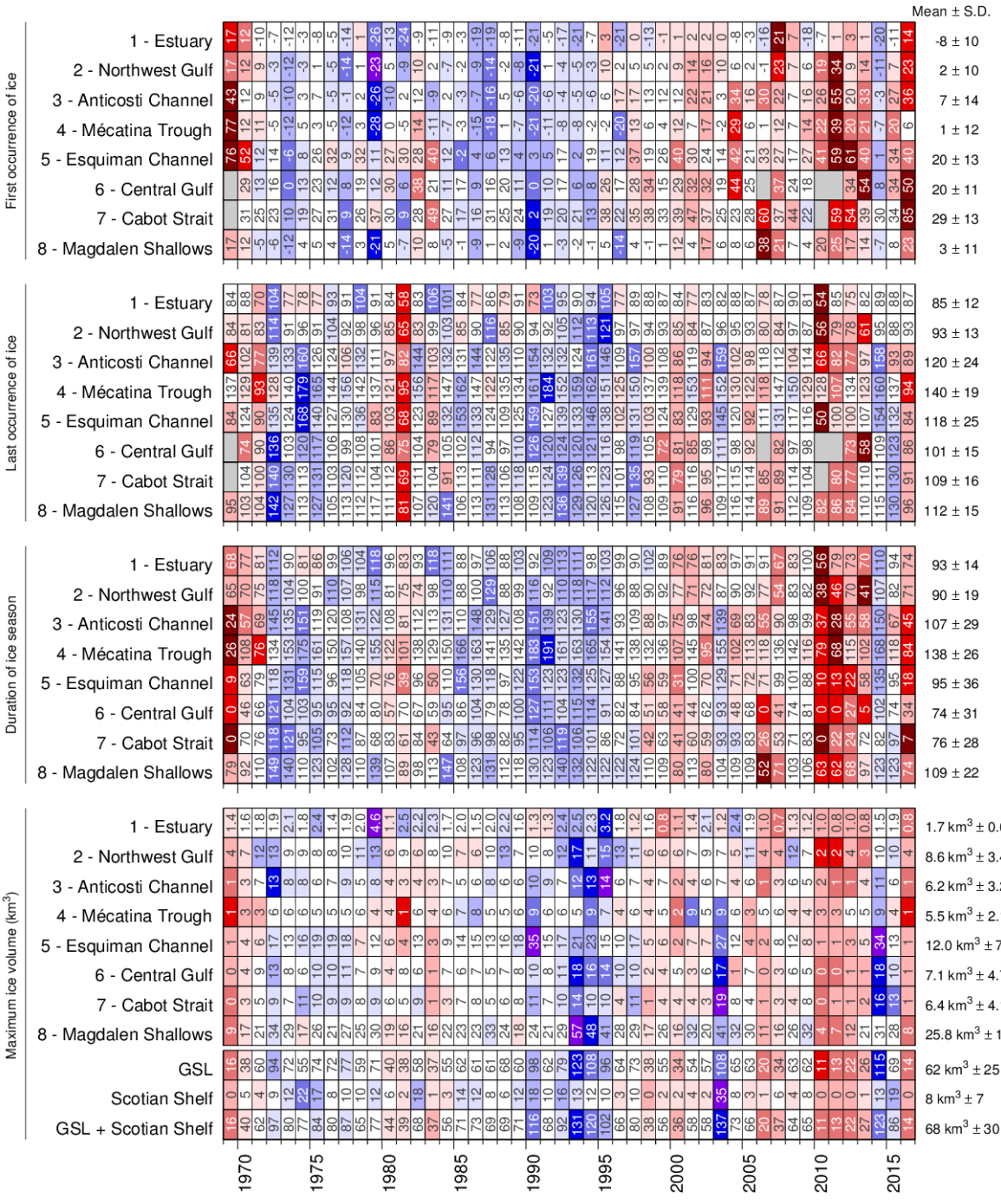

Figure 38. First and last day of ice occurrence, ice duration and maximum seasonal ice volume by region. The time when ice was first and last seen in days from the beginning of each year is indicated for each region, and the colour code expresses the anomaly based on the 1981–2010 climatology, with blue representing earlier first occurrence and later last occurrence. The threshold is 5% of the largest ice volume ever recorded in the region. Numbers in the table are the actual day of the year or volume, but the colour coding is according to normalized anomalies based on the climatology of each region. Duration is the numbers of days that the threshold was exceeded. All results based on weekly data.

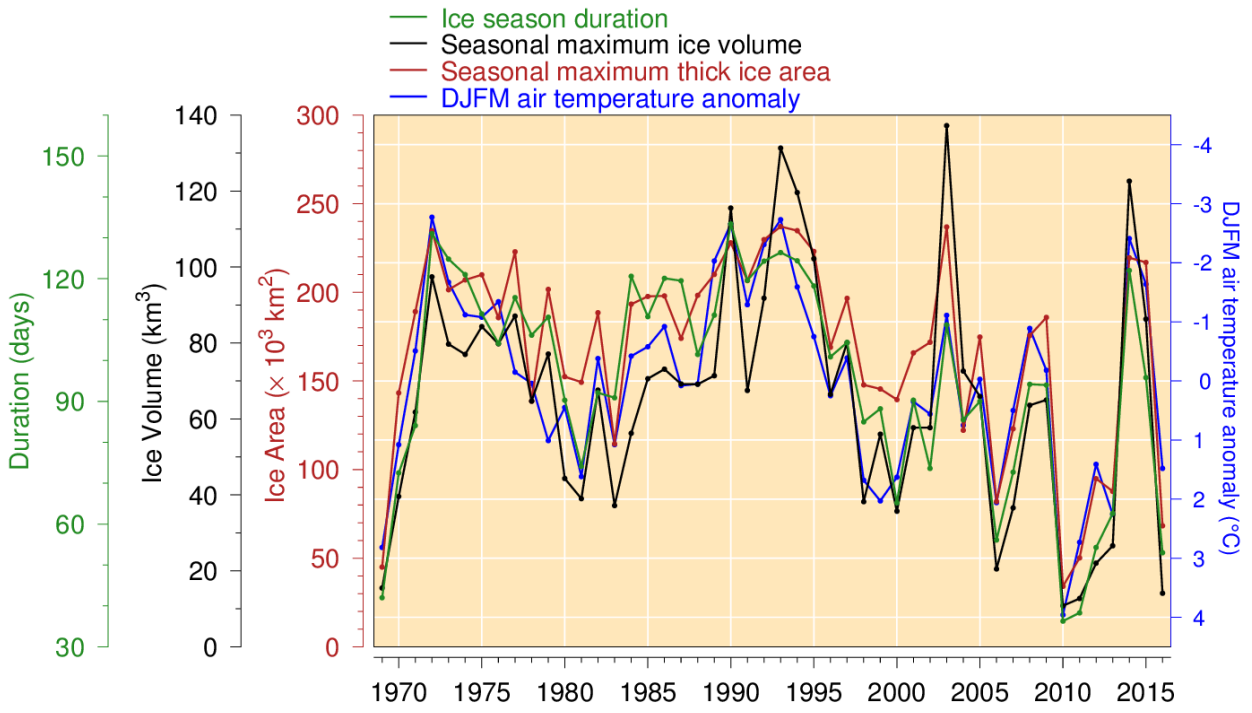

Figure 39. Seasonal maximum ice volume and area including the portion on the Scotian Shelf (excluding ice less than 15 cm thick), ice season duration and December-to-March air temperature anomaly (Figure adapted from Hammill and Galbraith 2012, but here not excluding small floes and adding February and March data to the air temperature anomalies). All sea-ice products are based on weekly data. Linear relations indicate losses of 17 km^3, 30,000 km^2 and 14 days of sea-ice season for each 1°C increase in winter air temperature (R^2 of 0.74, 0.80 and 0.76 respectively).

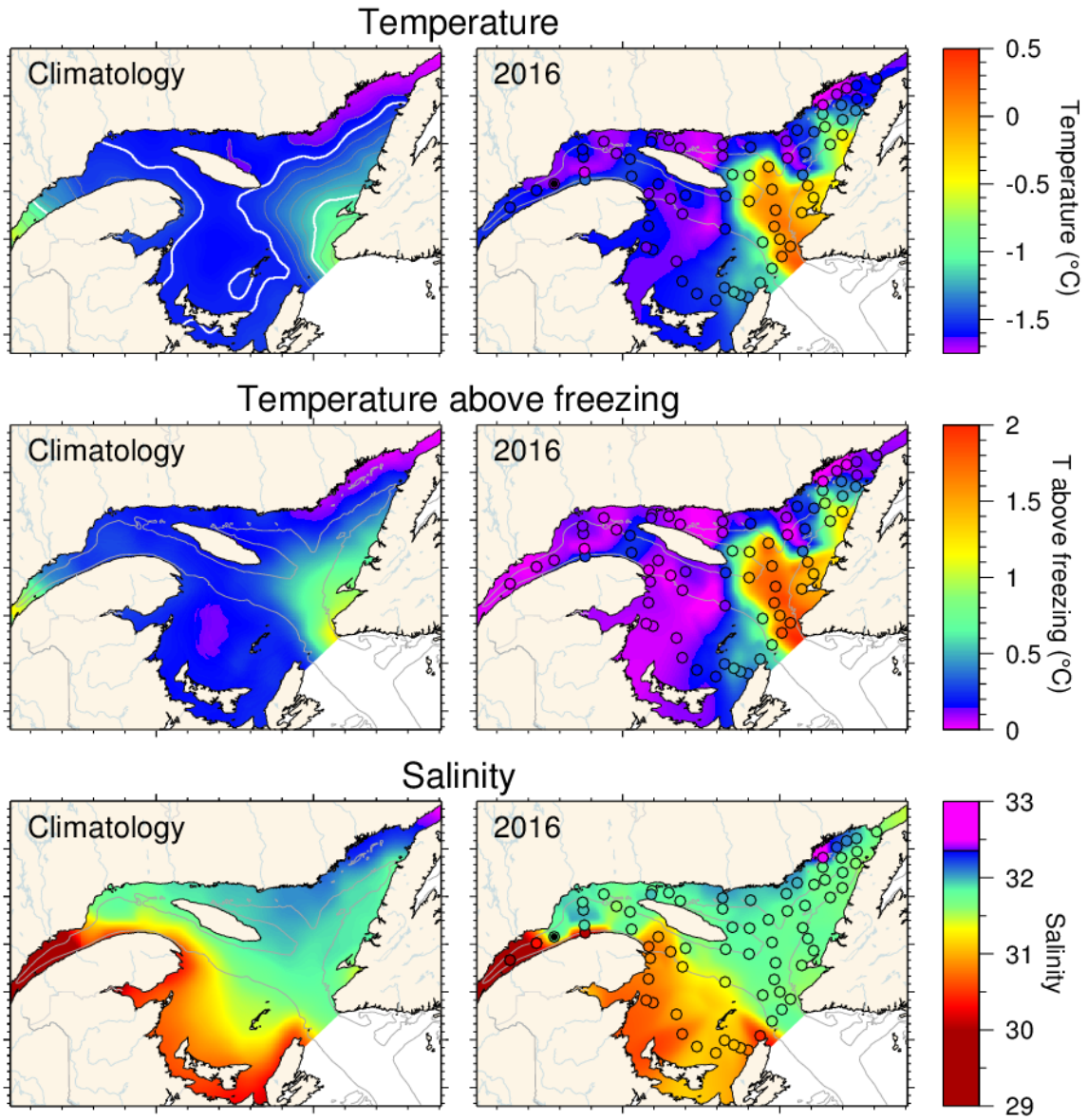

Figure 40. Winter surface layer characteristics from the March 2016 survey compared with climatological means: surface water temperature (upper panel), temperature difference between surface water temperature and the freezing point (middle panel), and salinity (lower panel). Symbols are coloured according to the value observed at the station, using the same colour palette as the interpolated image. A good match is seen between the interpolation and the station observations where the station colours blend into the background. Black symbols indicate missing or bad data. The climatologies are based on 1996-2016 for salinity but exclude 2010 as an outlier for temperature and temperature above freezing.

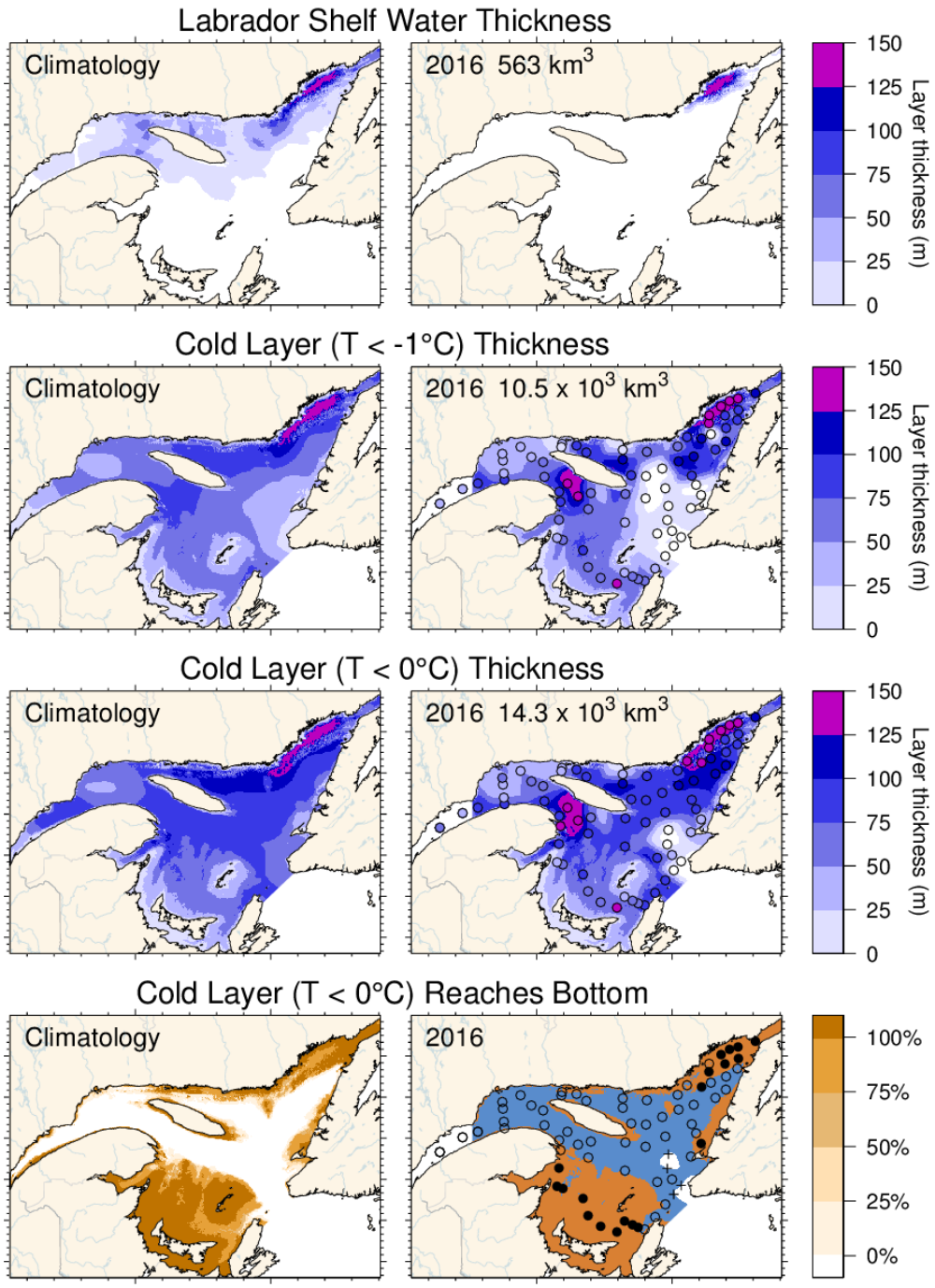

Figure 41. Winter surface layer characteristics from the March 2016 survey compared with climatological means: estimates of the thickness of the Labrador Shelf water intrusion (upper panels), cold layer (T<-1°C, T<0°C) thickness (middle panels), and maps indicating where the cold layer (T<0°C) reaches the bottom (in brown; lower panels). Station symbols are coloured according to the observed values as in Fig. 40. For the lower panels, the stations where the cold layer reached the bottom are indicated with filled circles while open circles represent stations where the layer did not reach the bottom. Integrated volumes are indicated for the first six panels (including an approximation for the Estuary but excluding the Strait of Belle Isle). The climatologies are based on 1997-2016 for the Labrador Shelf water intrusion, 1996-2016 for the cold layer (T<0°C) but excludes 2010 for T<-1°C.

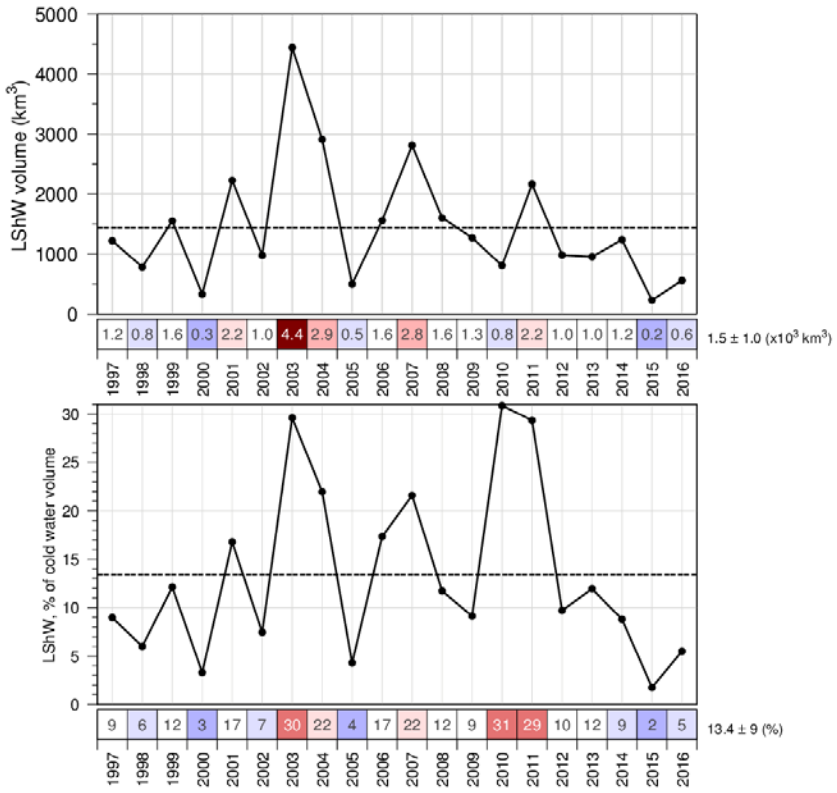

Figure 42. Estimated volume of cold and saline Labrador Shelf water that flowed into the Gulf over the winter through the Strait of Belle Isle. The bottom panel shows the volume as a percentage of total cold-water volume (<-1ºC). The numbers in the boxes are actual values colour-coded according to their 1997-2016 climatology anomaly.

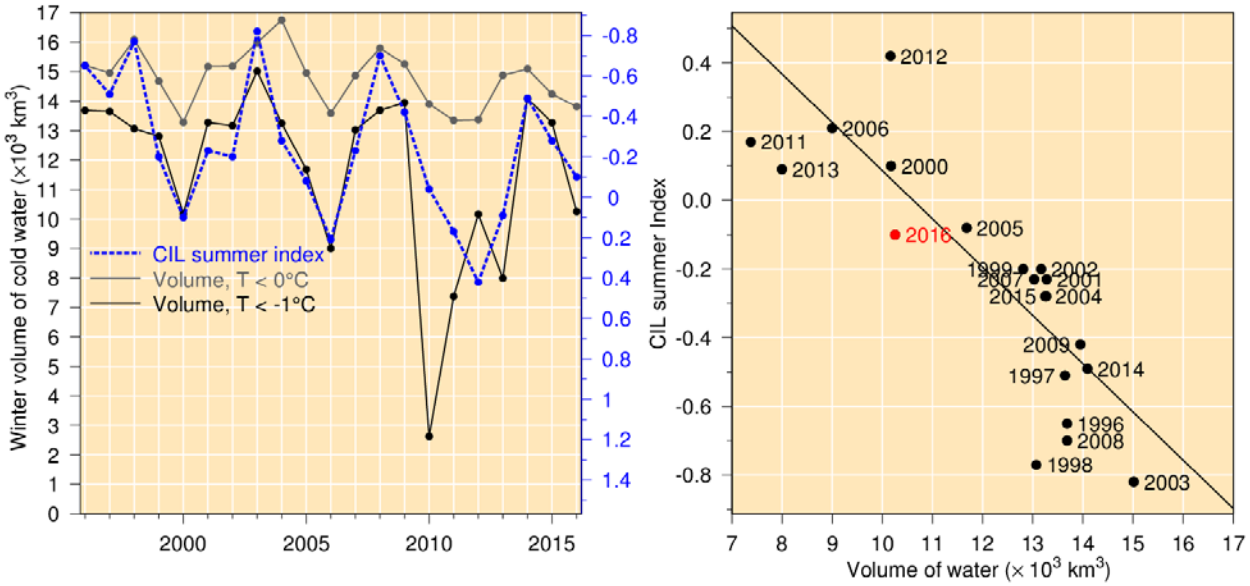

Figure 43. Left panel: winter surface cold (T<-1°C and T<0°C) layer volume (excluding the Estuary and the Strait of Belle Isle) time series (black and grey lines) and summer CIL index (blue dashed line). Right panel: Relation between summer CIL index and winter cold-water volume with T<-1°C (regression for 1996-2014 data pairs, excluding 1998 [see Galbraith 2006] as well as the 2010 and 2011 mild winters). Note that the CIL scale in the left panel is reversed.

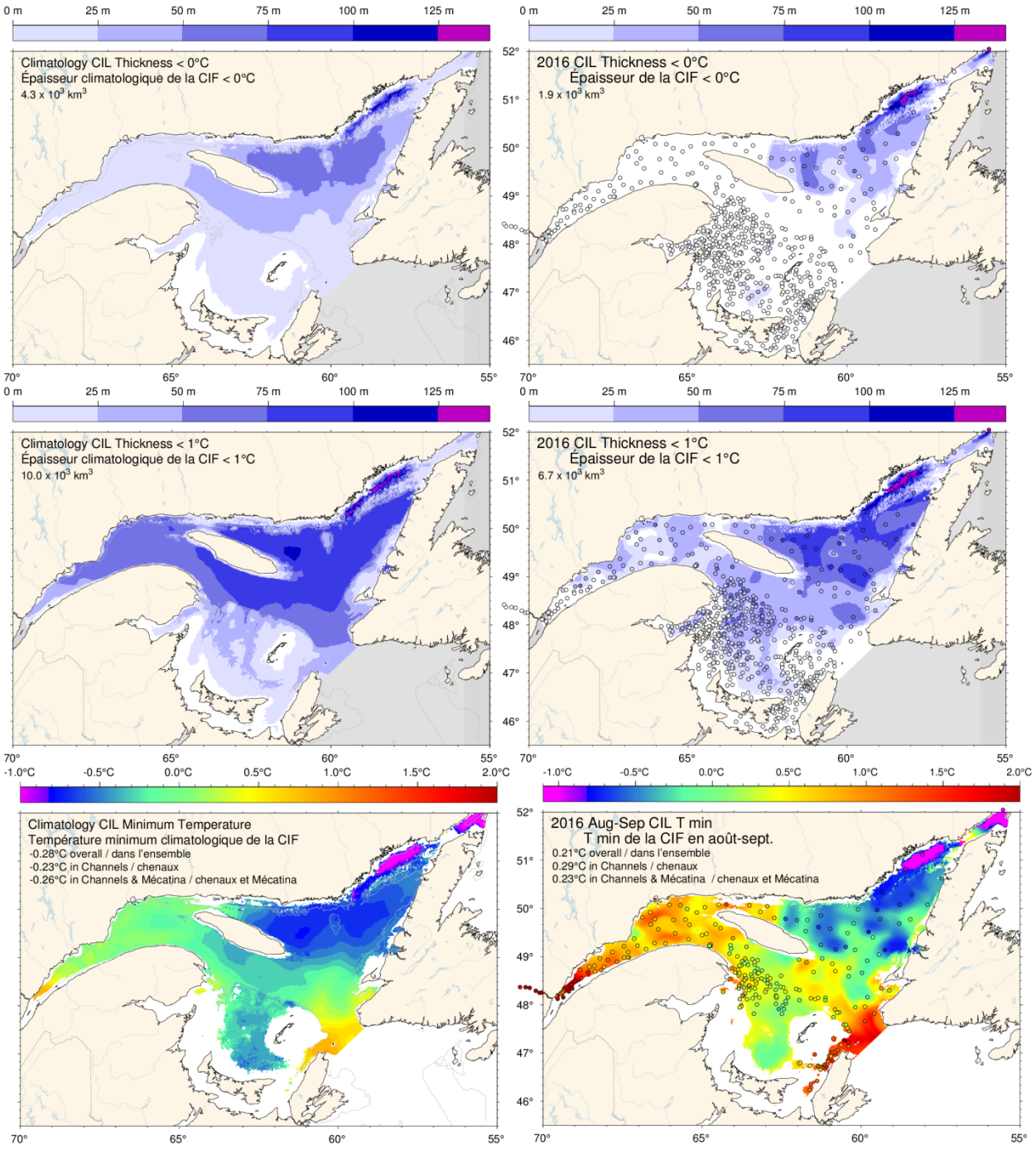

Figure 44. Cold intermediate layer thickness (T<0ºC, top panels; T<1ºC, middle panels) and minimum temperature (bottom panels) in August and September 2016 (right) and 1985-2010 climatology (left). Station symbols are colour-coded according to their CIL thickness and minimum temperature. Numbers in the upper and middle panels are integrated CIL volumes and in the lower panels are monthly average temperatures.

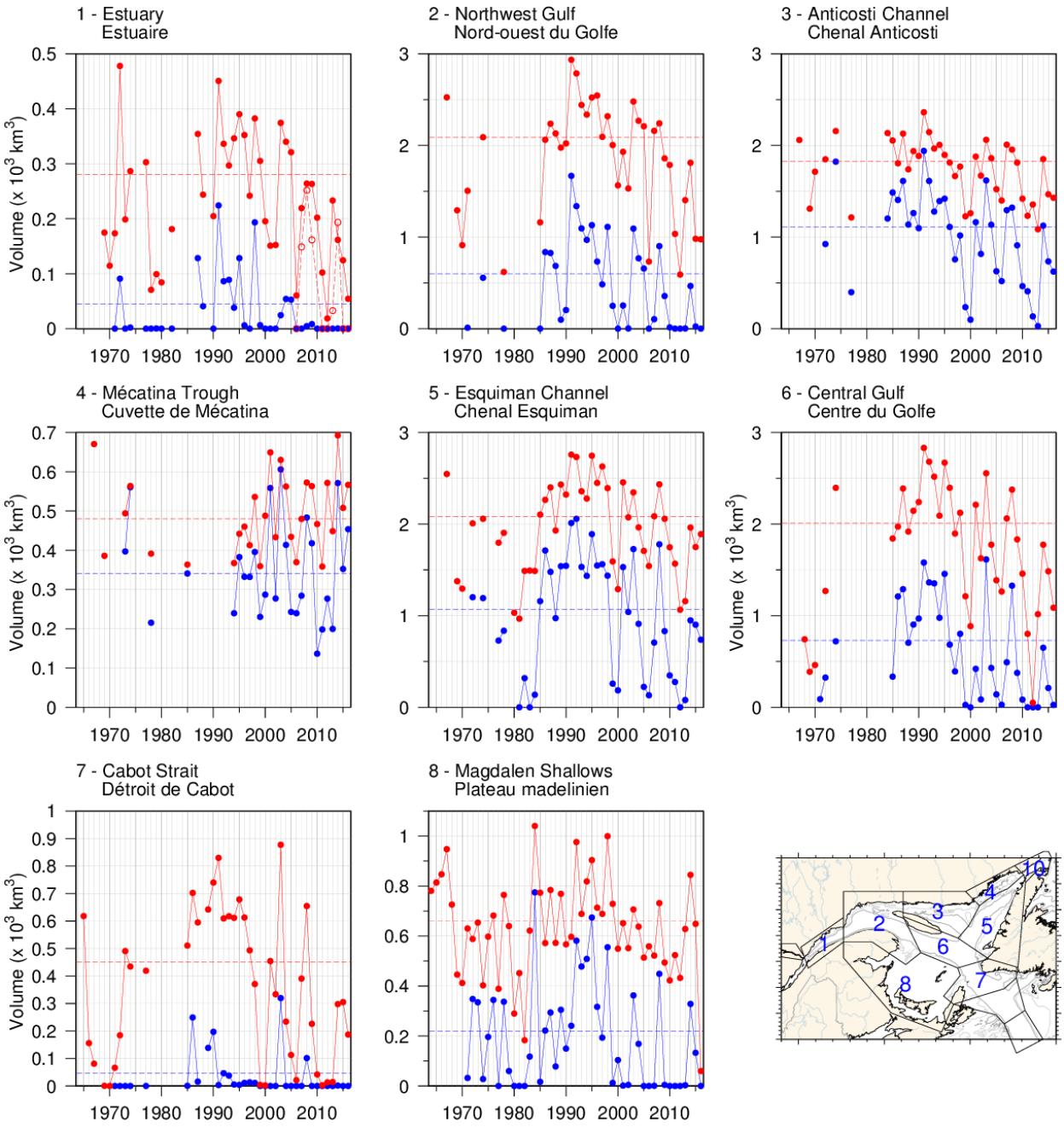

Figure 45. Volume of the CIL colder than 0ºC (blue) and colder than 1ºC (red) in August and September (primarily region 8 in September). The volume of the CIL colder than 1ºC in November for available years since 2006 is also shown for the St. Lawrence Estuary (dashed line).

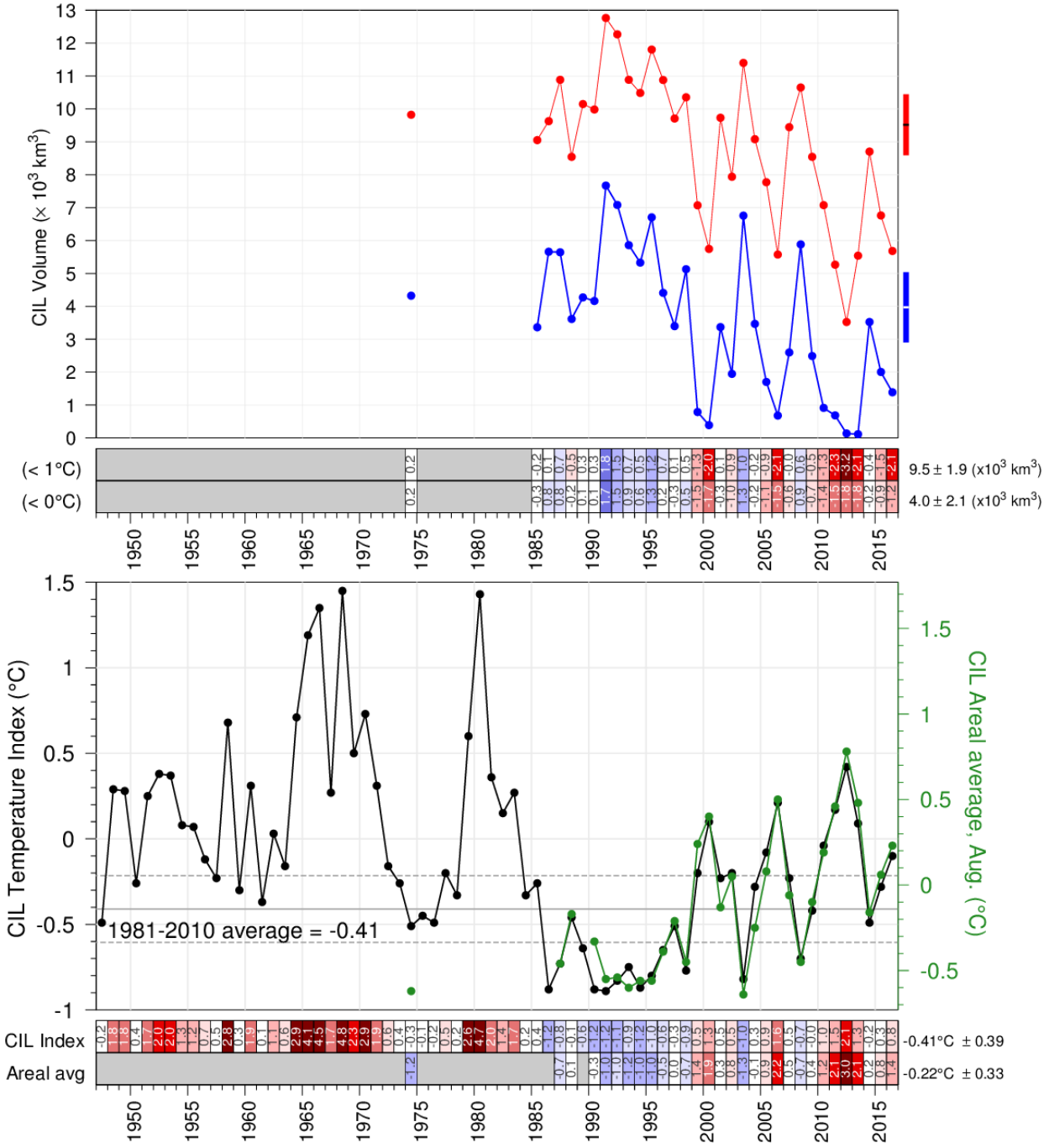

Figure 46. CIL volume (top panel) delimited by 0ºC (in blue) and 1ºC (in red), and minimum temperature index (bottom panel) in the Gulf of St. Lawrence. The volumes are integrals of each of the annual interpolated thickness grids such as those shown in the top panels of Fig. 44 excluding Mécatina Trough and the Strait of Belle Isle. Rectangles on right side show mean ± 0.5 SD. In the lower panel, the black line is the updated Gilbert and Pettigrew (1997) index interpolated to 15 July (with dashed lines showing mean ± 0.5 SD) and the green line is the spatial average of each of the annual interpolated grid such as those shown in the two bottom panels of Fig. 44, excluding Mécatina Trough, the Strait of Belle Isle and the Magdalen Shallows. The numbers in the boxes are normalized anomalies relative to 1980-2010 climatologies constructed using all available years.

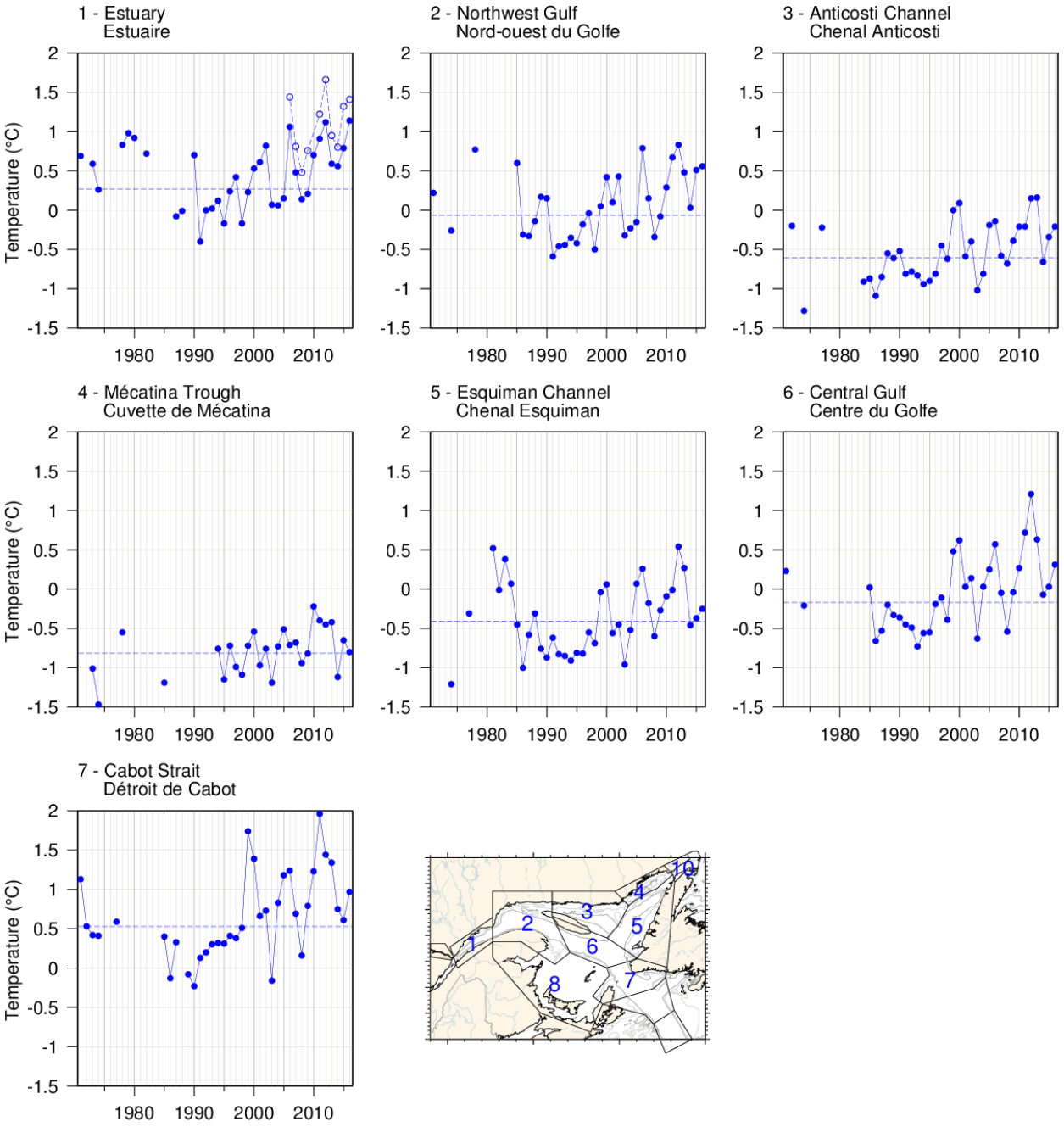

Figure 47. Temperature minimum of the CIL spatially averaged for the seven areas where the CIL minimum temperature can be clearly identified. The spatial average of the November CIL temperature minimum for available years since 2006 is also shown for the St. Lawrence Estuary (dashed line).

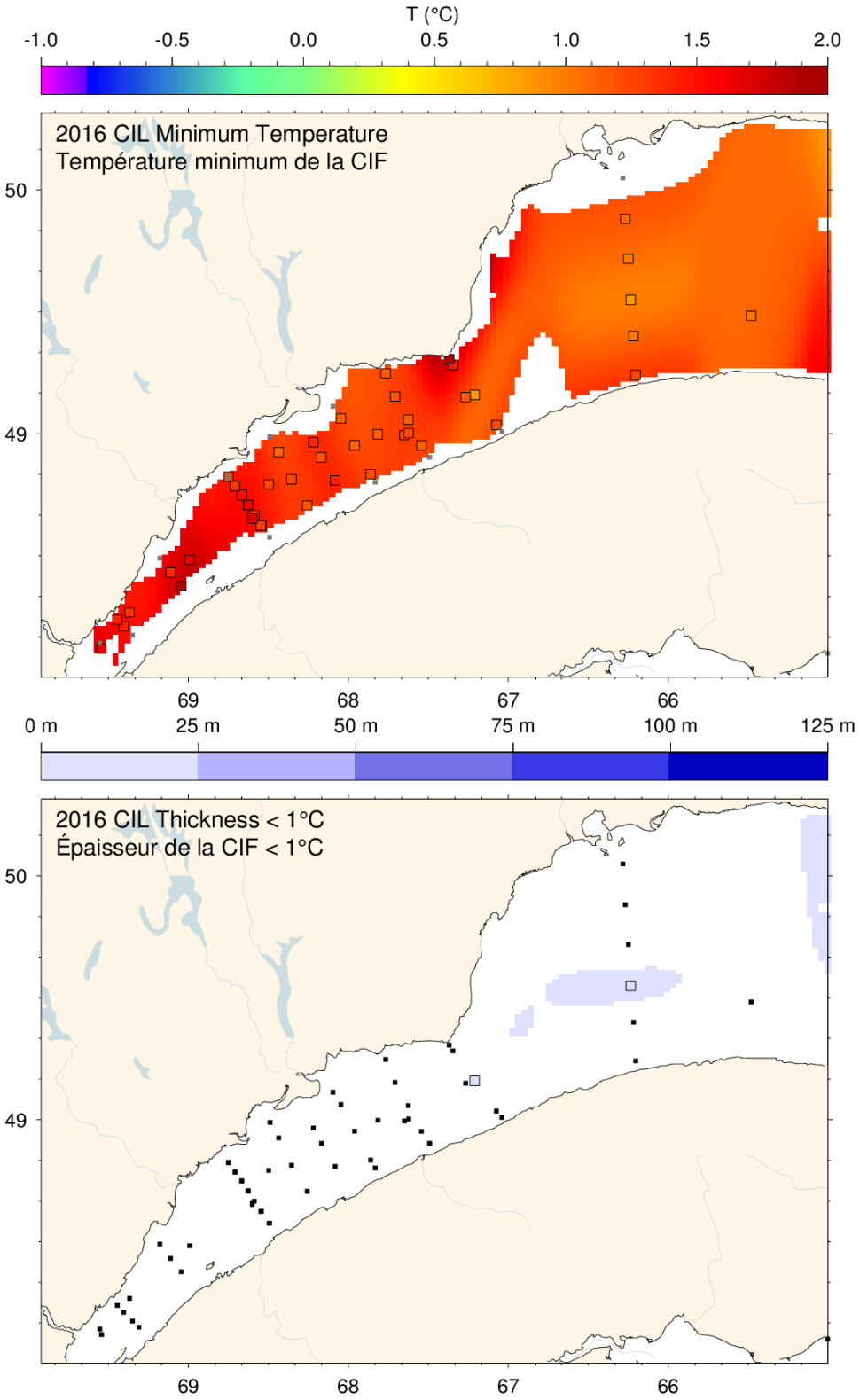

Figure 48. Cold intermediate layer minimum temperature and thickness (T<1°C) in November 2016 in the St. Lawrence Estuary.

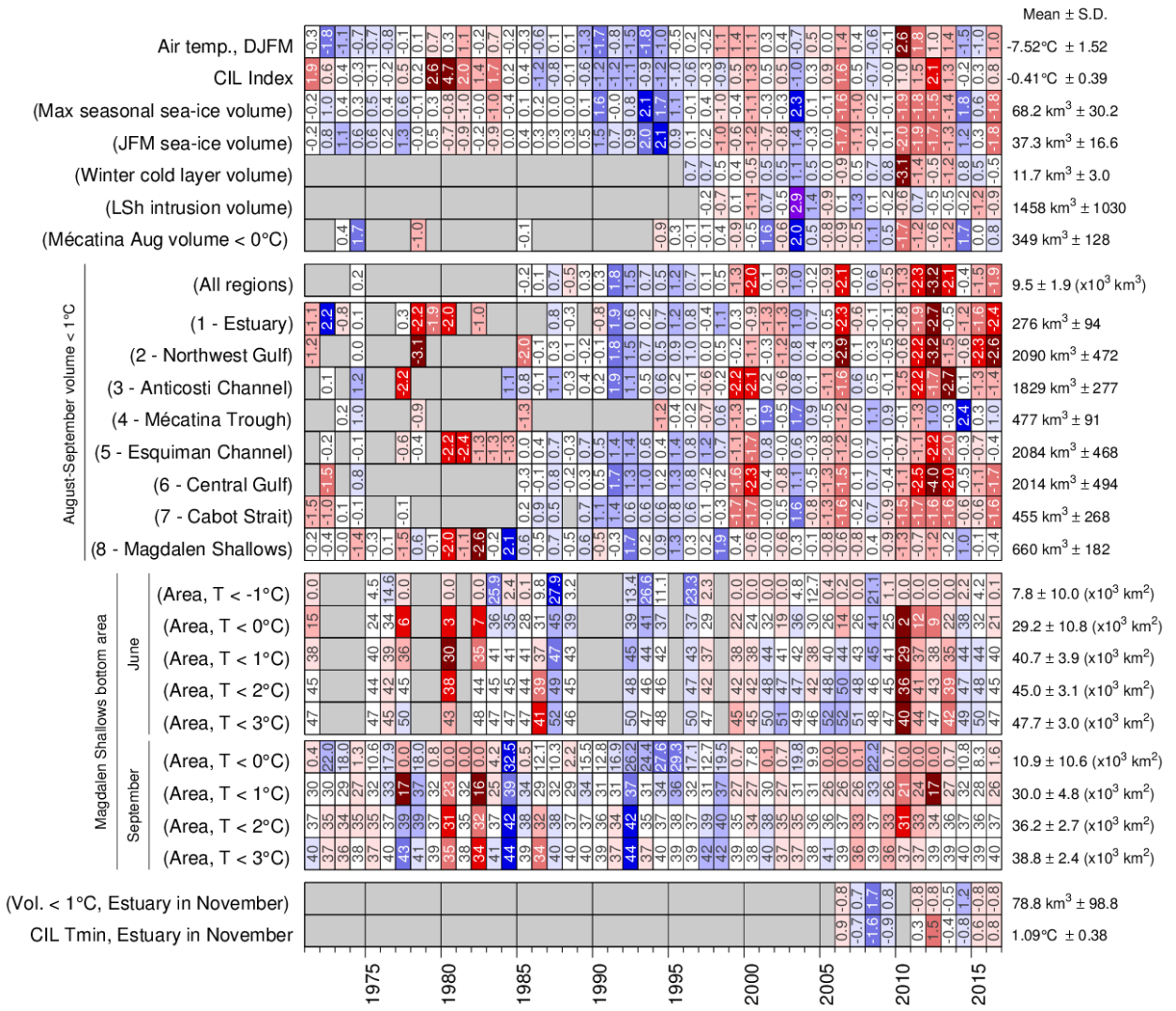

Figure 49. Winter and summertime CIL related properties. The top block shows the scorecard time series for Dec-Jan-Feb-March air temperature (Fig. 5), the Gilbert and Pettigrew (1997) CIL index, yearly maximum sea-ice volume (Gulf + Scotian Shelf), Dec-Jan-Feb average sea-ice volume, winter (March) cold-layer (<-1°C) volume, volume of Labrador Shelf Water intrusion into the Gulf observed in March, and the August–September volume of cold water (<0°C) observed in the Mécatina Trough. Labels in parentheses have their colour coding reversed (blue for high values). The second block shows scorecard time series for August–September CIL volumes (<1°C) for all eight regions and for the entire Gulf when available. The third block shows the scorecard time series for the bottom areas of the Magdalen Shallows covered by waters colder than 0, 1, 2, and 3°C during the June and September survey. The last block shows the November survey CIL volume (<1°C) and average CIL minimum temperature in the Estuary. Numbers in cells express anomalies in units of standard deviation, except for bottom areas which are expressed in units of area (×10³ km²) (because of the occurrence of zeros).

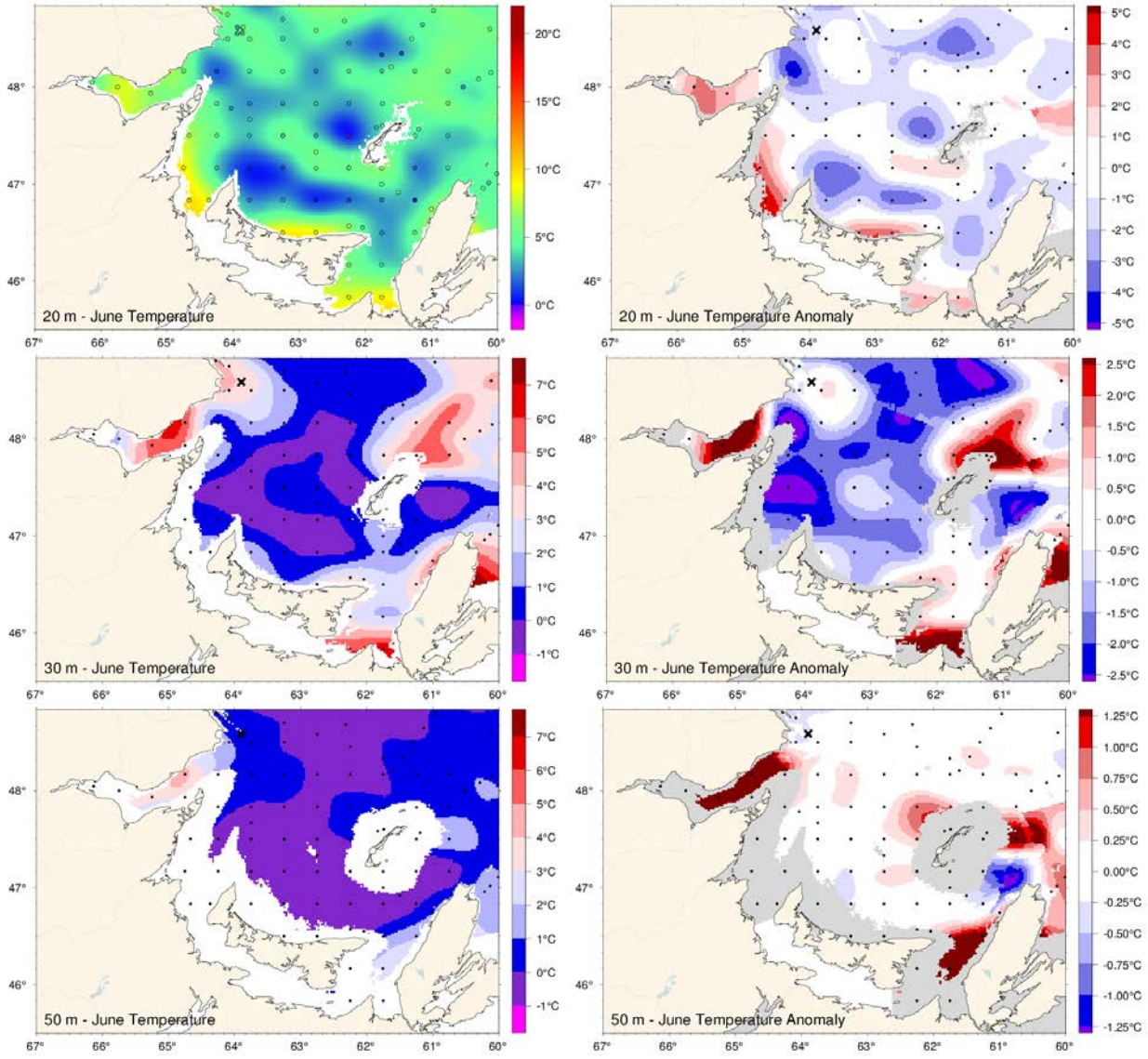

Figure 50. June depth-layer temperature and anomaly fields on the Magdalen Shallows at 10, 20 and 50 m. Anomalies are based on 1971-2010 climatologies for all available years (appearing on Fig. 51) The black outline delimits Region 8 (Fig. 2) and the gray outlines delimit western and eastern regions of the Magdalen Shallows (Fig. 22).

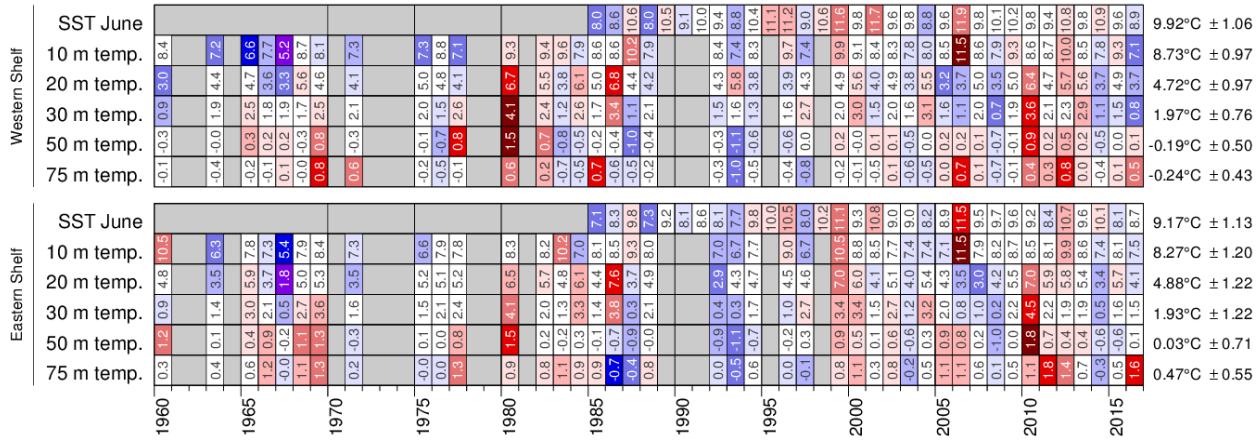

Figure 51. Depth-layer average temperature anomalies for western and eastern Magdalen Shallows for the June mackerel survey. The SST data are June averages from NOAA remote sensing repeated from Fig. 23. The SST colour-coding is based on the 1985-2010 climatology and the numbers are mean temperatures in ºC. The colour-coding of the 10 to 75 m lines are according to normalized anomalies based on the 1981-2010 climatologies, but the numbers are mean temperatures in ºC.

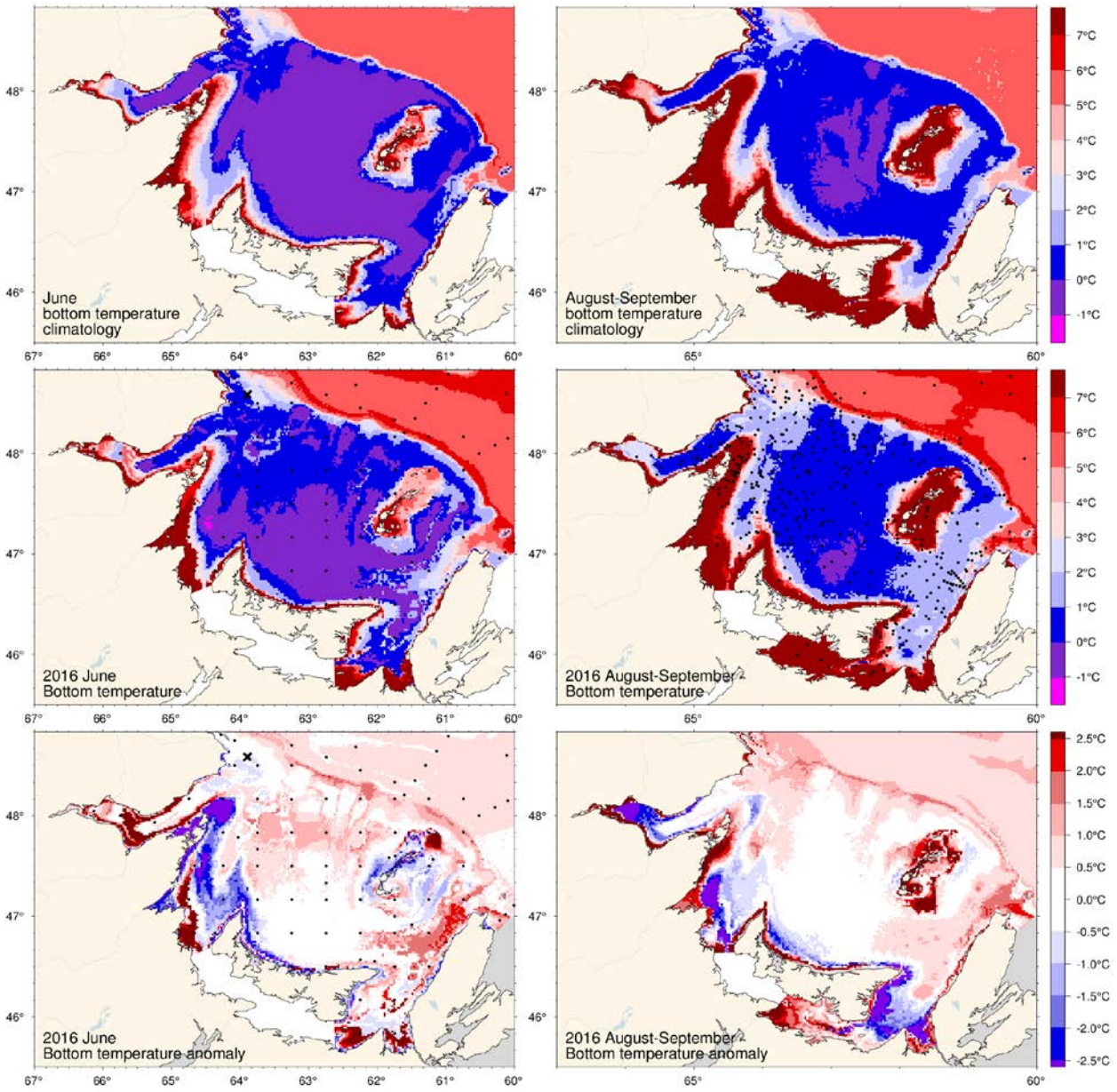

Figure 52. June (left) and August-September (right) bottom temperature climatology (top), 2016 observations (middle) and anomaly (bottom).

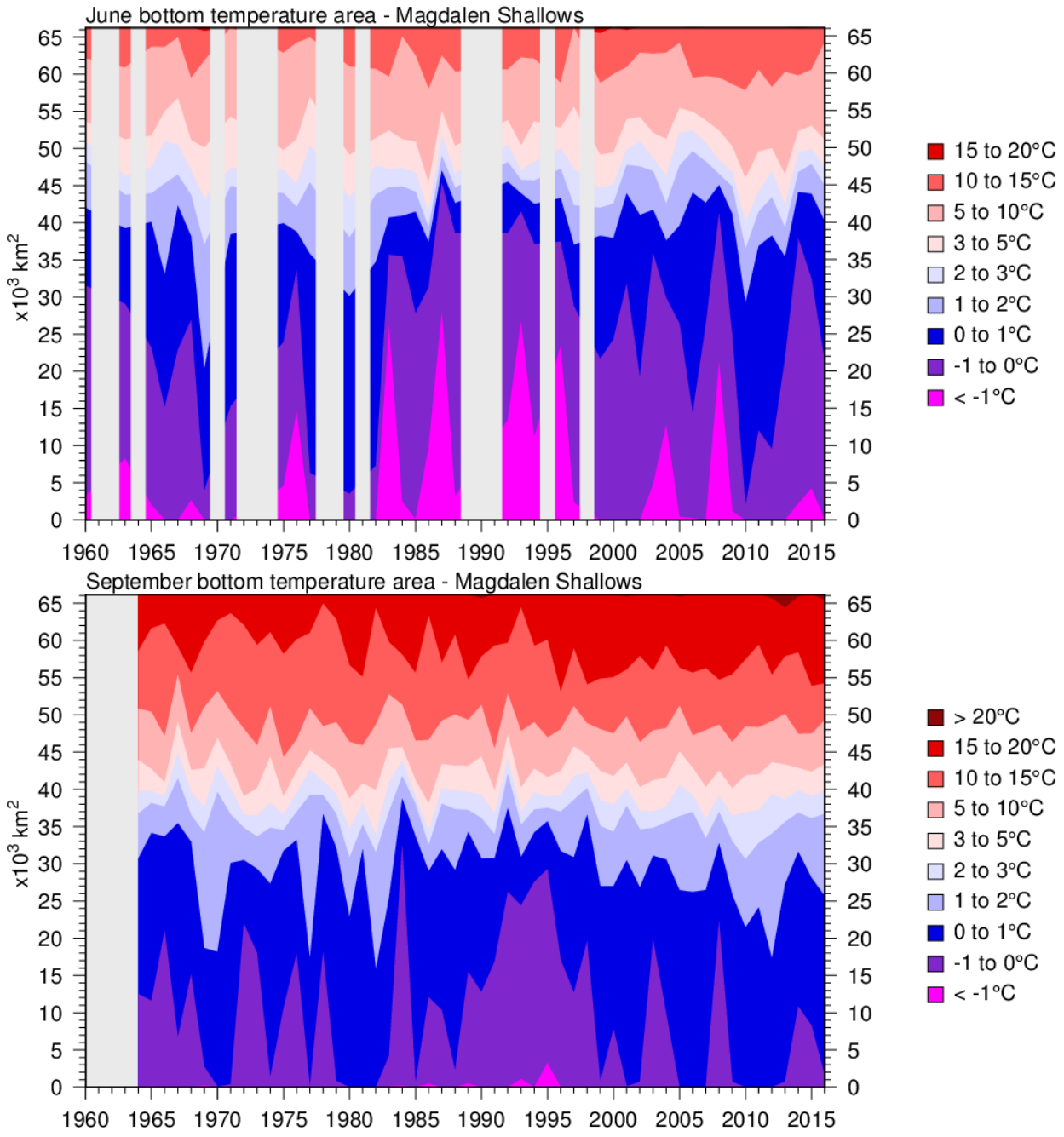

Figure 53. Time series of the bottom areas covered by different temperature bins in June (top) and August-September (bottom) for the Magdalen Shallows (region 8). Data are mostly from September for the bottom panel.

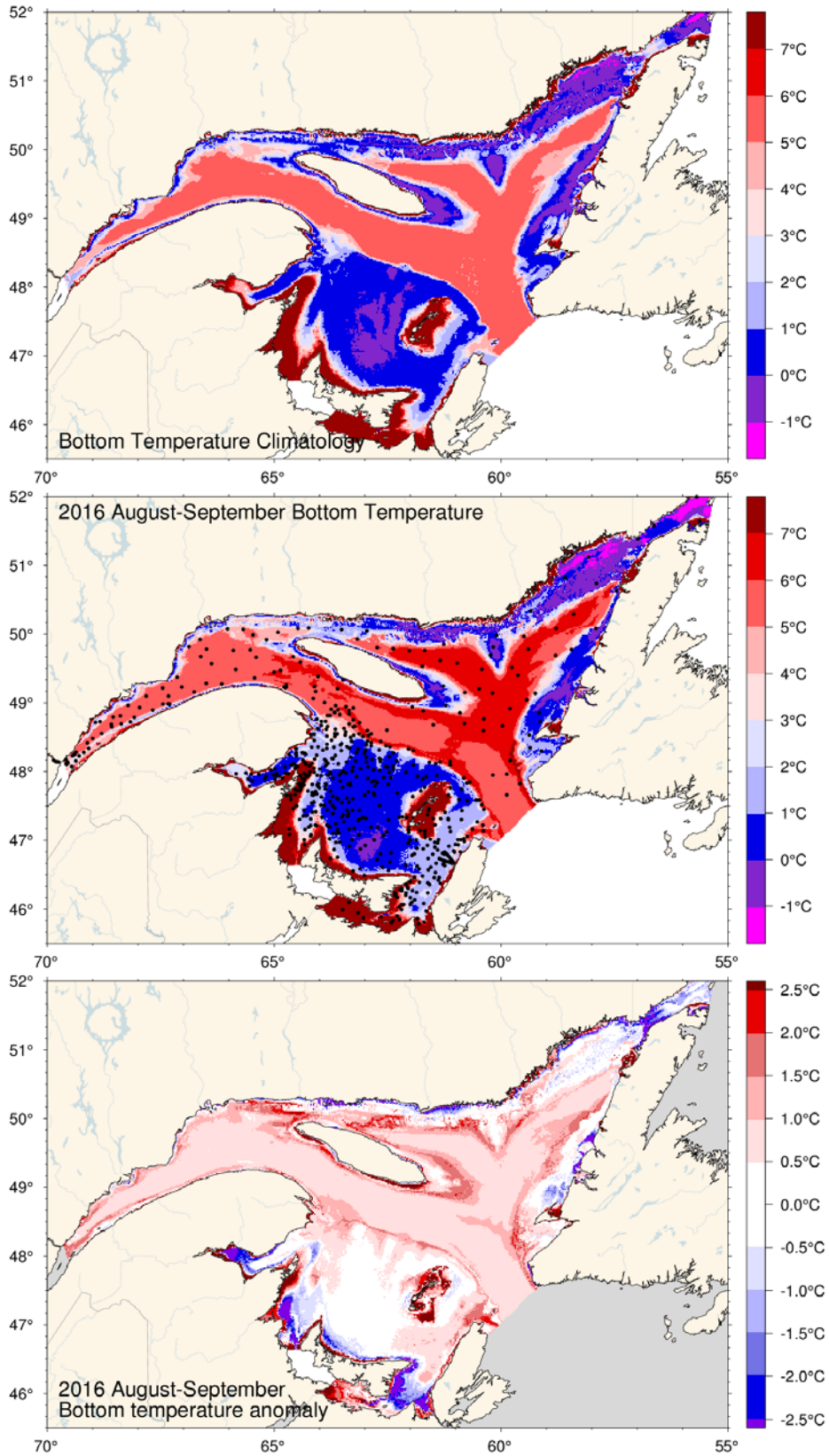

Figure 54. August-September bottom temperature climatology (top), 2016 observations (middle) and anomaly (bottom).

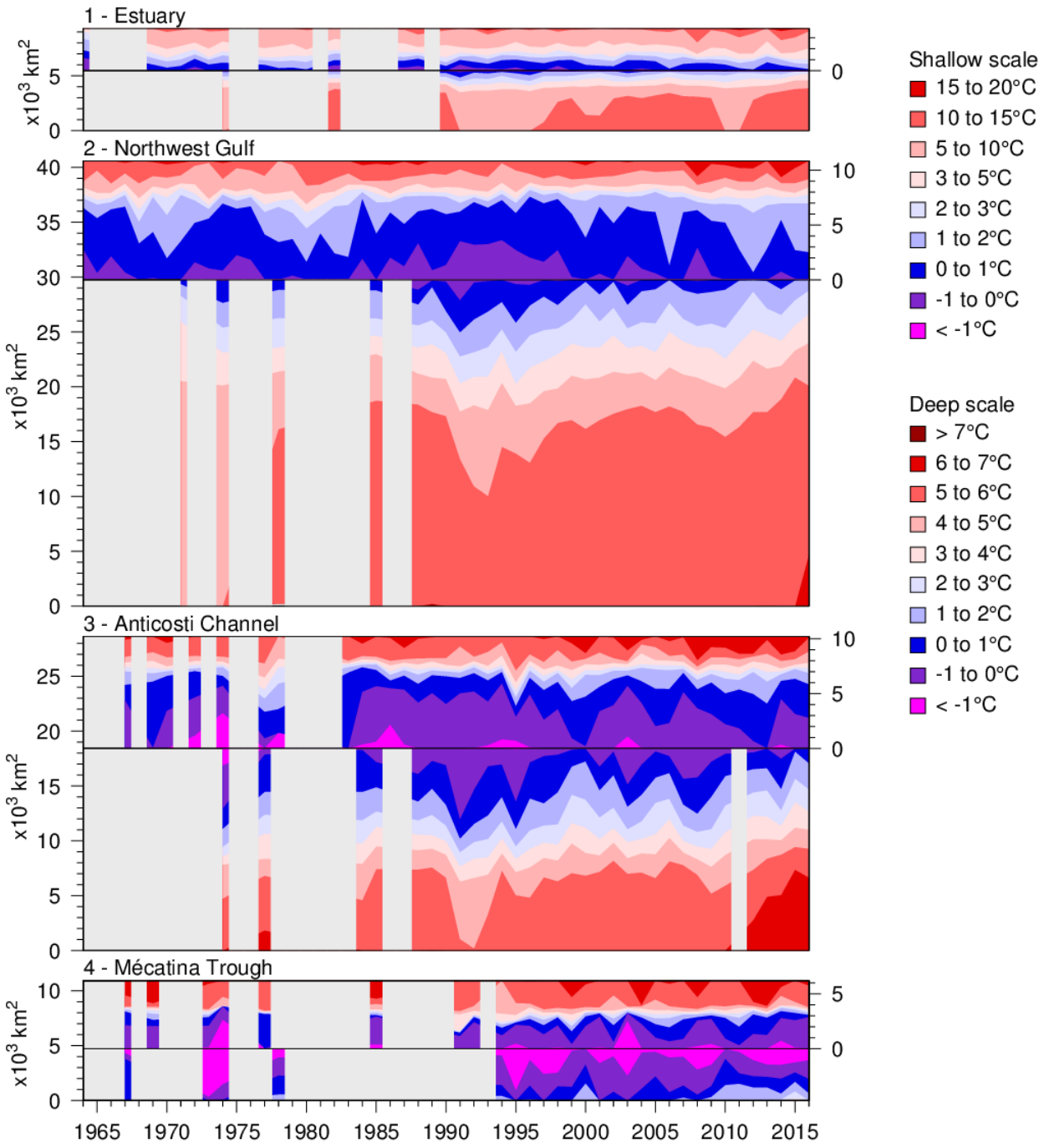

Figure 55. Time series of the bottom areas covered by different temperature bins in August and September for regions 1 to 4. The panels are separated by a black horizontal line into shallow (<100m) and deep (>100 m) areas to distinguish between warmer waters above and below the CIL. The shallow areas are shown on top using the area scale on the right-hand side and have warmer waters shown starting from the top end. The deep areas are shown below the horizontal line and have warmer waters starting at the bottom end. The CIL areas above and below 100 m meet near the horizontal line.

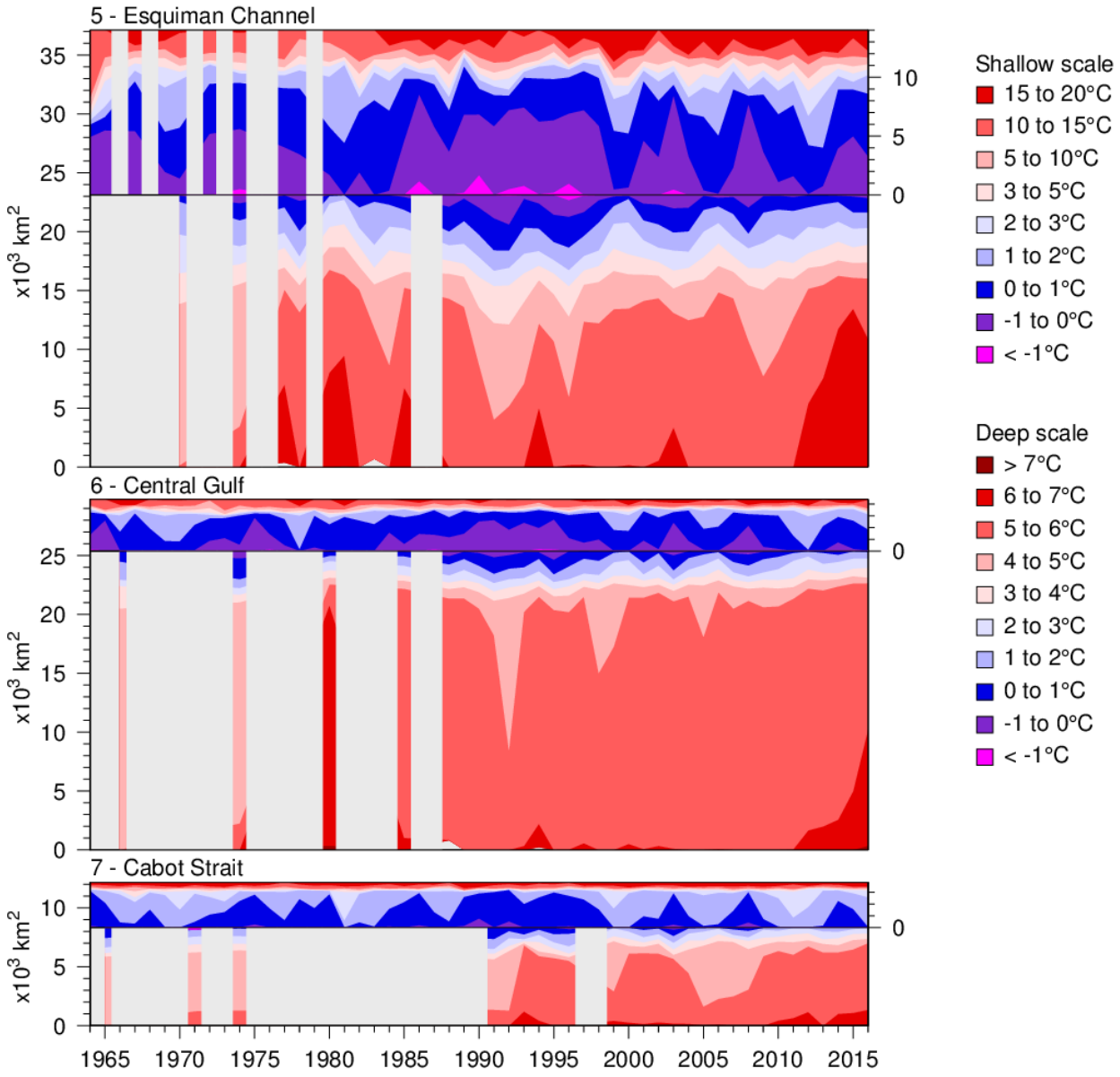

Figure 56. Time series of the bottom areas covered by different temperature bins in August and September for regions 5 to 7. The panels are separated into shallow (<100 m) and deep (>100 m) areas to distinguish between warmer waters above and below the CIL See Fig. 55 caption.

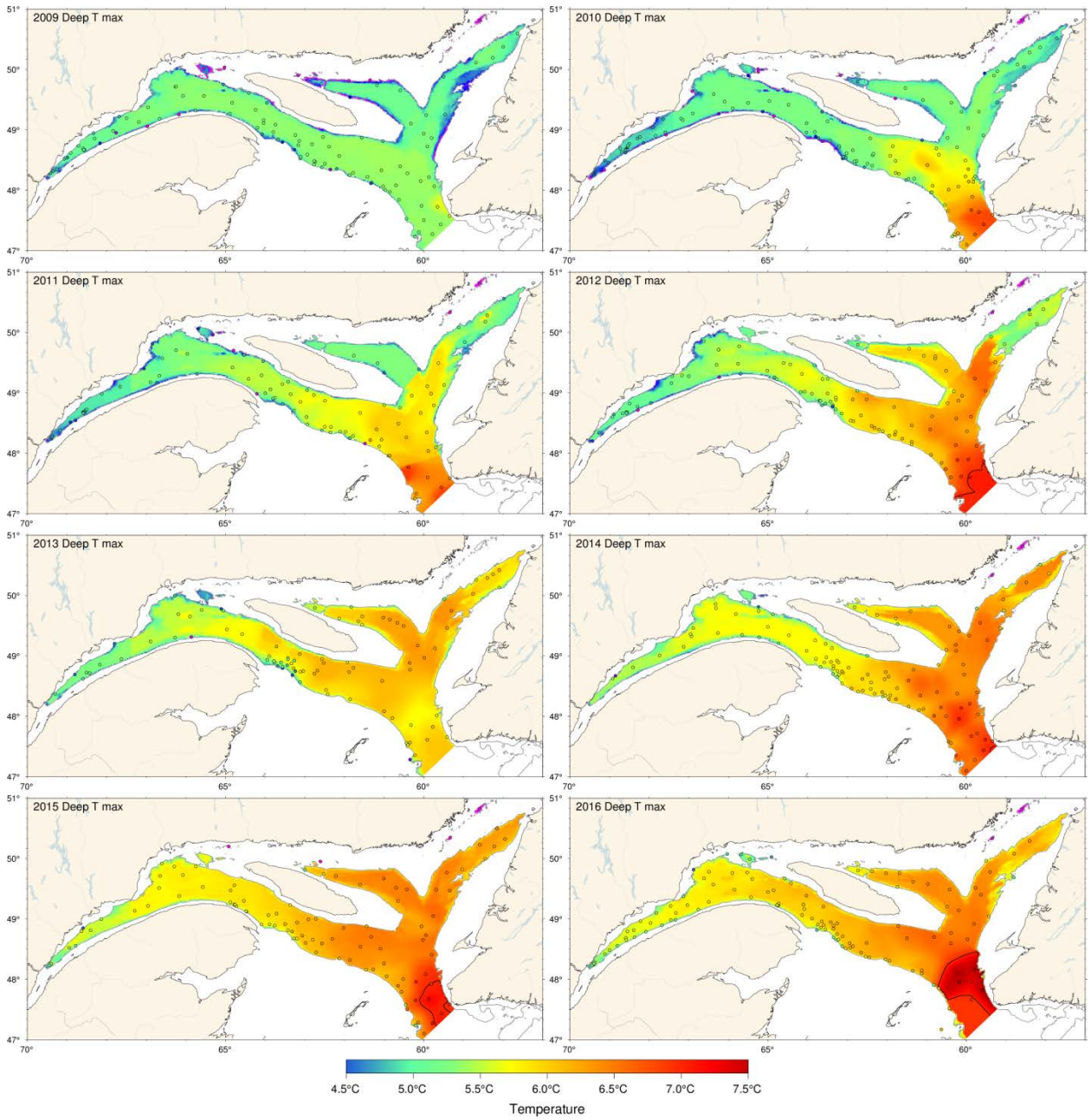

Figure 57. Map of the deep temperature maximum found typically between 200 and 300 m, 2009-2016. Maps are interpolated from August-September data available for each year.

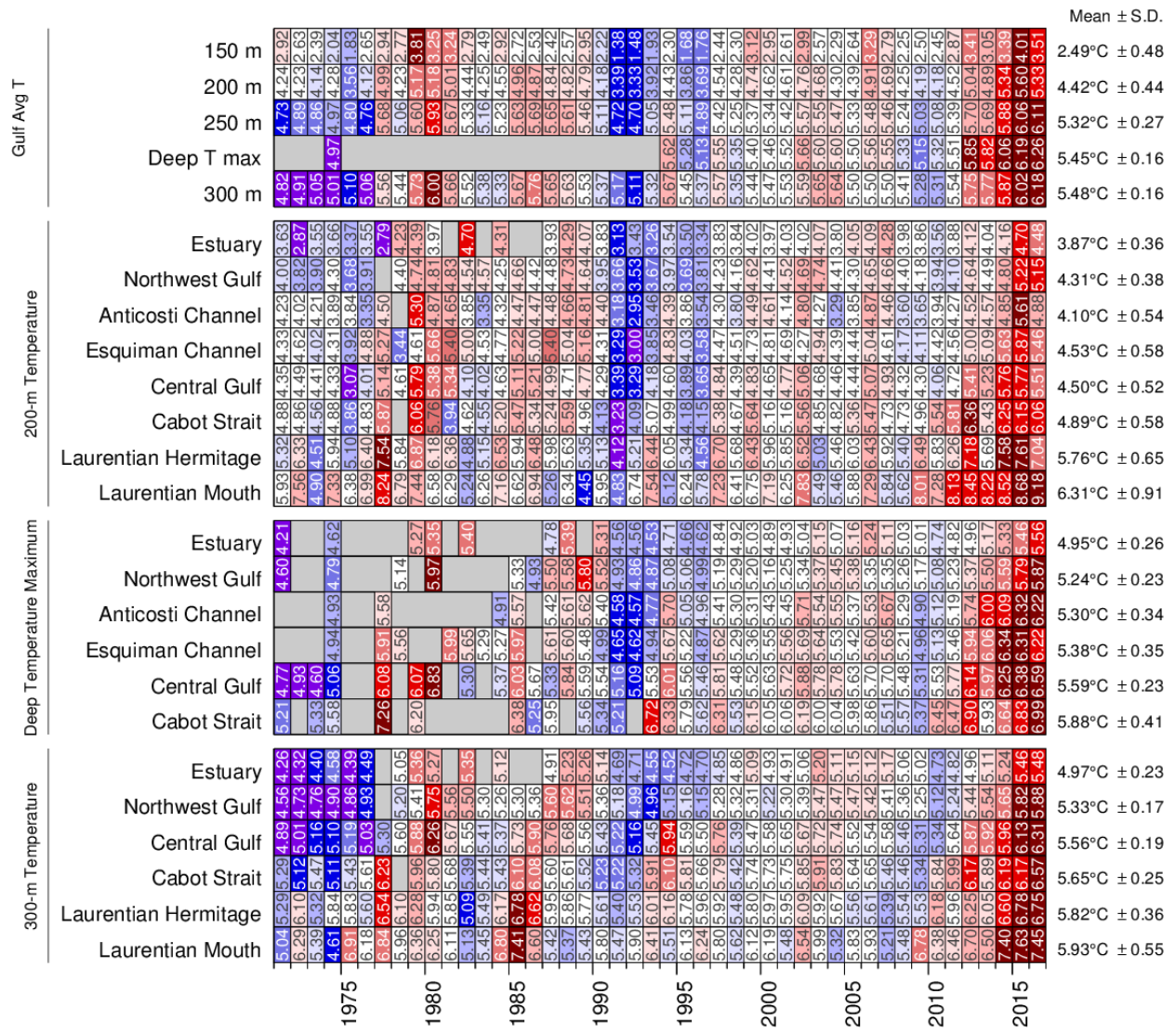

Figure 58. Deep layer temperature. Gulf averages for temperature are shown for 150, 200, 250, 300 m, as well as for the deep temperature maximum usually found between 200 and 300 m. Regional averages are shown for 200 and 300m, and deep temperature maximum. The numbers on the right are the 1981–2010 climatological means and standard deviations. The numbers in the boxes are normalized anomalies.

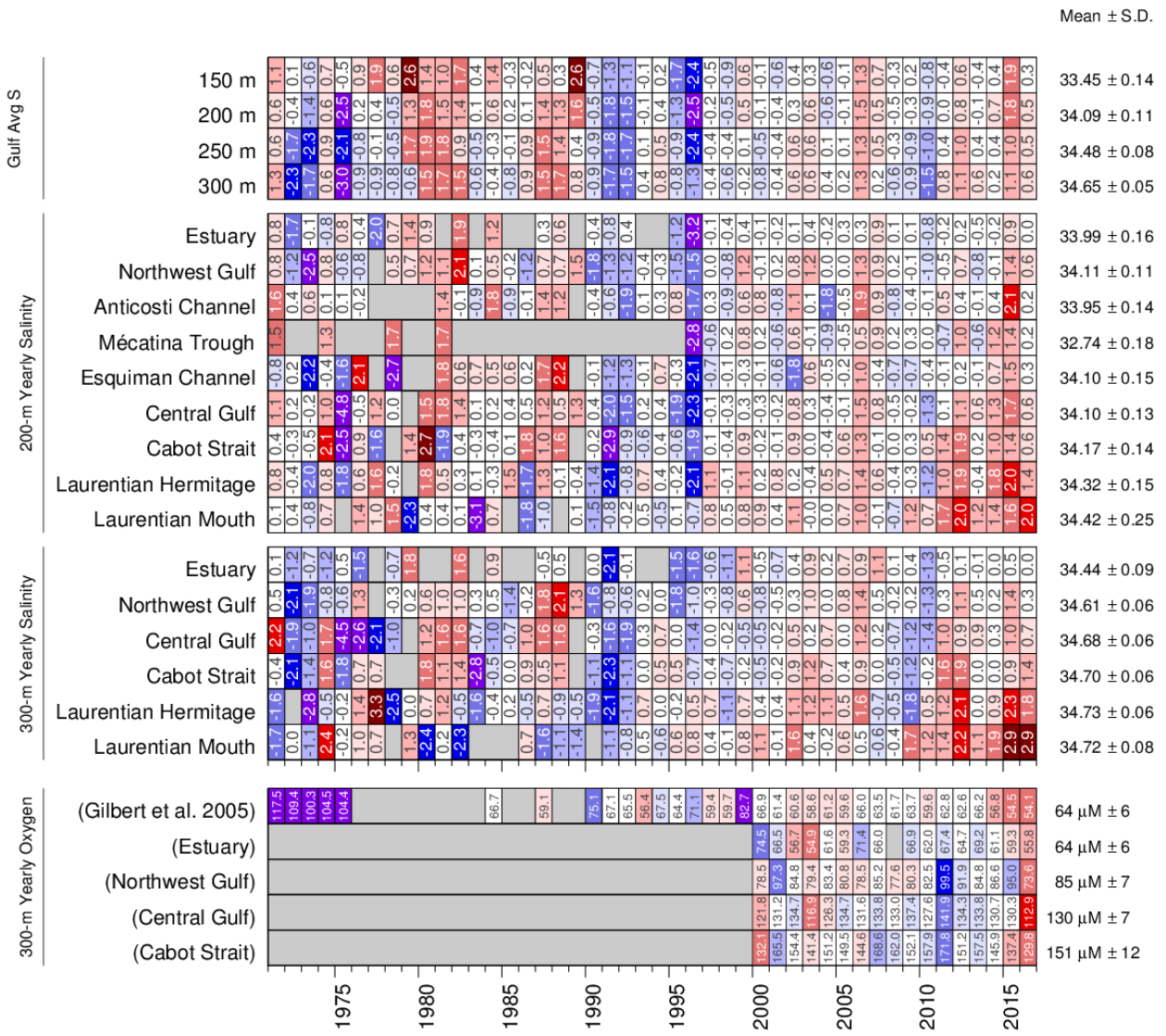

Figure 59. Deep layer salinity and dissolved oxygen. Gulf averages for salinity are shown for 150, 200, 250, and 300 m. Regional averages are shown for 200 and 300m. Dissolved oxygen is shown with an inverted colour scheme for the updated Gilbert et al. 2005 time series as well as recent regional averages at 300 m obtained using a Seabird SBE43 CTD sensor. The numbers on the right are the 1981–2010 climatological means and standard deviations. The numbers in the boxes are normalized anomalies, except for oxygen where physical values are shown for easier comparison between the Gilbert et al. 2005 time series and the CTD data.

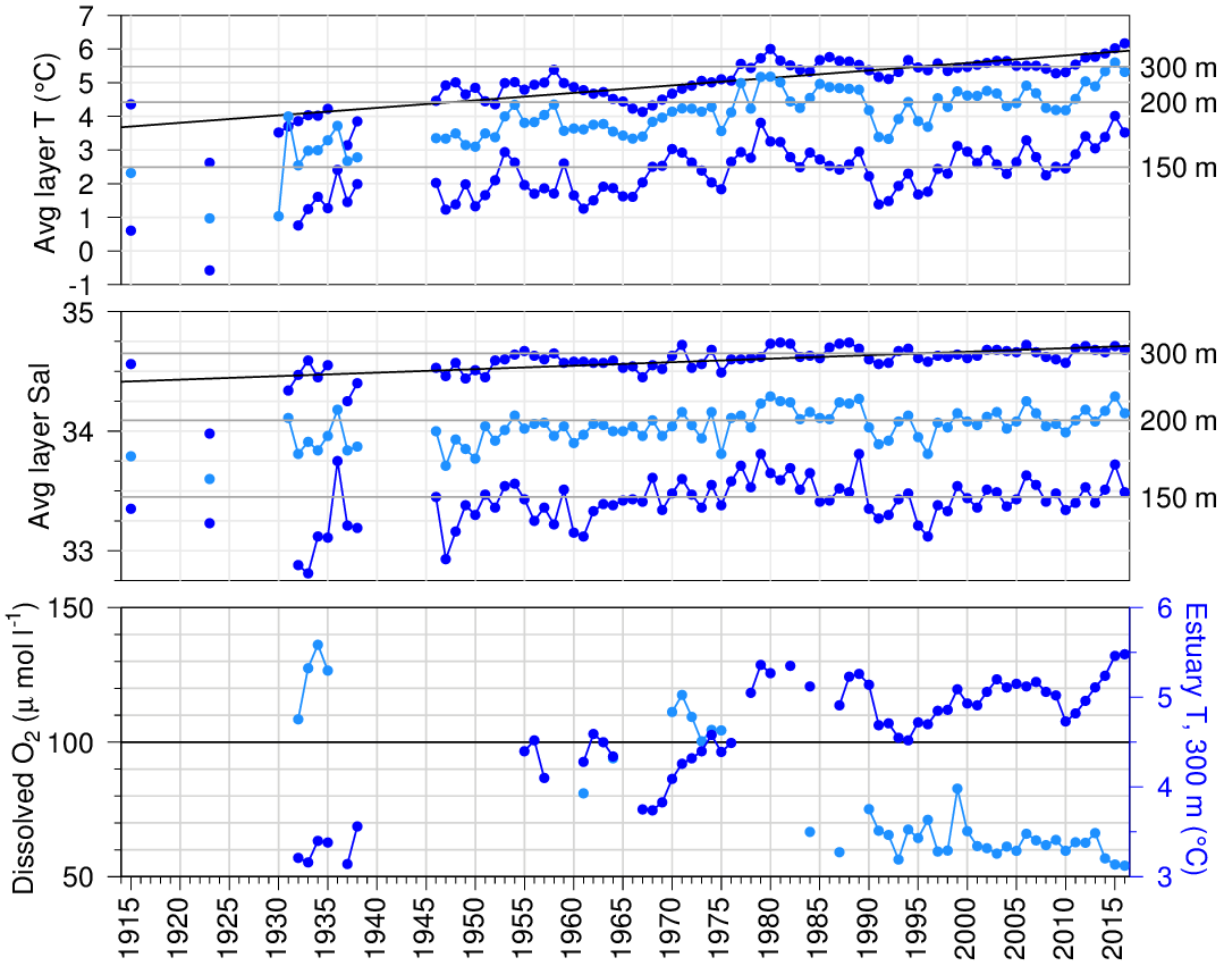

Figure 60. Layer-averaged temperature and salinity time series for the Gulf of St. Lawrence and dissolved oxygen between 295 m and the bottom in the deep central basin of the St. Lawrence Estuary. The temperature and salinity panels show the 150 m, 200 m, and 300 m annual averages and the horizontal lines are 1981–2010 means. Sloped lines show linear regressions for temperature and salinity at 300 m of respectively 2.2°C and 0.3 per century. The horizontal line in the oxygen panel corresponds roughly to 30% saturation and marks the threshold of hypoxic conditions. In addition to the dissolved oxygen time series (light blue), the lower panel also shows temperature (dark blue) at 300 m in the Estuary. The horizontal line at 100 µ mol l^{-1} corresponds to about 30% saturation.

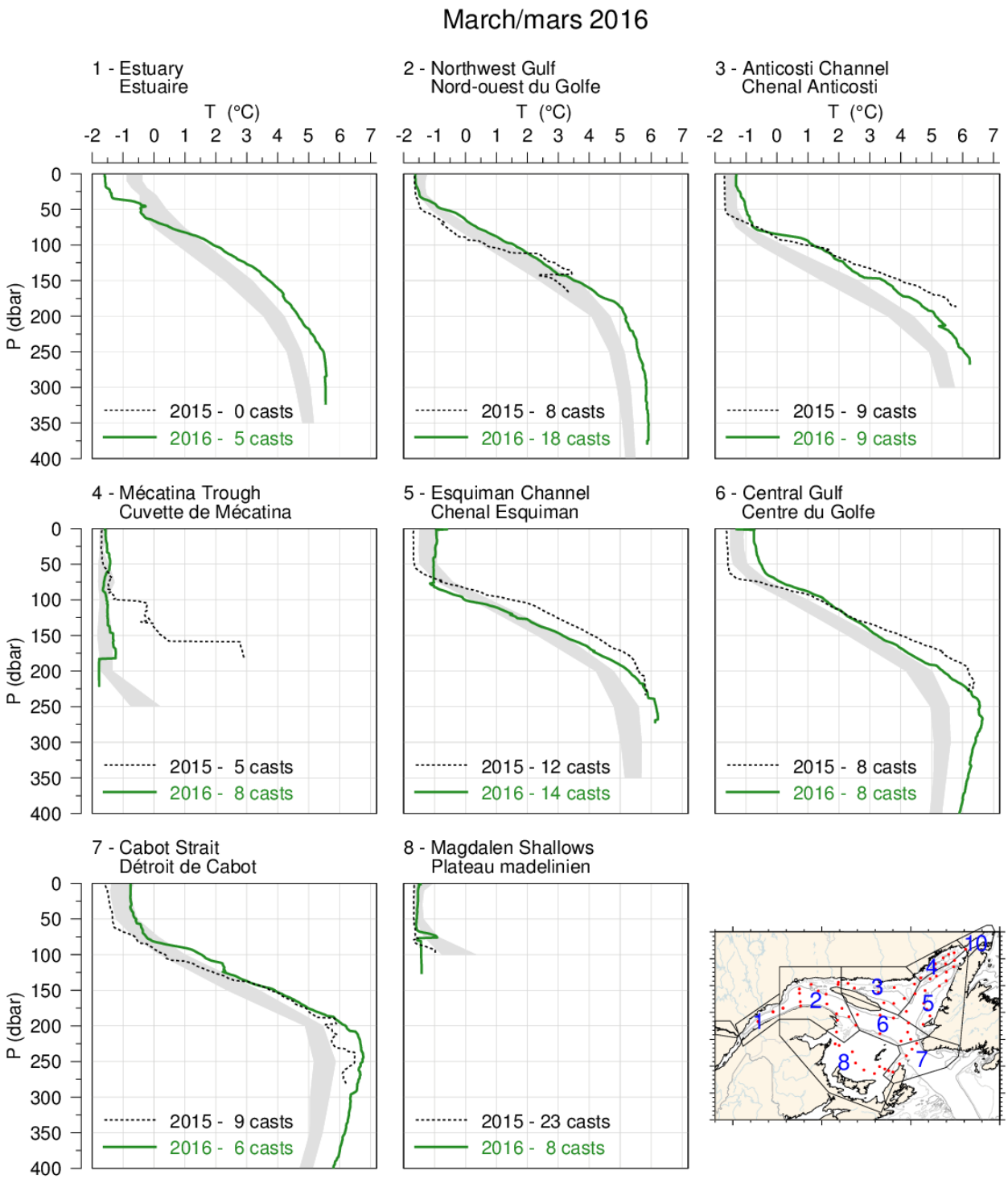

Figure 61. Mean temperature profiles observed in each region of the Gulf during the March 2016 survey. The shaded area represents the 1981–2010 (but mostly 1996–2010) climatological monthly mean ± 0.5 SD. Mean profiles for 2015 are also shown for comparison.

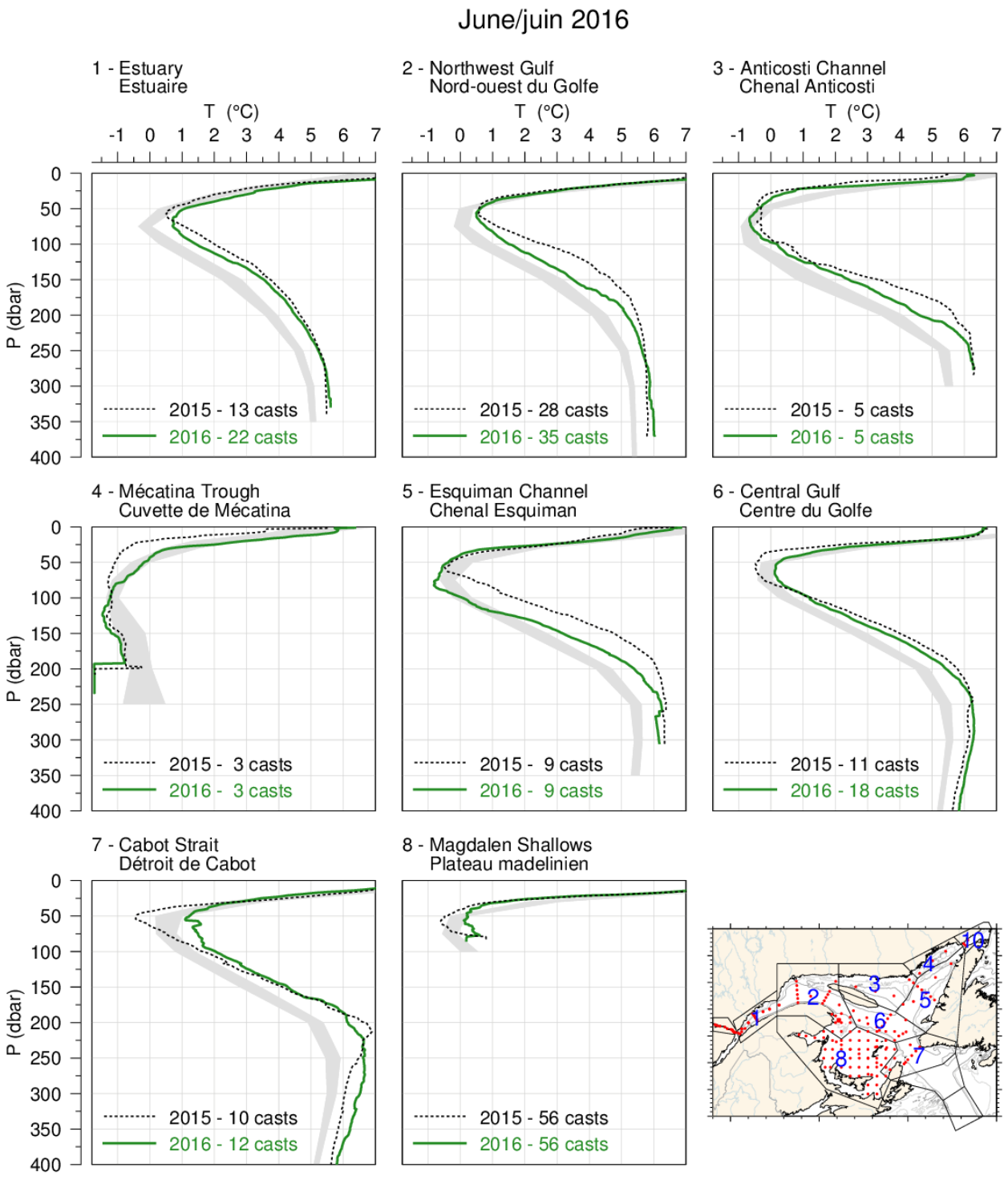

Figure 62. Mean temperature profiles observed in each region of the Gulf during June 2016. The shaded area represents the 1981–2010 climatological monthly mean ± 0.5 SD. Mean profiles for 2015 are also shown for comparison.

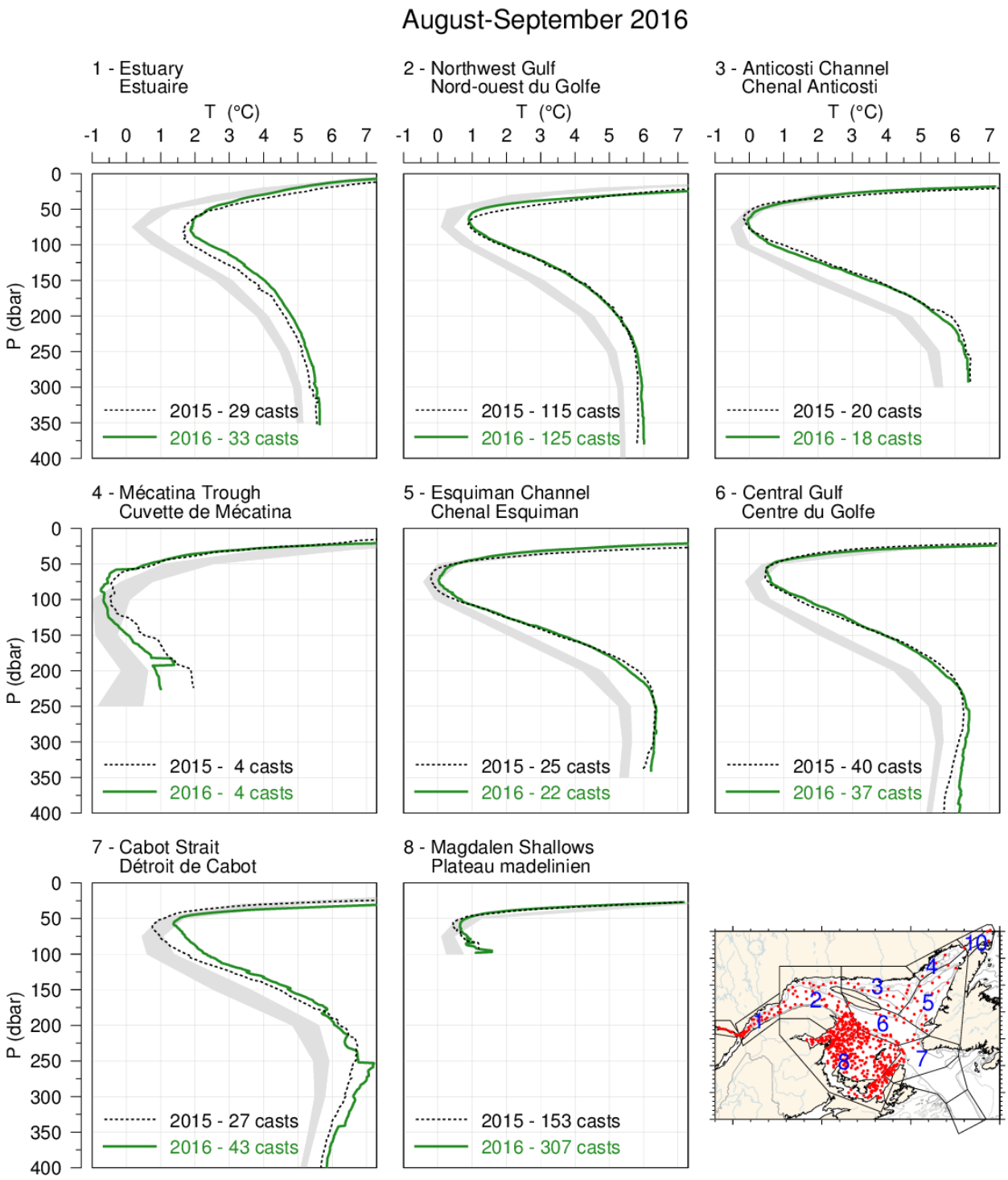

Figure 63. Mean temperature profiles observed in each region of the Gulf during August and September 2016. The shaded area represents the 1981–2010 climatological monthly mean ± 0.5 SD for August for regions 1 through 7 and for September for region 8. Mean profiles for 2015 are also shown for comparison.

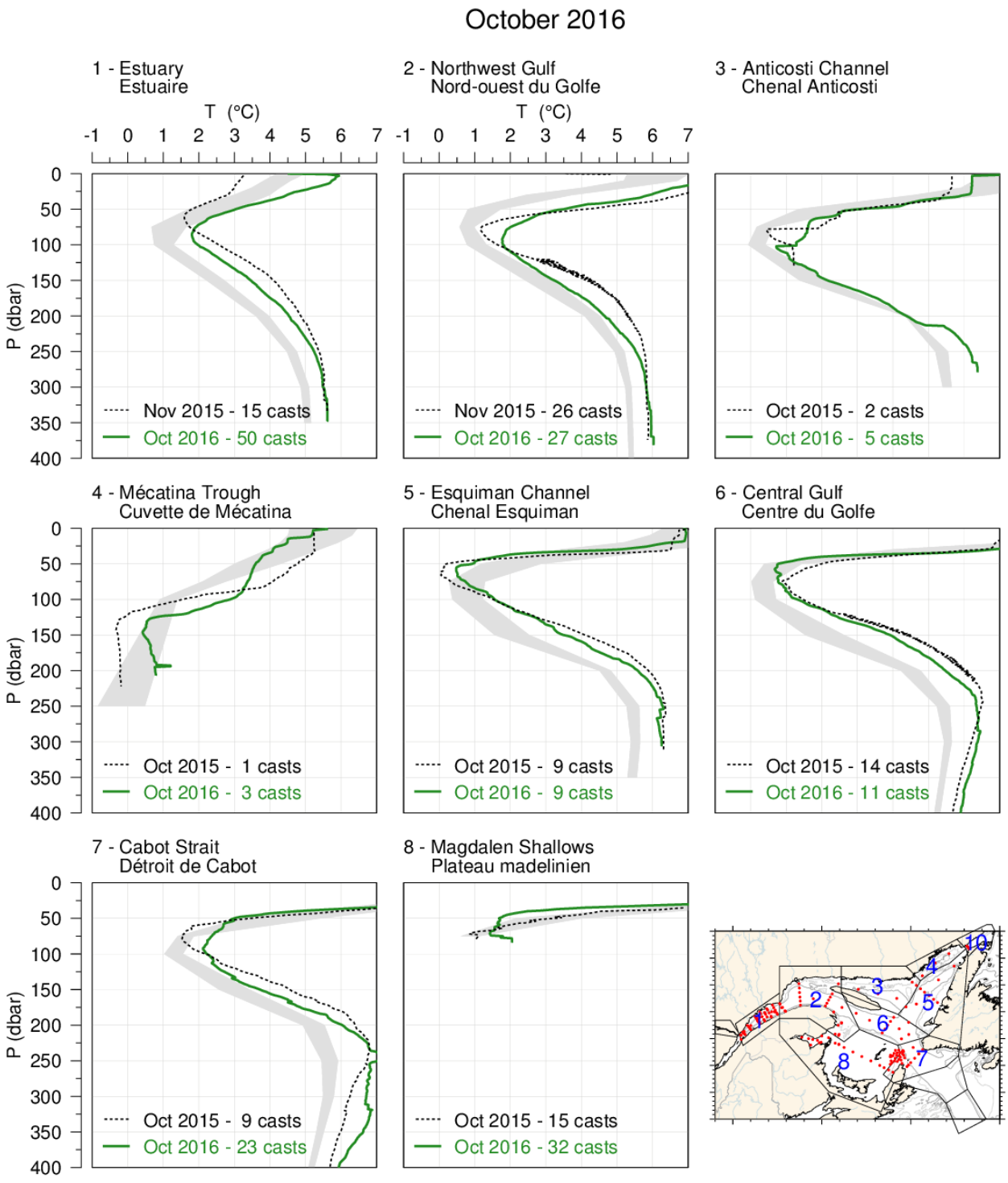

Figure 64. Mean temperature profiles observed in each region of the Gulf during the October 2016 AZMP survey. The shaded area represents the 1981–2010 climatological monthly mean ± 0.5 SD. Mean profiles for 2015 are also shown for comparison.

1 - Estuary / Estuaire

	2015			2016			
	June	Aug	Nov	Mar	June	Aug	Oct
0 m	7.4	10.1	3.0	-1.63	8.1	9.2	5.9
10 m	5.6	8.2	3.0	-1.63	6.4	6.6	5.7
20 m	3.4	6.1	2.9	-1.64	4.1	5.0	5.2
30 m	2.4	4.8	2.7	-1.65	2.9	3.9	4.4
50 m	1.2	2.5	1.8	0.1	1.1	2.3	3.0
75 m	1.1	1.4	1.6	0.2	0.8	1.8	1.9
100 m	2.1	1.8	2.5	1.4	1.5	2.5	2.0
150 m	3.8	3.8	4.0	3.3	3.5	4.1	3.5
200 m	4.69	4.79	4.81	4.54	4.53	4.87	4.54
250 m	5.23	5.29	5.33	5.59	5.22	5.31	5.24
300 m	5.43	5.50	5.55	5.63	5.53	5.53	5.51
350 m	5.46	5.52	5.57		5.61	5.63	5.61

2 - Northwest Gulf / Nord-ouest du Golfe

	2015				2016			
	Mar	June	Aug	Nov	Mar	June	Aug	Oct
0 m	-1.64	8.1	14.9	4.1	-1.62	8.9	15.3	7.2
10 m	-1.64	6.6	11.1	4.1	-1.62	6.6	13.5	7.3
20 m	-1.62	4.1	6.0	4.0	-1.55	3.8	8.8	6.6
30 m	-1.60	2.1	3.9	3.6	-1.48	2.3	5.0	5.9
50 m	-1.42	0.5	1.3	2.7	-0.68	0.6	1.1	3.4
75 m	-0.58	0.8	1.1	1.9	0.4	0.8	1.0	1.9
100 m	0.3	2.1	2.0	1.9	1.5	1.5	1.9	1.8
150 m	3.7	4.3	4.2	4.3	3.3	3.5	4.1	3.3
200 m		5.33	5.22	5.53	5.17	5.17	5.24	4.65
250 m		5.70	5.71	5.79	5.58	5.63	5.79	5.53
300 m		5.79	5.81	5.83	5.84	5.88	5.92	5.83
350 m		5.79	5.82	5.84	5.87	5.95	5.95	5.91
400 m			5.81		5.88		6.01	6.02

3 - Anticosti Channel / Chenal Anticosti

	2015				2016			
	Mar	June	Aug	Oct	Mar	June	Aug	Oct
0 m	-1.70	5.5	16.8	5.7	-1.32	6.3	13.6	6.2
10 m	-1.69	3.6	15.9	5.7	-1.32	5.6	11.8	6.2
20 m	-1.69	1.2	7.5	5.6	-1.28	1.7	6.0	6.2
30 m	-1.69	-0.1	3.3	5.4	-1.17	0.3	2.5	6.0
50 m	-1.66	-0.3	0.1	3.1	-1.00	-0.4	0.3	3.0
75 m	-0.60	-0.3	-0.0	1.9	-0.76	-0.6	-0.0	1.6
100 m	0.7	0.2	1.0	1.1	1.2	0.2	0.7	1.3
150 m	4.0	3.4	3.6		2.9	2.4	3.5	2.2
200 m		5.67	5.54		5.00	4.61	5.53	4.39
250 m		6.24	6.32		6.04	6.16	6.22	6.16

4 - Mécatina Trough / Cuvette de Mécatina

	2015				2016			
	Mar	June	Aug	Oct	Mar	June	Aug	Oct
0 m	-1.70	3.6	12.0	5.2	-1.56	5.8	14.6	5.2
10 m	-1.70	2.5	10.0	5.2	-1.56	5.3	13.5	5.2
20 m	-1.69	-0.1	6.3	5.2	-1.53	2.9	8.3	4.5
30 m	-1.71	-0.7	3.5	5.2	-1.52	0.7	3.3	4.1
50 m	-1.64	-1.1	0.9	4.8	-1.42	-0.2	0.6	3.6
75 m	-1.45	-1.3	-0.4	4.1	-1.62	-0.8	-0.5	3.4
100 m	-1.11	-1.2	-0.4	1.5	-1.54	-1.2	-0.7	2.9
150 m	0.2	-0.9	0.5	-0.3	-1.41	-1.2	0.1	0.5
200 m		-0.72	2.60	-0.20	-1.77	-0.78	1.45	0.82

5 - Esquiman Channel / Chenal Esquiman

	2015				2016			
	Mar	June	Aug	Oct	Mar	June	Aug	Oct
0 m	-1.69	5.5	15.0	6.7	-0.98	6.6	16.6	6.9
10 m	-1.68	4.9	14.6	6.7	-0.94	5.6	15.4	6.9
20 m	-1.68	3.5	11.4	6.5	-0.93	4.0	8.1	6.5
30 m	-1.68	1.8	5.4	6.5	-0.98	1.0	3.5	5.0
50 m	-1.65	-0.3	0.4	0.2	-1.03	-0.4	0.5	0.9
75 m	-0.63	0.4	-0.2	0.3	-1.02	-0.8	0.0	0.7
100 m	1.5	1.7	0.5	1.5	-0.02	0.1	0.7	1.6
150 m	4.2	4.8	3.4	4.1	3.1	3.2	3.6	3.5
200 m	5.67	6.10	5.84	5.88	5.28	5.39	5.57	5.58
250 m		6.32	6.32	6.30	6.16	6.23	6.35	6.29
300 m		6.33	6.29	6.31		6.16	6.34	6.25

6 - Central Gulf / Centre du Golfe

	2015				2016			
	Mar	June	Aug	Nov	Mar	June	Aug	Oct
0 m	-1.63	6.7	16.8	5.0	-0.74	6.6	17.1	7.9
10 m	-1.62	6.5	15.1	5.0	-0.74	6.4	16.6	7.9
20 m	-1.62	4.3	8.4	4.9	-0.73	4.6	10.8	7.9
30 m	-1.59	1.0	3.8	4.7	-0.67	2.2	4.0	6.9
50 m	-1.58	-0.4	1.2	3.1	-0.53	0.2	0.6	0.9
75 m	-0.57	-0.2	0.4	1.3	0.1	0.2	0.6	0.8
100 m	1.4	1.3	1.3	1.1	1.5	1.2	1.5	1.4
150 m	4.0	4.0	3.8	3.8	3.2	3.5	4.0	3.8
200 m	6.20	5.79	5.85	5.64	5.17	5.44	5.70	5.31
250 m		6.19	6.32	6.63	6.56	6.24	6.41	6.22
300 m		6.10	6.19	6.29	6.41	6.27	6.41	6.24
350 m		5.87	5.85	5.96	6.20	6.05	6.16	6.08
400 m		5.65	5.68	5.78	5.89	5.85	6.06	5.92
450 m		5.62	5.65	5.65	5.77	5.72	5.86	5.80

7 - Cabot Strait / Détroit de Cabot

	2015				2016			
	Mar	June	Aug	Oct	Mar	June	Aug	Nov
0 m	-1.56	7.4	16.0	12.4	-0.75	7.6	17.1	9.5
10 m	-1.50	7.2	15.7	12.1	-0.76	7.2	15.9	9.4
20 m	-1.47	5.4	10.9	11.8	-0.76	4.5	4.8	9.3
30 m	-1.42	2.7	5.3	8.1	-0.73	2.7	2.4	8.7
50 m	-1.34	-0.4	1.6	1.9	-0.58	1.2	1.4	4.6
75 m	-0.62	0.4	0.7	1.5	-0.25	1.5	1.6	3.5
100 m	0.3	1.6	1.4	2.2	1.5	2.0	2.0	2.5
150 m	3.8	4.1	4.5	4.6	3.9	4.3	4.2	3.9
200 m	5.88	6.67	6.41	6.39	6.19	6.14	6.09	6.29
250 m	6.48	6.48	6.75	6.73	6.74	6.66	6.76	7.16
300 m	6.17	6.05	6.39	6.25	6.36	6.51	6.62	6.81
350 m		5.85	5.92	5.98	6.17	6.21	6.34	6.62
400 m		5.62	5.67	5.68	5.80	5.80	5.85	5.93
450 m		5.58	5.61	5.59	5.64	5.73	5.77	5.80
500 m			5.62	5.59	5.65	5.71	5.75	5.80

8 - Magdalen Shallows / Plateau madelinien

	2015				2016			
	Mar	June	Sep	Oct	Mar	June	Sep	Oct
0 m	-1.64	9.9	16.3	12.3	-1.50	8.2	16.1	12.8
10 m	-1.66	8.8	16.2	12.4	-1.53	7.8	15.9	12.7
20 m	-1.67	4.7	12.5	12.0	-1.53	4.8	13.1	11.8
30 m	-1.67	1.5	5.9	8.5	-1.54	1.6	5.6	7.2
50 m	-1.67	-0.4	0.8	2.4	-1.57	0.2	0.8	1.4
75 m	-1.62	-0.2	0.6	1.0	-0.93	0.4	0.7	1.7
100 m	-0.98		1.2		-1.43		1.4	

Figure 65. Depth-layer monthly average temperature summary for months during which the eight Gulf-wide oceanographic surveys took place in 2015 and 2016. The colour-coding is according to the temperature anomaly relative to the monthly 1981–2010 climatology of each region.

1 - Estuary / Estuaire

	2015			2016			
	June	Aug	Nov	Mar	June	Aug	Oct
Strat.	4.8	4.1	1.9	1.01	5.7	3.8	2.9
0 m	26.3	27.3	29.9	30.4	25.0	28.0	28.0
10 m	27.4	28.1	30.2	30.3	26.3	28.9	28.5
20 m	29.2	29.1	30.7	30.4	28.4	29.9	29.3
30 m	30.3	30.1	31.3	30.5	29.9	30.6	30.2
50 m	31.6	31.3	32.1	31.7	31.3	31.7	31.3
75 m	32.3	32.2	32.8	32.1	32.1	32.5	32.1
100 m	33.1	32.8	33.2	32.6	32.7	33.1	32.7
150 m	33.8	33.7	33.8	33.5	33.6	33.8	33.5
200 m	34.13	34.17	34.16	34.00	34.01	34.15	34.01
250 m	34.38	34.40	34.40	34.48	34.32	34.35	34.32
300 m	34.48	34.50	34.52	34.50	34.47	34.46	34.44
350 m	34.50	34.51	34.52		34.52	34.51	34.49

2 - Northwest Gulf / Nord-ouest du Golfe

	2015				2016			
	Mar	June	Aug	Nov	Mar	June	Aug	Oct
Strat.	0.17	3.2	4.3	1.1	0.30	3.5	4.7	2.0
0 m	31.4	28.7	28.9	30.4	31.4	28.4	28.3	29.6
10 m	31.5	29.3	29.6	30.6	31.4	29.2	28.8	29.8
20 m	31.5	30.2	30.7	30.7	31.5	30.4	29.8	30.2
30 m	31.5	31.0	31.3	31.0	31.5	31.1	30.7	30.6
50 m	31.7	31.9	32.0	31.6	31.8	31.9	31.8	31.6
75 m	32.0	32.6	32.6	32.4	32.2	32.3	32.4	32.2
100 m	32.3	33.1	33.0	32.9	32.7	32.7	32.9	32.6
150 m	33.6	33.9	33.8	33.9	33.4	33.5	33.8	33.4
200 m		34.31	34.26	34.34	34.18	34.20	34.23	34.00
250 m		34.56	34.52	34.56	34.42	34.46	34.53	34.39
300 m		34.67	34.68	34.70	34.63	34.63	34.65	34.59
350 m		34.73	34.75	34.73	34.71	34.72	34.73	34.66
400 m			34.76		34.81		34.77	34.73

3 - Anticosti Channel / Chenal Anticosti

	2015				2016			
	Mar	June	Aug	Oct	Mar	June	Aug	Oct
Strat.	0.05	1.5	3.8	0.7	0.06	1.6	3.2	0.8
0 m	31.8	30.9	30.3	31.1	31.9	30.7	30.2	31.1
10 m	31.9	31.2	30.4	31.1	31.9	31.2	30.5	31.1
20 m	31.9	31.7	31.2	31.1	31.9	31.8	31.2	31.1
30 m	31.9	31.9	31.6	31.2	31.9	31.9	31.7	31.2
50 m	31.9	32.1	32.1	31.6	31.9	32.0	32.0	31.7
75 m	32.2	32.4	32.4	32.1	32.0	32.2	32.3	32.0
100 m	32.6	32.7	32.8	32.8	32.6	32.5	32.6	32.3
150 m	33.7	33.5	33.6		33.3	33.1	33.5	33.1
200 m		34.25	34.24		34.02	33.90	34.21	33.81
250 m		34.55	34.61		34.41	34.50	34.56	34.49

4 - Mécatina Trough / Cuvette de Mécatina

	2015				2016			
	Mar	June	Aug	Oct	Mar	June	Aug	Oct
Strat.	0.05	1.8	2.3	0.4	0.17	1.1	3.0	0.4
0 m	32.1	30.3	30.7	31.0	32.0	31.2	30.5	31.2
10 m	32.1	30.9	30.9	31.0	32.0	31.3	30.6	31.2
20 m	32.1	31.8	31.4	31.0	32.0	31.6	31.0	31.4
30 m	32.1	32.0	31.6	31.1	32.0	31.8	31.5	31.5
50 m	32.2	32.2	31.9	31.4	32.2	32.0	31.9	31.6
75 m	32.4	32.4	32.2	31.7	32.3	32.2	32.2	31.7
100 m	32.4	32.5	32.5	32.1	32.3	32.4	32.4	31.8
150 m	32.9	32.8	33.0	32.7	32.6	32.6	32.7	32.5
200 m		32.93	33.35	32.72	32.70	32.73	32.98	32.72

5 - Esquiman Channel / Chenal Esquiman

	2015				2016			
	Mar	June	Aug	Oct	Mar	June	Aug	Oct
Strat.	-0.01	1.0	2.9	1.4	0.10	1.2	3.4	1.3
0 m	31.9	31.3	30.7	31.0	31.7	31.2	30.6	31.1
10 m	31.8	31.4	30.7	31.0	31.7	31.4	30.8	31.1
20 m	31.8	31.7	31.0	31.0	31.8	31.7	31.3	31.2
30 m	31.8	31.8	31.4	31.0	31.8	31.8	31.7	31.4
50 m	31.8	32.0	31.8	32.0	31.8	32.0	31.9	32.1
75 m	32.1	32.5	32.2	32.4	31.9	32.2	32.2	32.4
100 m	32.8	33.0	32.6	32.9	32.3	32.5	32.5	32.7
150 m	33.7	33.9	33.5	33.7	33.3	33.4	33.5	33.4
200 m	34.23	34.40	34.30	34.33	34.08	34.14	34.19	34.21
250 m		34.63	34.58	34.59	34.48	34.52	34.58	34.56
300 m		34.60	34.75	34.57		34.50	34.66	34.52

6 - Central Gulf / Centre du Golfe

	2015				2016			
	Mar	June	Aug	Nov	Mar	June	Aug	Oct
Strat.	0.01	1.2	4.0	0.8	0.06	1.3	4.0	1.6
0 m	31.8	31.2	29.7	30.6	31.7	30.8	29.8	30.8
10 m	31.8	31.2	30.0	30.6	31.7	30.9	30.0	30.8
20 m	31.8	31.4	30.9	30.7	31.7	31.1	30.6	30.8
30 m	31.9	31.7	31.4	30.8	31.7	31.5	31.2	31.0
50 m	31.9	32.0	31.9	31.4	31.8	31.8	31.8	32.0
75 m	32.1	32.3	32.3	32.2	32.0	32.1	32.2	32.3
100 m	32.8	32.9	32.8	32.6	32.6	32.6	32.7	32.7
150 m	33.7	33.7	33.7	33.6	33.4	33.5	33.6	33.5
200 m	34.41	34.30	34.34	34.27	34.03	34.17	34.25	34.11
250 m		34.58	34.63	34.63	34.53	34.55	34.60	34.52
300 m		34.73	34.77	34.76	34.71	34.73	34.76	34.69
350 m		34.81	34.85	34.85	34.82	34.82	34.82	34.82
400 m		34.86	34.88	34.87	34.87	34.87	34.89	34.84
450 m		34.88	34.89	34.90	34.89	34.91	34.91	34.90

7 - Cabot Strait / Détroit de Cabot

	2015				2016			
	Mar	June	Aug	Oct	Mar	June	Aug	Nov
Strat.	0.32	1.8	3.4	2.7	0.15	1.6	3.4	1.6
0 m	31.2	30.3	30.1	29.7	31.2	30.2	30.9	30.4
10 m	31.3	30.4	30.2	29.7	31.2	30.4	31.0	30.4
20 m	31.5	30.7	30.8	29.9	31.2	30.9	31.5	30.5
30 m	31.5	31.1	31.3	30.4	31.3	31.1	31.9	30.7
50 m	31.6	31.7	31.8	31.4	31.4	31.4	32.1	31.6
75 m	32.0	32.3	32.2	32.4	31.5	32.1	32.4	32.2
100 m	32.4	32.8	32.6	32.9	32.5	32.7	32.7	32.5
150 m	33.6	33.7	33.8	33.8	33.6	33.7	33.6	33.4
200 m	34.29	34.53	34.43	34.43	34.36	34.32	34.31	34.19
250 m	34.62	34.72	34.69	34.73	34.61	34.62	34.64	34.62
300 m	34.64	34.78	34.79	34.80	34.77	34.77	34.84	34.77
350 m		34.85	34.86	34.86	34.82	34.86	34.88	34.91
400 m		34.88	34.89	34.89	34.87	34.90	34.90	34.91
450 m		34.89	34.90	34.92	34.88	34.91	34.92	34.91
500 m			34.91	34.92	34.88	34.92	34.92	34.91

8 - Magdalen Shallows / Plateau madelinien

	2015				2016			
	Mar	June	Sep	Oct	Mar	June	Sep	Oct
Strat.	0.27	2.7	4.2	2.7	0.08	2.2	4.4	3.2
0 m	30.9	29.4	28.9	29.4	30.9	29.5	28.6	29.4
10 m	30.9	29.7	29.0	29.5	30.9	29.7	28.7	29.5
20 m	31.0	30.5	29.7	29.6	30.9	30.1	29.2	29.9
30 m	31.1	31.0	30.6	30.2	31.0	30.8	30.3	30.4
50 m	31.2	31.4	31.6	31.2	31.0	31.3	31.5	31.6
75 m	31.6	32.1	32.2	32.1	31.2	32.1	32.1	32.3
100 m	31.9		32.6		31.2		32.6	

Figure 66. Depth-layer monthly average stratification and salinity summary for months during which the eight Gulf-wide oceanographic surveys took place in 2015 and 2016. Stratification is defined as the density difference between 50 m and the surface and its colour-coding is reversed (blue for positive anomaly).

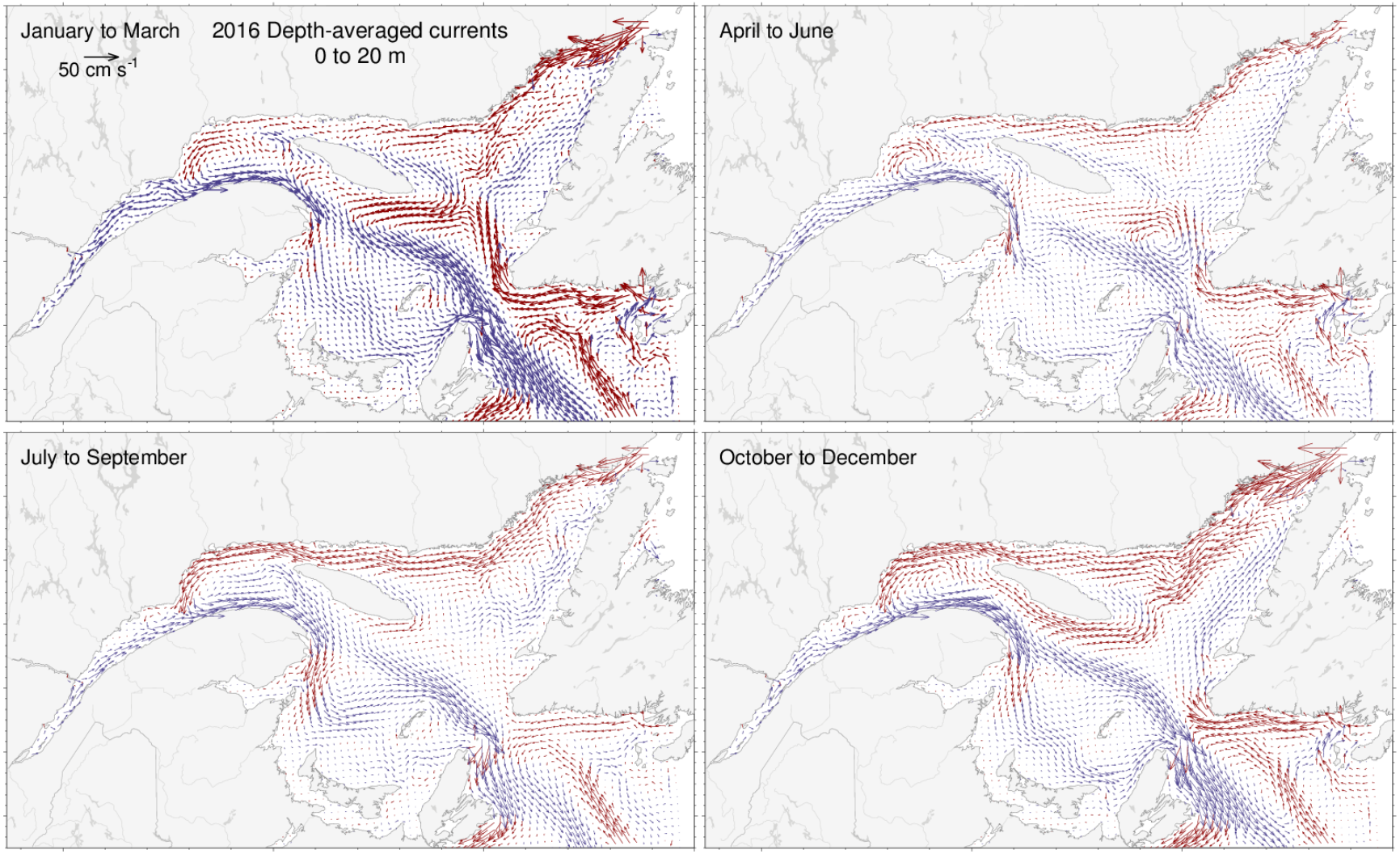

Figure 67. Depth-averaged currents from 0 to 20 m for each three-month period of 2016.

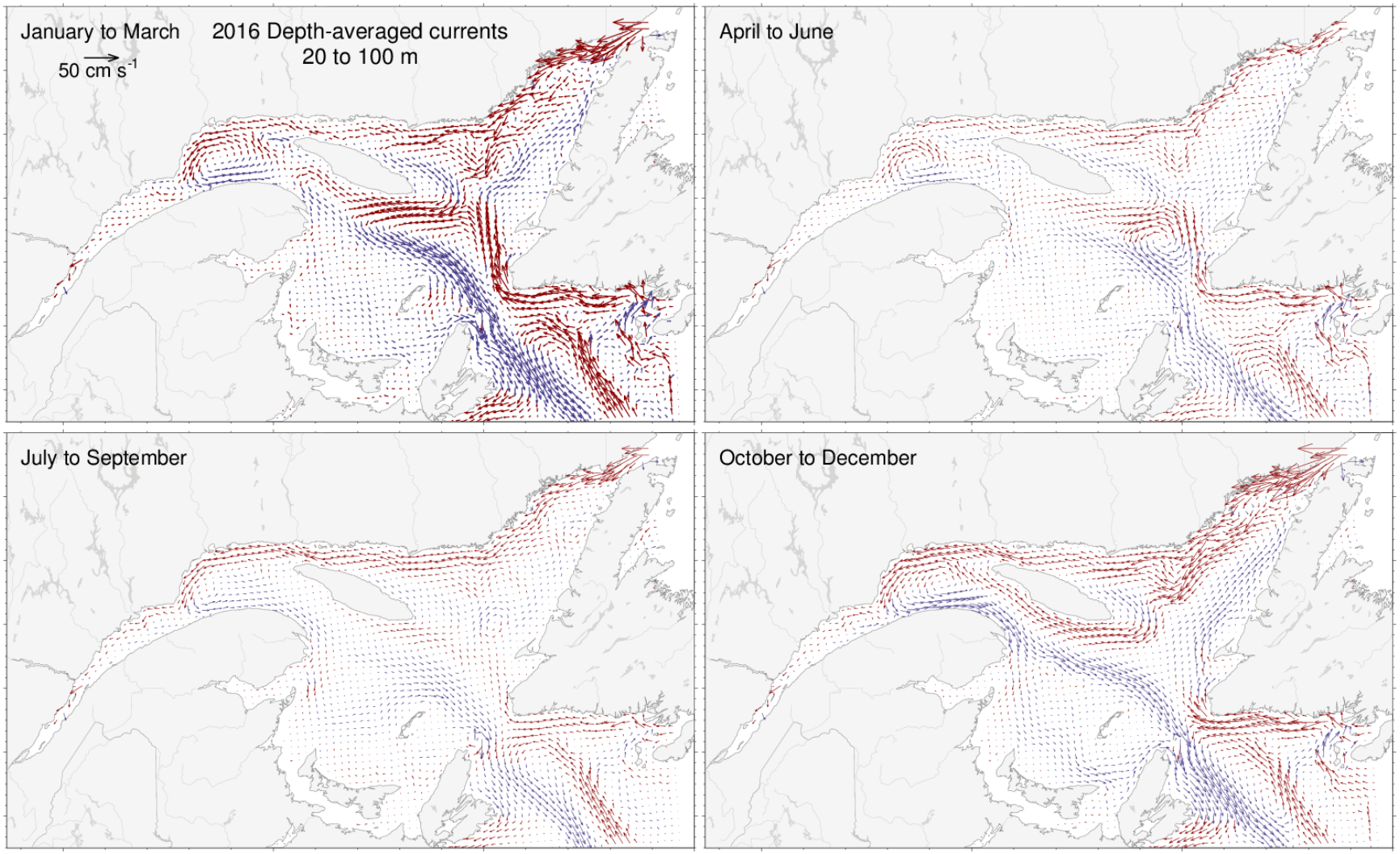

Figure 68. Depth-averaged currents from 20 to 100 m for each three-month period of 2016.

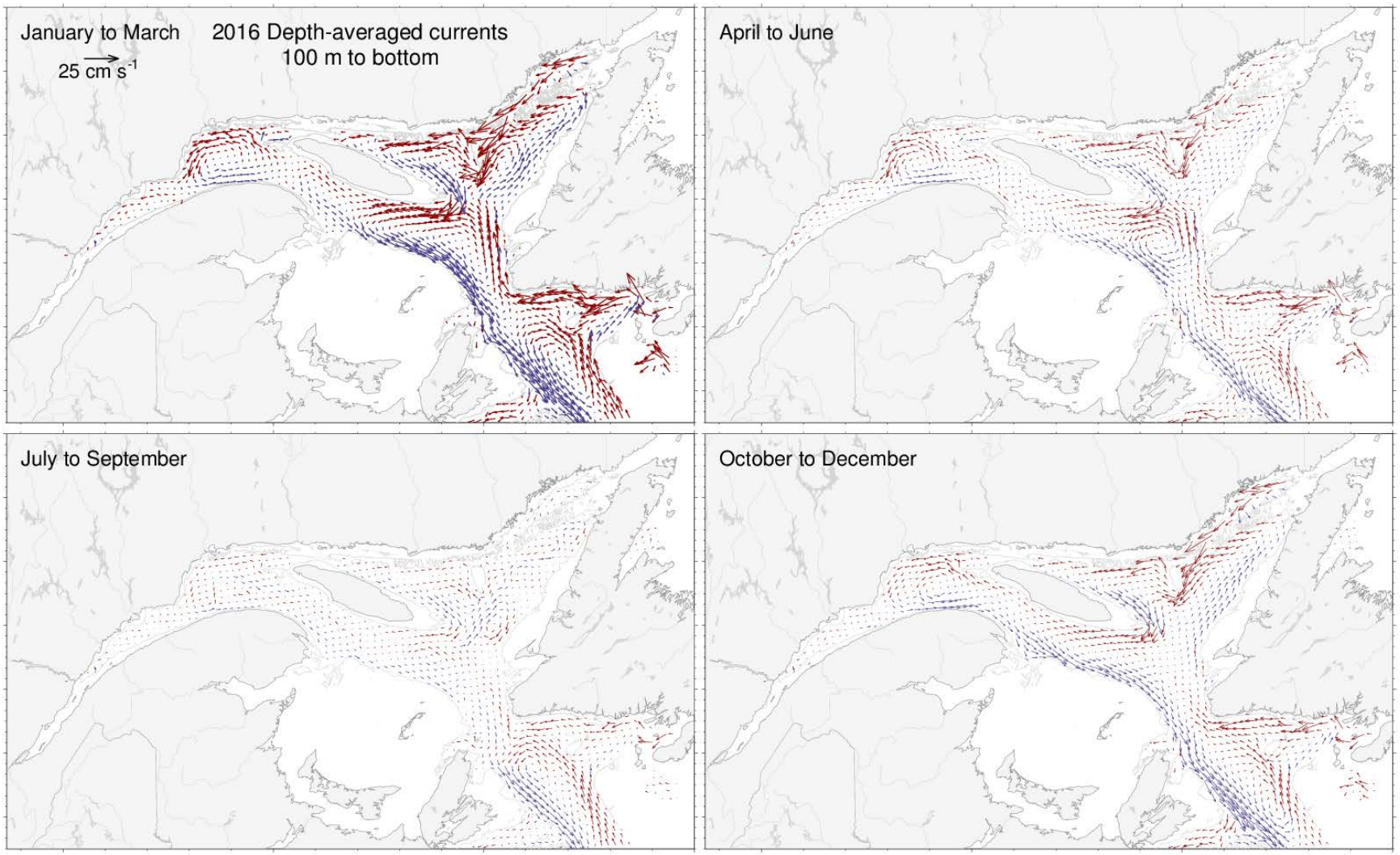

Figure 69. Depth-averaged currents from 100 m to the bottom for each three-month period of 2016.

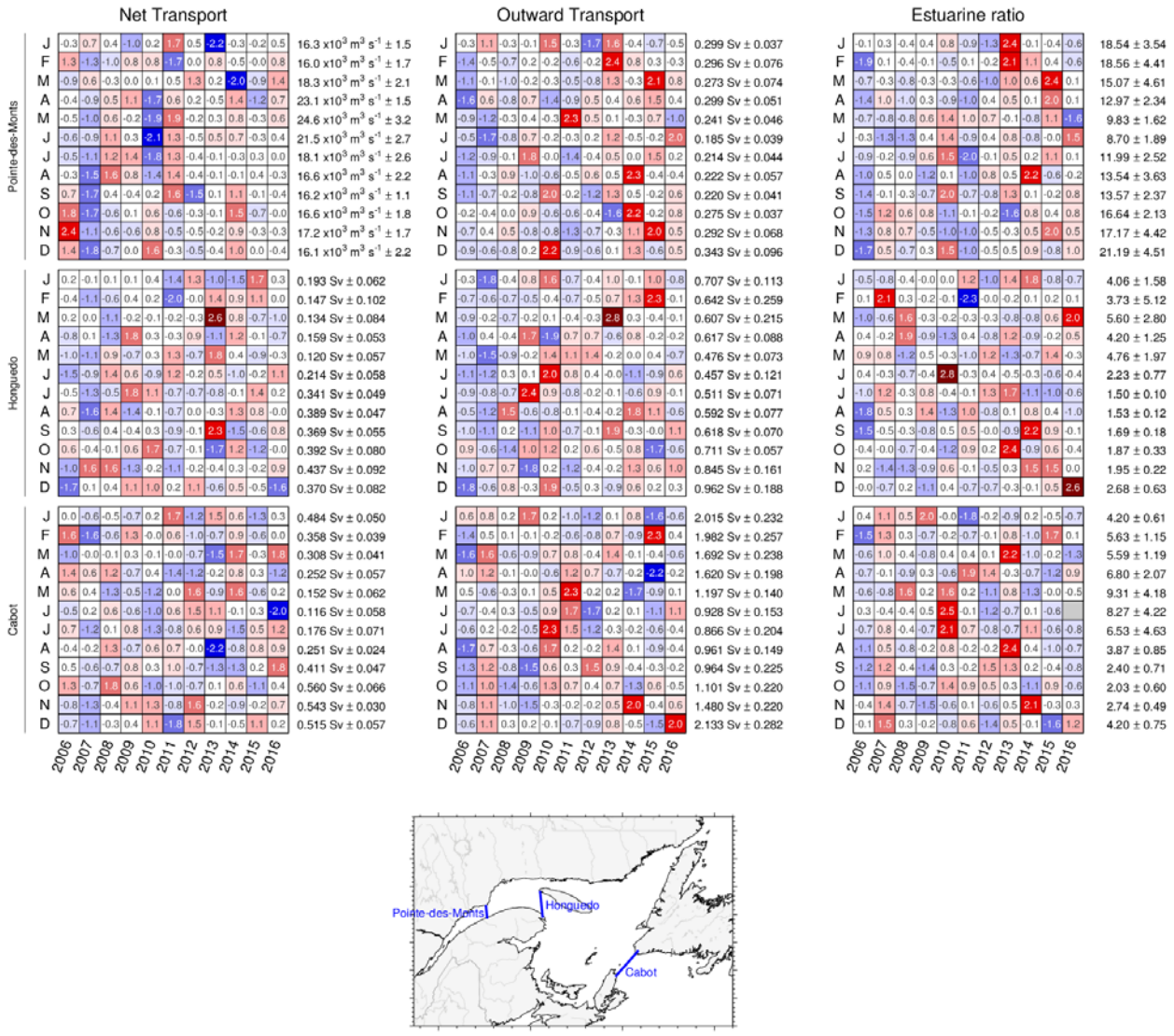

Figure 70. Monthly averaged modelled transports and estuarine ratio across sections of the Gulf of St. Lawrence since 2006. The numbers on the right are the 2006–2016 means and standard deviations. The numbers in the boxes are normalized anomalies. Colours indicate the magnitude of the anomaly. Sv (Sverdrup) are units of transport equal to 10^6 m^3s^{-1}.

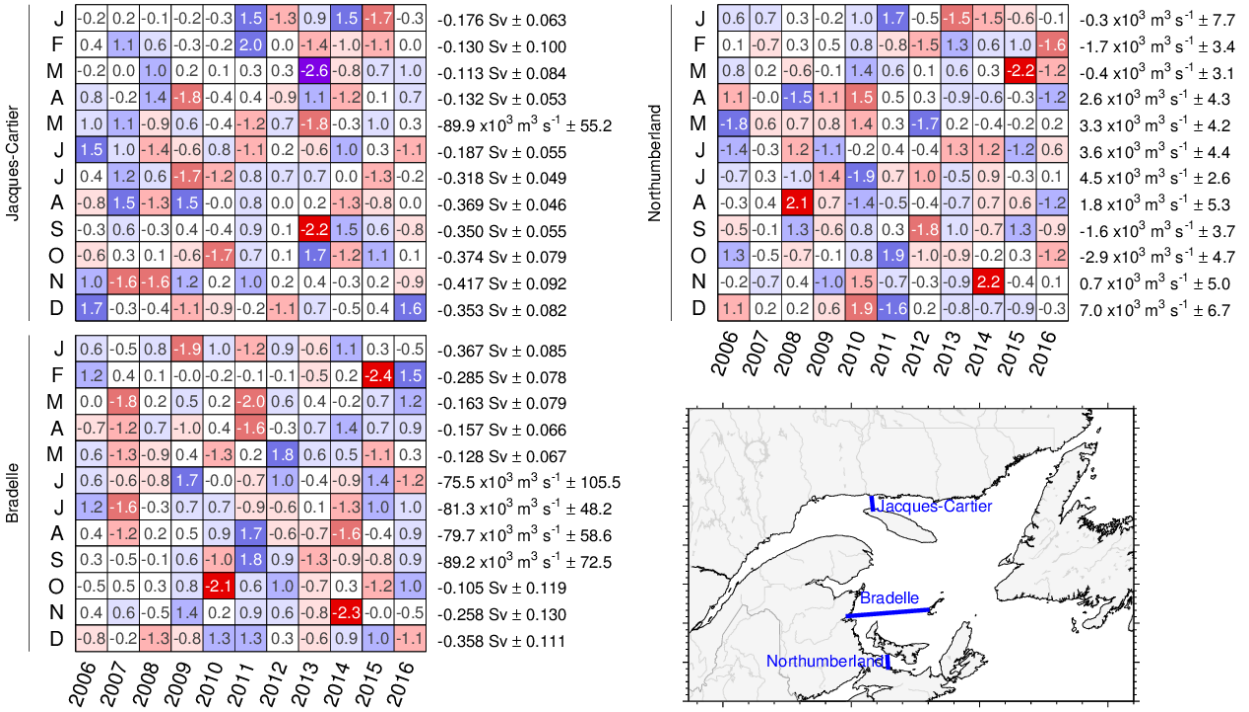

Figure 71. Monthly averaged modelled transports across sections of the Gulf of St. Lawrence since 2006. The numbers on the right are the 2006–2016 means and standard deviations, with positive values toward east and north. The numbers in the boxes are normalized anomalies. Colours indicate the magnitude of the anomaly (e.g., negative anomalies are still shown in red when the mean transport is negative across the section).

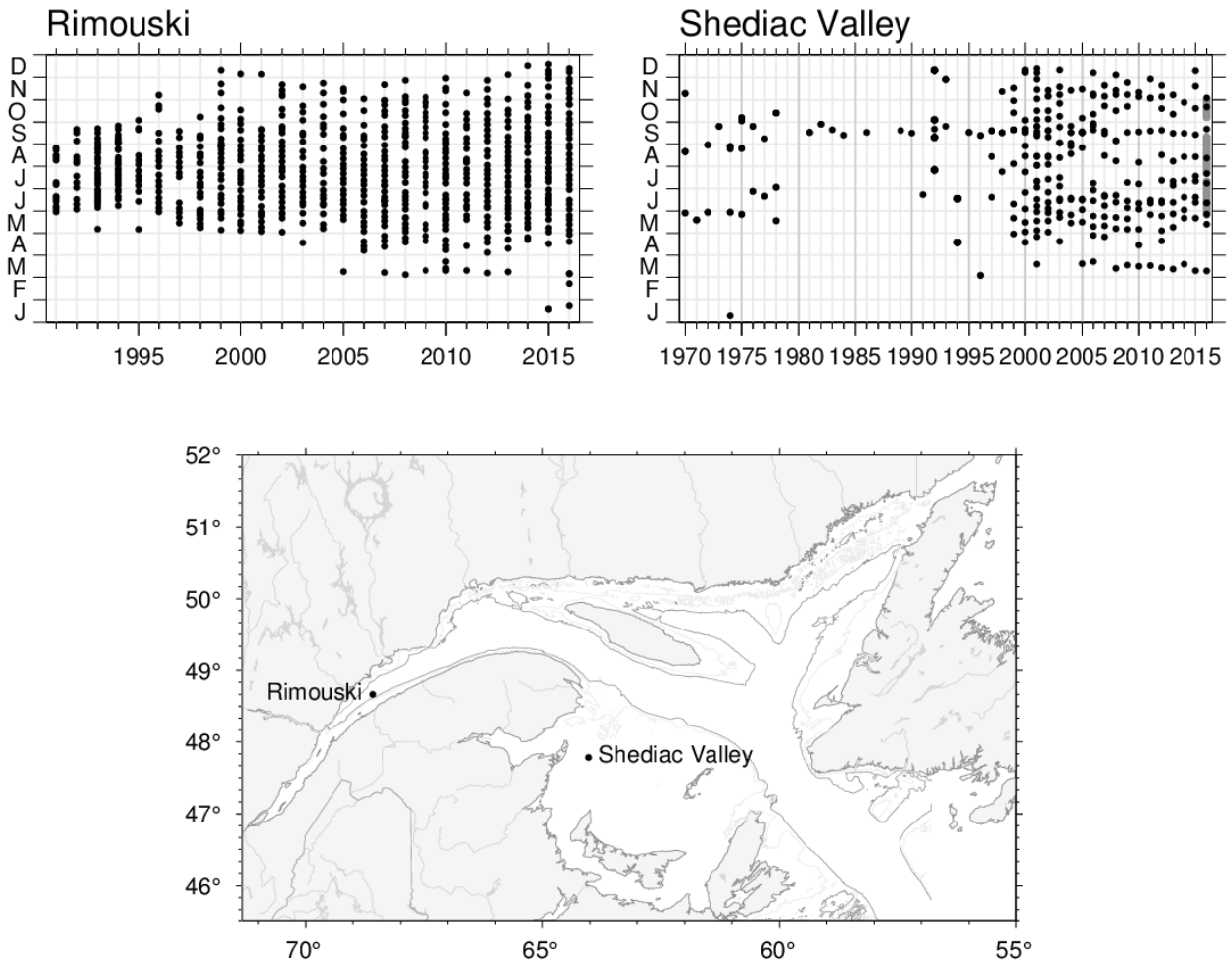

Figure 72. Sampling frequency and positions of the AZMP stations Rimouski and Shediac Valley. Gray overlay in 2016 at Shediac Valley shows span of 866 temperature and salinity profiles made by an automatic oceanographic buoy.

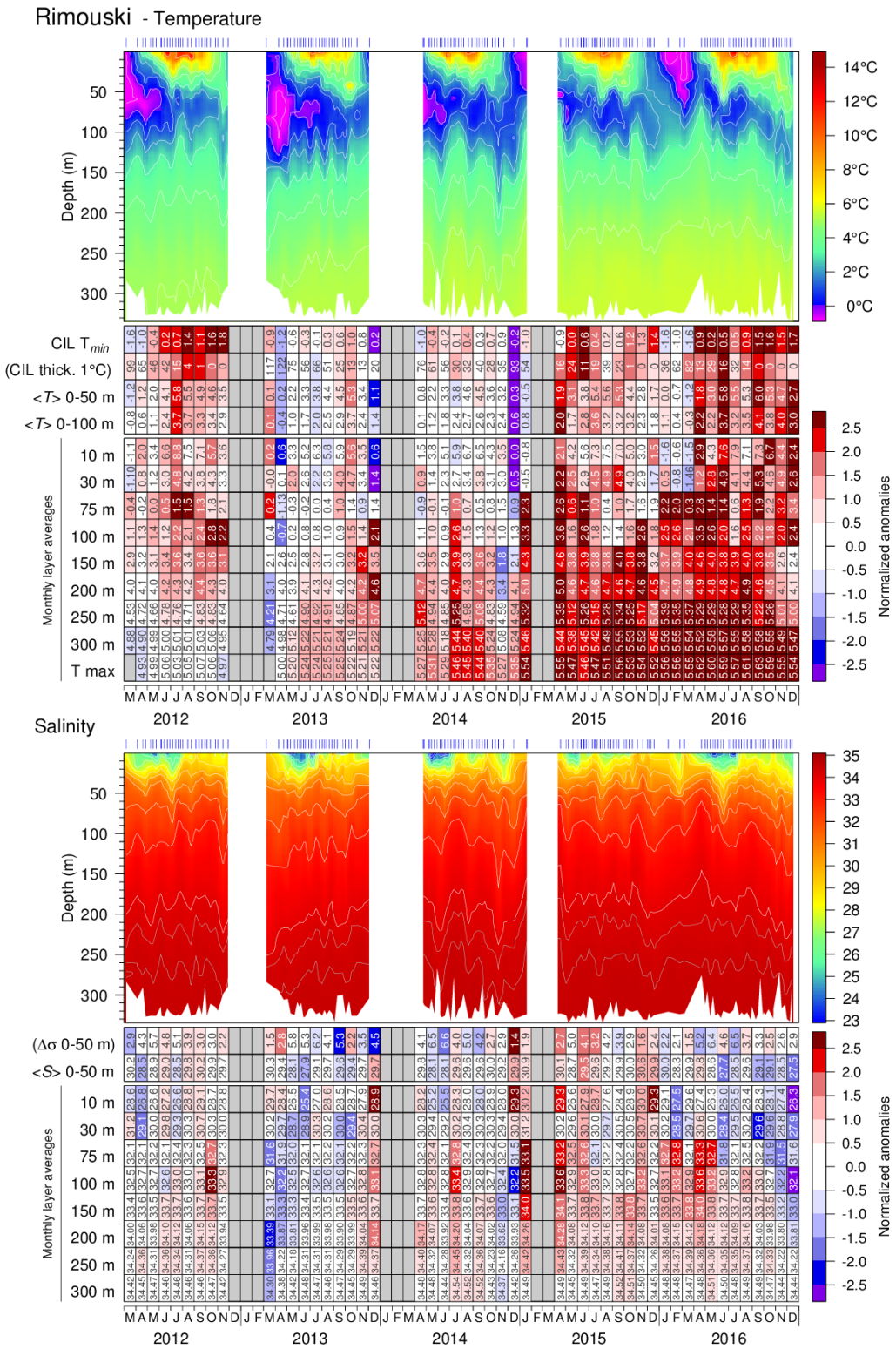

Figure 73. Isotherm (top) and isohaline (bottom) time series at the Rimouski station; tick marks above indicate sample dates. The scorecard tables are monthly layer averages colour-coded according to the anomaly relative to the 1991–2010 monthly climatology for the station (yearly climatology for 250 m and deeper). Thickness of the CIL and stratification have reversed colour codes where red indicates thinner CIL (warmer water) and less stratification (higher surface salinity).

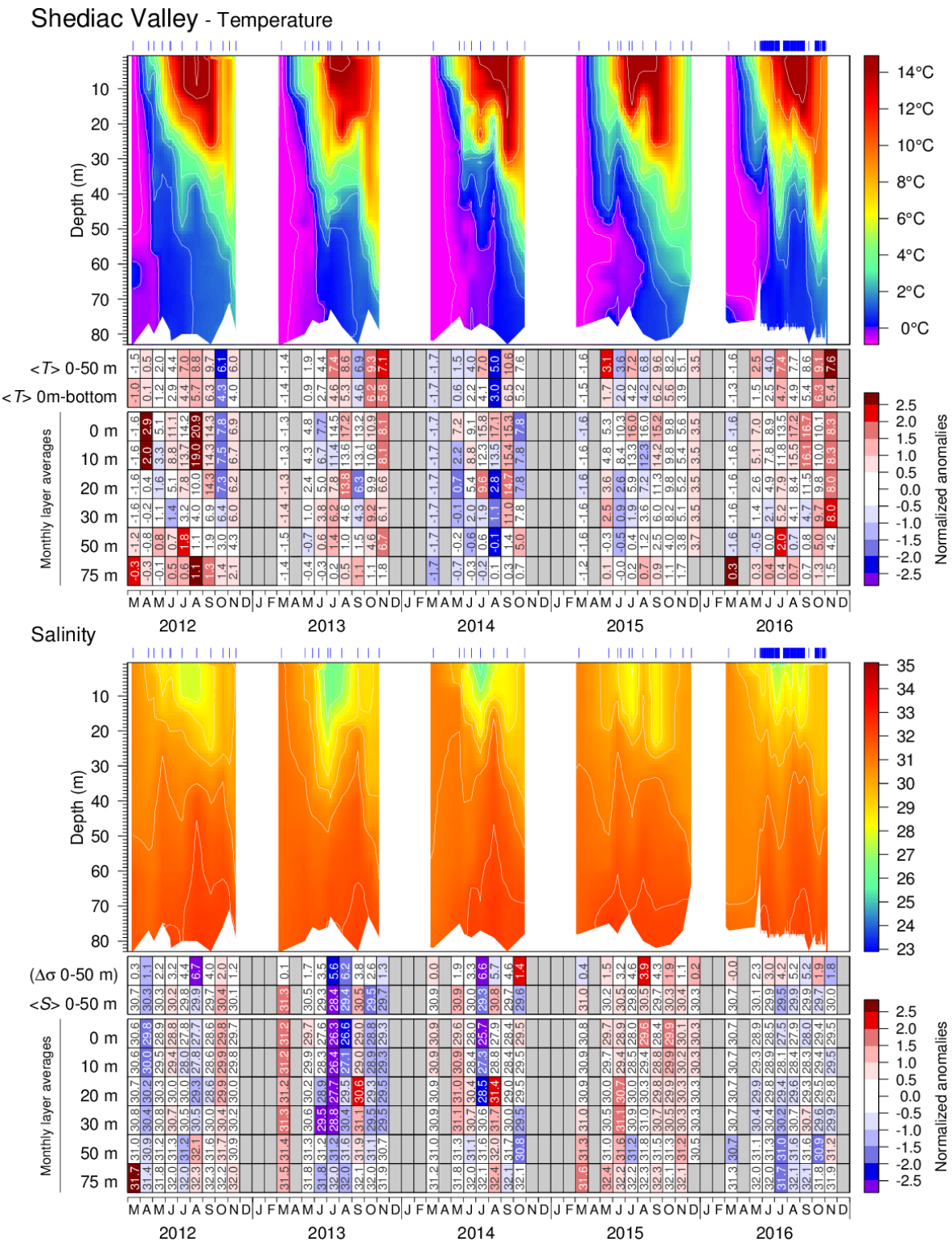

Figure 74. Isotherm (top) and isohaline (bottom) time series at the Shediac Valley station; tick marks above indicate sample dates (including from automatic buoy starting in 2016). Scorecard tables are monthly layer averages colour-coded according to the anomaly relative to the 1981–2016 monthly climatology for the station (input to climatology is sparse prior to 1999). The 10, 20, 30 and 75 m monthly layer averages for June-September 2015 are from mooring data.

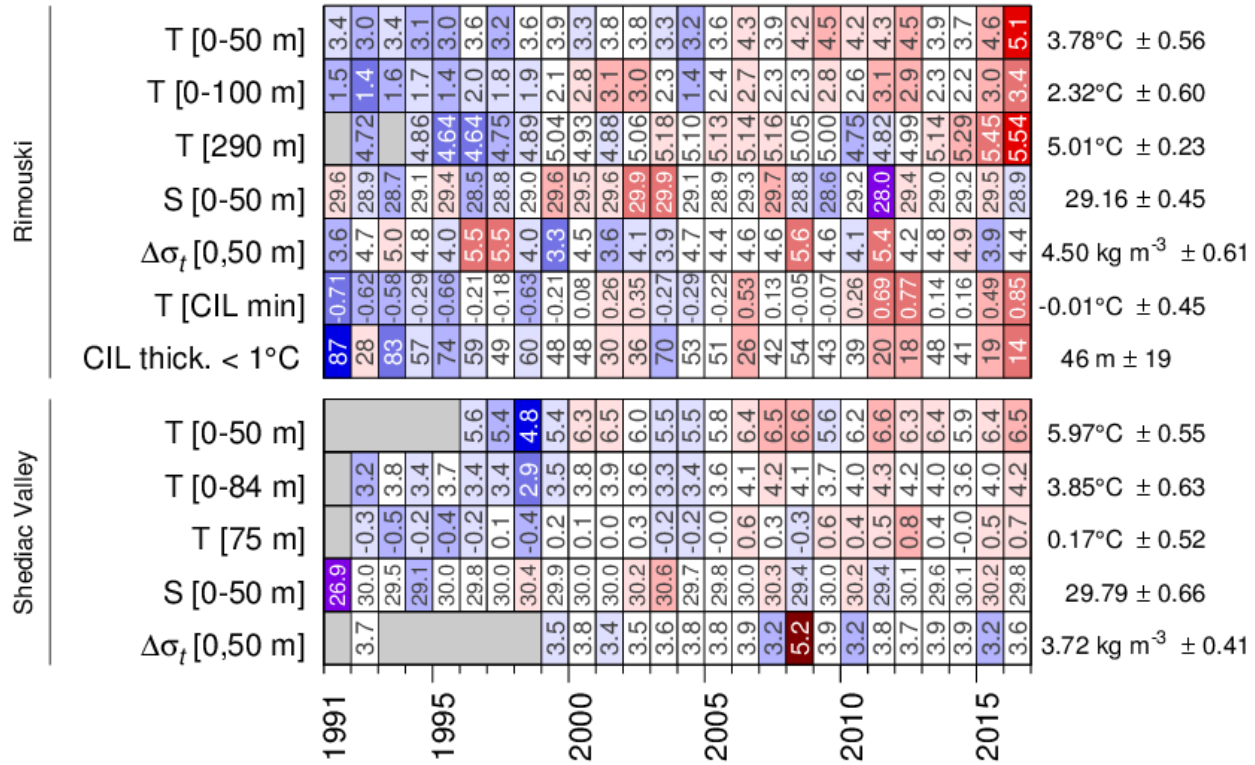

Figure 75. May to October temperature and salinity layer averages, stratification expressed as the density difference between 0 and 50 m, and CIL temperature minimum and thickness (T<1°C) for the fixed monitoring stations. Numbers in panels are monthly average values colour-coded according to the anomaly relative to the 1991–2016 timeseries. Three months of anomaly data, between May and October, are required to show an average anomaly for any given year, except for deep water temperature at Rimouski station. Temperatures at 290 m and 75 m at Rimouski station and Shediac Valley station are considered to represent near-bottom temperatures.

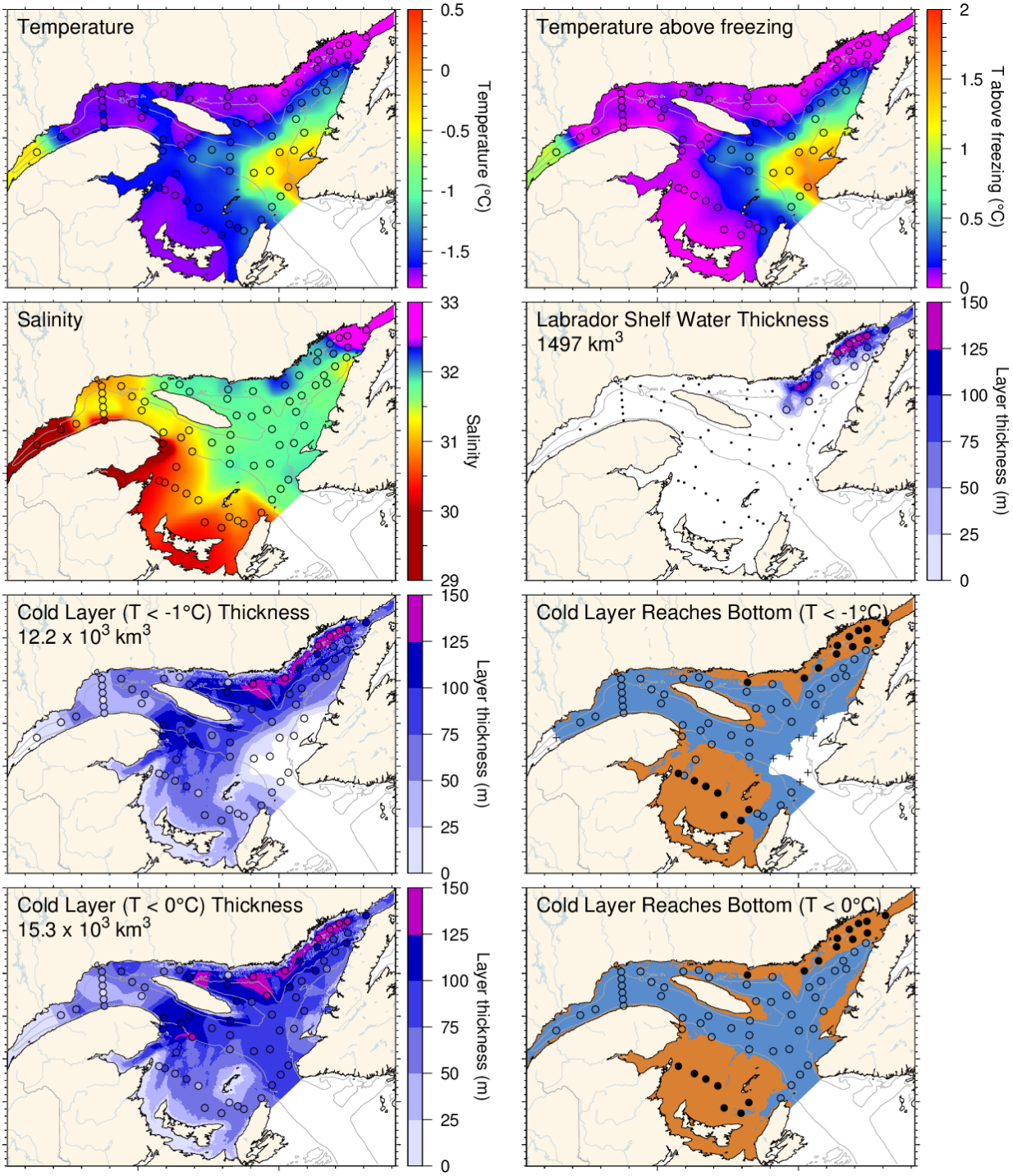

Figure 76. March 2017 surface cold layer characteristics: surface water temperature (upper left), temperature difference with the freezing point (upper right), salinity (second row left), estimate of the thickness of the Labrador Shelf water intrusion (second row right), and cold layer (T<-1°C and <0°C) thicknesses and where they reach bottom. The symbols are coloured according to the value observed at the station, using the same colour palette as the interpolated image. A good match is seen between the interpolation and the station observations where the station colours blend into the background.

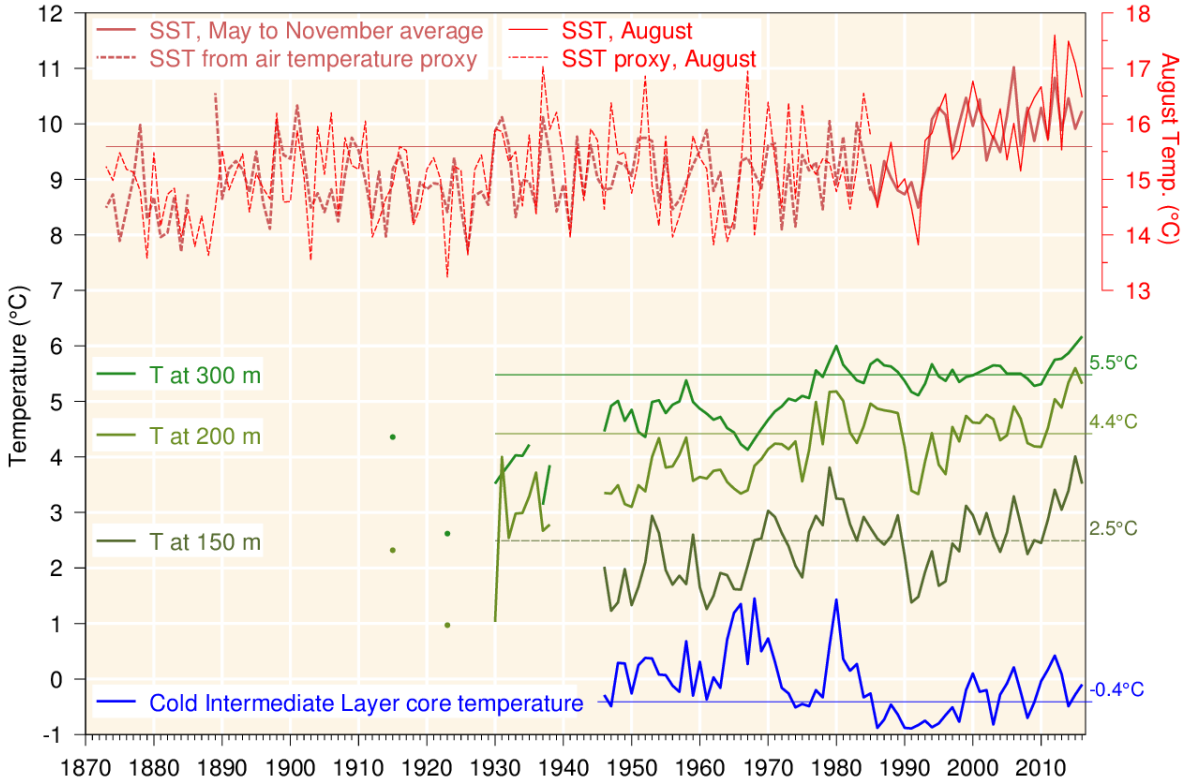

Figure 77. Water temperatures in the Gulf of St. Lawrence. May–November SST averaged over the Gulf excluding the Estuary (1985–2016, red line), completed by a proxy based on April–November air temperature (1873–1984, red dashed line; average of all AHCCD stations in Fig. 4 but excluding Estuary stations at Baie Comeau and Mont-Joli). August SST is shown using temperature scale offset by 6°C; its proxy is based on the average air temperature in July and August. Layer-averaged temperature for the Gulf of St. Lawrence at 150, 200 and 300 m (green lines). Cold intermediate layer minimum temperature index in the Gulf of St. Lawrence (blueline). SST air temperature proxy is similar to that of Galbraith et al. (2012). Climatological averages based on the 1981-2010 period are indicated by thin lines labeled on the right side. Figure adapted from (Benoît et al. 2012).

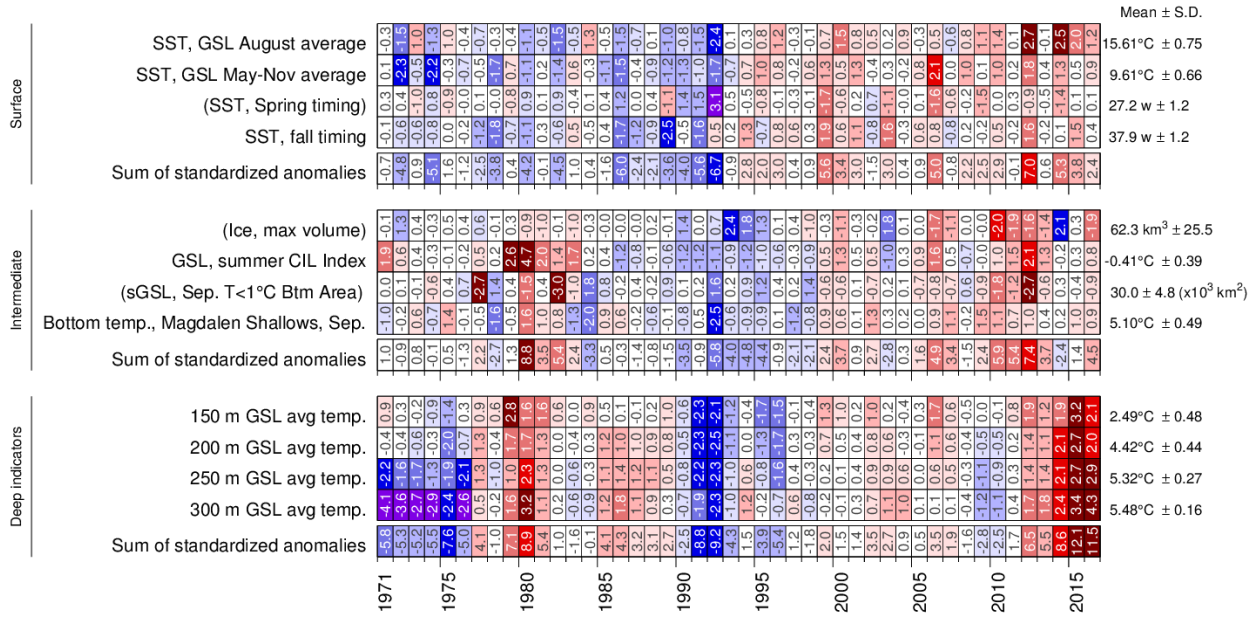

Figure 78. Surface, intermediate (and sea-ice) and deep indicators used in the composite climate index (Fig. 79).

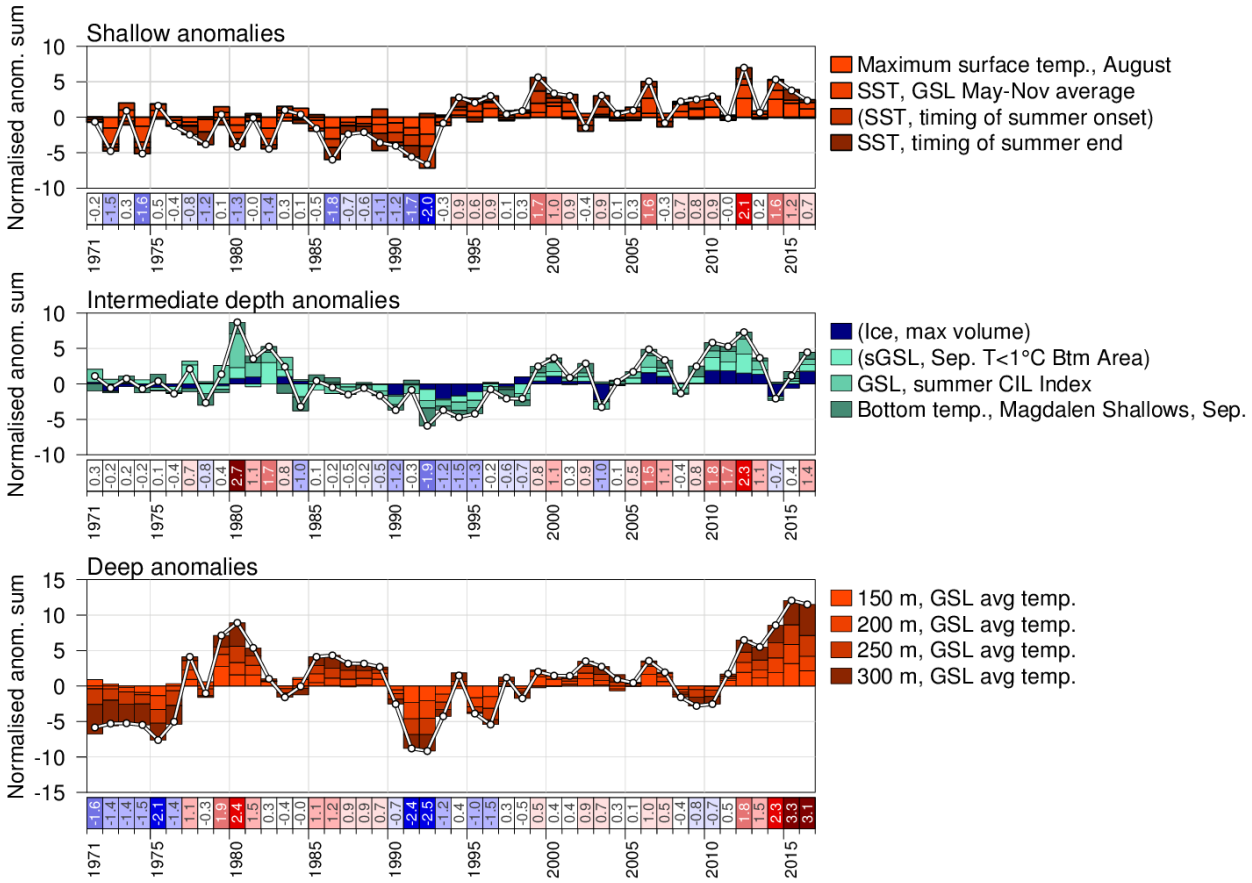

Figure 79. Composite climate indices (white lines and dots) derived by summing various normalized anomalies from different parts of the environment (colored boxes stacked above the abscissa are positive anomalies, and below are negative). Top panel sums anomalies representing shallow temperature anomalies, middle panel sums intermediate depth temperature anomalies and sea-ice (all related to winter formation), and bottom panel sums deep temperature anomalies.